

Electronic Thesis and Dissertation Repository

8-11-2017 12:00 AM

Distinct Roles of GABA(A)R Signaling in the Regulation of Two Human T lymphocyte Lines

Ying Lin, *The University of Western Ontario*

Supervisor: Dr. Wei-Yang Lu, *The University of Western Ontario*

A thesis submitted in partial fulfillment of the requirements for the Master of Science degree in
Physiology and Pharmacology

© Ying Lin 2017

Follow this and additional works at: <https://ir.lib.uwo.ca/etd>



Part of the [Cellular and Molecular Physiology Commons](#)

Recommended Citation

Lin, Ying, "Distinct Roles of GABA(A)R Signaling in the Regulation of Two Human T lymphocyte Lines" (2017). *Electronic Thesis and Dissertation Repository*. 4742.
<https://ir.lib.uwo.ca/etd/4742>

This Dissertation/Thesis is brought to you for free and open access by Scholarship@Western. It has been accepted for inclusion in Electronic Thesis and Dissertation Repository by an authorized administrator of Scholarship@Western. For more information, please contact wlsadmin@uwo.ca.

Abstract

In response to antigen presentation, helper T lymphocytes (T_H cells) initiate store-operated Ca^{2+} entry (SOCE) and differentiate into effector subtypes such as T_H1 and T_H2 cells. These cells play essential roles in adaptive immunity and the pathogenesis of various autoimmune and allergic diseases. The differentiation and activity of T_H cells are also critically regulated by paracrine and autocrine soluble factors in the cell microenvironment. Previous studies have reported that T_H cells produce gamma-aminobutyric acid (GABA) via glutamic acid decarboxylase (GAD) and express A-type GABA receptors ($GABA_A$ Rs), forming an autocrine GABA signaling system. In addition, GABA executes anti-inflammatory actions in T_H1 -autoimmune diseases. This project sought to examine whether autocrine GABA signaling distinctively regulates the function of different T_H effector cells using two unique lines of human T_H cells: Jurkat and CCRF-CEM. Our results showed that Jurkat and CCRF-CEM cells exhibited features of T_H1 and T_H2 phenotypes, respectively, and express different levels of $GABA_A$ R subunits. Selective blockade of $GABA_A$ Rs differentially affected cell metabolic activity, CRTh2 expression, NFAT expression, and store-operated Ca^{2+} entry (SOCE) in the two cell lines. In conclusion, our results suggest that by modulating SOCE, autocrine GABA signaling uniquely regulates the activity of different T_H subtypes.

Keywords

GABA, $GABA_A$ R, GAD, T_H cells, Jurkat, CCRF-CEM, MTT, CRTh2, NFAT, Thapsigargin, SOCE, Bicuculline

Co-Authorship Statement

All experiments and analyses were performed by Amy Lin (unless stated otherwise). Flow cytometry assays were performed with assistance from Meerah Vijeyakumaran (MSc candidate, Cameron Lab, Department of Pathology and Toxicology, Western University) and qPCR assays were performed by Tharsan Kanagalingam (MSc candidate, Cameron Lab, Department of Pathology and Toxicology, Western University). This thesis was reviewed by Dr. Wei-Yang Lu and Dr. Lisa Cameron.

Acknowledgements

This project would not have been possible without the help of several individuals. First and foremost, I would like to thank my supervisor Dr. Wei-Yang Lu for his patience, encouragement and guidance throughout my time in the lab. I was extremely lucky to have a supervisor who always had his office door open and was willing to put a hold on his own tasks to answer a question or discuss a problem with me. His positivity and passion for research made my graduate school experience one that I will never forget.

Next, I would like to thank the past and present members of our lab: Yun-Yan Xiang (Yanna), Matthew Maksoud, Vasiliki Tellios, Jacob Poirier, Dong An, Yimo Wang, and Alison Bell. Not only did we have many insightful discussions about our research, but we also shared plenty of laughter and meaningful conversations outside of the lab. In particular, I would like to thank Yanna for teaching me how to perform all the experiments. Her organizational skills and professionalism are traits that I aspire to have.

I would like to thank our collaborator Dr. Lisa Cameron as well as her lab members Meerah Vijeyakumaran and Tharsan Kanagalingam for their contributions towards this project. Dr. Cameron offered much-needed expertise on T cell immunology and greatly contributed to the development of this project. Meerah assisted me with the flow cytometry experiments and Tharsan performed qPCR assays that helped rationalize the cell lines we used. I would also like to extend my gratitude to the rest of my advisory committee, Dr. Ruud Velhuizen and Dr. Stan Leung, for their guidance and helpful suggestions.

Last but not least, thank you to my family (Mom, Dad, Alan) for always supporting me in whatever I chose to do and for bringing me home-cooked food when I needed it the most. I hope to always make you all proud.

Table of Contents

Abstract.....	ii
Co-Authorship Statement.....	iii
Acknowledgements.....	iv
Table of Contents.....	v
List of Figures.....	ix
List of Abbreviations	xi
Chapter 1: Introduction	1
1.1 Overview.....	1
1.2 Immune System	2
1.2.1 Innate Immunity.....	2
1.2.2 Adaptive Immunity	3
1.2.3 Antigen Presentation Process.....	6
1.2.4 G-Protein Coupled Receptors	7
1.2.5 CRTh2 Receptor	7
1.3 Store Operated Calcium Entry (SOCE).....	8
1.3.1 TCR Signaling Cascade.....	8
1.3.2 CRAC Channels.....	9
1.3.3 SOCE Regulation.....	10
1.3.4 Thapsigargin-induced SOCE	10
1.4 T cell Development.....	12
1.4.1 T _H Cell Differentiation.....	15

1.4.2 T _H Cell Regulation of Macrophage Polarization	17
1.4.3 Unique CD4 ⁺ Cell Lines	19
1.5 Gamma-Aminobutyric Acid	22
1.5.1 GABA _A R Structure	23
1.5.2 Chloride Transporters	25
1.5.3 GABA Signaling Outside of the CNS	26
1.5.4 GABA in the Immune System	26
1.5.5 GABA in Autoimmune Diseases	28
1.6 Rationale	29
1.7 General Hypothesis	31
1.8 Objectives	31
Chapter 2: Materials and Methods	32
2.1 Cell Cultures	32
2.2 Cell Proliferation	32
2.3 MTT Assay	33
2.4 Immunocytochemistry	34
2.5 Cell Size Analysis	36
2.6 Mitogenic Stimulation of Cells	36
2.7 Western Blot	37
2.8 Calcium-Dependent Fluorescence Imaging	40
2.9 Flow Cytometry	42
2.10 Statistical Analyses	42
Chapter 3: Results.....	43

3.1 Characterization of Jurkat and CCRF-CEM Lines	43
3.1.1 CCRF-CEM cells proliferate faster than Jurkat cells	43
3.1.2 Jurkat cells are larger than CCRF-CEM cells.....	45
3.1.3 Both cell lines express CRAC channel components.....	48
3.1.4 Larger SOCE magnitude observed in Jurkat cells in response to thapsigargin	50
3.2 Expression of GABA Signaling Proteins.....	53
3.2.1 Glutamic acid decarboxylase is expressed in both cell lines	53
3.2.2 Various GABA _A R subunits are expressed in both cell lines	55
3.3 Effects of GABA _A R Signaling and Blockade on Functions of Jurkat and CCRF-CEM Lines.....	58
3.3.1 GABA _A R blockade enhances cell metabolic activity in Jurkat cells.....	58
3.3.2 GABA _A R blockade enhances CRTh2 surface expression in CCRF-CEM cells ...	60
3.3.3 GABA _A R blockade increases nuclear NFATc2 expression in Jurkat cells	62
3.3.4 GABA _A R blockade differentially regulates SOCE in the two cell lines	65
3.3.5 GABA _A R subunit expression changes following mitogenic stimulation	68
Chapter 4: Discussion	71
4.1 Summary of results	71
4.2 Unique features of Jurkat and CCRF-CEM cells.....	71
4.2.1 Cell size, proliferation and metabolism	72
4.2.2 CRAC channels and SOCE.....	73
4.2.3 Active form of NFAT	75
4.2.4 Autocrine GABA signaling system	76
4.3 GABA signaling in Jurkat and CCRF-CEM Cells	77

4.3.1 Role of GABA signaling on cell metabolism and receptor protein expression.....	77
4.3.2 Effects of GABA signaling on SOCE and NFAT expression	78
4.3.3 Potential mechanisms by which autocrine GABA signaling regulates SOCE	79
4.3.4 KCC and NKCC	82
4.4 GABA _A R plasticity during T _H cell activation.....	83
4.5 Roles of GABA signaling in T _H 1 and T _H 2 diseases	83
4.6 Limitations and future studies.....	85
4.7 Conclusions and significance.....	86
Chapter 5: References	88
Appendices.....	103
Curriculum Vitae	110

List of Figures

Figure 1.1 Components of the innate and adaptive immune systems.....	5
Figure 1.2 Store-operated calcium entry in T lymphocytes.....	11
Figure 1.3 T cell development in the thymus	14
Figure 1.4 Differentiation of naïve T _H cells into various effector subtypes.	18
Figure 1.5 Comparison of mRNA levels of T _H 1 and T _H 2 markers in Jurkat and CCRF-CEM cells.	21
Figure 1.6 Illustration of a GABA _A R formed from two α , two β , and one γ subunit.	24
Figure 1.7 Proposed mechanism of GABA _A R signaling in T lymphocytes.	30
Figure 3.1 Proliferation of Jurkat and CCRF-CEM cells under culture conditions.....	44
Figure 3.2 Analysis of average cell size of Jurkat and CCRF-CEM cells.....	47
Figure 3.3 Protein expression of STIM1 and Orai1 in Jurkat and CCRF-CEM cells.	49
Figure 3.4 Thapsigargin-induced Ca ²⁺ influx in Jurkat and CCRF-CEM cells.	52
Figure 3.5 Protein expression and localization of glutamic acid decarboxylase (GAD) in Jurkat and CCRF-CEM cells.	54
Figure 3.6 Protein expression of GABA _A R- α 1, β 1, and β 3 subunits in cell lines.	57
Figure 3.7 Effects of GABA and bicuculline on cell metabolic activity.....	59
Figure 3.8 Flow cytometric analysis of surface CRTh2 receptor expression.	61
Figure 3.9 Protein expression of nuclear NFATc2 in Jurkat and CCRF-CEM cells.....	64
Figure 3.10 Effects of GABA and bicuculline pre-treatment on TG-induced Ca ²⁺ entry.	67

Figure 3.11 Effect of PHA/PMA stimulation on GABA_AR-β3 expression in the cell lines. . 69

Figure 3.12 Effect of PHA/PMA stimulation on GABA_AR-β1 expression in the cell lines. . 70

Figure 4.1 Proposed mechanism of how GABA_AR signaling differentially acts on Jurkat and CCRF-CEM cells. 81

Figure 6.1 Protein expression and localization of STIM1 and CD3 in Jurkat cells co-cultured with RAW 264.7 cells and isolated primary mixed splenocytes. 103

Figure 6.2 Protein expression and localization of NKCC1 in Jurkat and CCRF-CEM cells. 104

List of Abbreviations

APC	Antigen-presenting cell
CD4	Cluster of differentiation 4
CRAC	Calcium release-activated calcium
CRTh2	Chemoattractant receptor homologous to the T helper 2 Cell
DAG	Diacylglycerol
DN	Double negative
DP	Double positive
ER	Endoplasmic reticulum
GABA	Gamma-aminobutyric acid
GABA_AR	A-type gamma-aminobutyric acid receptor
GABA_BR	B-type gamma-aminobutyric acid receptor
GABA-T	Gamma-aminobutyric acid transaminase
GAD	Glutamic acid decarboxylase
GAT	Gamma-aminobutyric acid transporter

GPCR	G-protein coupled receptor
KCC	Potassium-chloride cotransporter
IFN-γ	Interferon gamma
IL	Interleukin
IP₃	Inositol trisphosphate
NFAT	Nuclear factor of activated T cells
NF-κB	Nuclear factor kappa-light-chain-enhancer of activated B cells
NKCC	Sodium-potassium-chloride cotransporter
MHC	Major histocompatibility complex
PAMP	Pathogen-associated molecular patterns
PGD₂	Prostaglandin D ₂
PHA	Phytohemagglutinin
PIP₂	Phosphatidylinositol 4,5-bisphosphate
PKC	Protein kinase C
PLC	Phospholipase C
PMA	Phorbol-12-myristate-13-acetate

PRR	Pattern recognition receptor
SERCA	Sarco/endoplasmic reticulum calcium-ATPase
SOCE	Store operated calcium entry
STIM1	Stromal interaction molecule 1
T1D	Type 1 Diabetes
T-bet	T-box transcription factor
TCR	T cell receptor
TGF-β	Transforming growth factor-beta
T_H	T helper
TNF-α	Tumor necrosis factor-alpha
V_m	Membrane potential

Chapter 1: Introduction

1.1 Overview

CD4⁺ T lymphocytes, also known as T helper (T_H) cells, play critical roles in the adaptive immune system. They assist B lymphocytes (B cells) in the generation of antibodies, regulate macrophage function, and produce cytokines to coordinate immune responses against foreign microorganisms¹. The differentiation of naïve T_H cells into effector subtypes including T_H1, T_H2 and T_H17 cells is necessary for the generation of specific adaptive immune responses. Dysregulation of this process could pave the way to a spectrum of autoimmune and inflammatory disorders. For example, it has long been thought that an imbalance between T_H1 and T_H2 cytokines contributes to the pathophysiology of asthma^{2,3}. The differentiation of T_H cells is initiated during antigen presentation and critically modulated by micro-environmental cues⁴, which include soluble factors released through paracrine and autocrine systems⁵⁻⁷. The exact mechanisms by which these factors regulate T_H cell differentiation and the functions of specific T_H cell subtypes is not well understood.

An increasing pool of evidence indicates that gamma-aminobutyric acid (GABA), the main inhibitory neurotransmitter in the central nervous system (CNS), also functions as a signaling molecule in cells outside of the CNS⁸. GABA signaling proteins, including the GABA-synthesis enzyme glutamic acid decarboxylase (GAD) and A-type GABA receptors (GABA_ARs), are present in T cells and macrophages⁹, implying that these immune cells are endowed with an autocrine GABA_AR signaling system. Indeed, GABA has been shown to play inhibitory roles in autoimmune and inflammatory diseases, which are largely T_H1 cell-mediated responses¹⁰. Recent studies in our lab have demonstrated that activation of GABA_ARs in macrophages restrains M1 polarization while enhancing M2 polarization.

Considering the analogous relationship between the T_H1/T_H2 and M1/M2 systems, we proposed that GABA_AR signaling may also differentially modulate different T_H cell subtypes. This thesis project sought to investigate if, and how, autocrine GABA signaling affects the activities and functions of two unique human T_H cell lines: Jurkat and CCRF-CEM.

1.2 Immune System

The human immune system is a complex host defense network consisting of multiple layers of cellular and molecular components (illustrated in **Figure 1.1**). It plays a critical role in protecting the body against infections and diseases caused by foreign microorganisms, toxins and viruses. The immune system is generally classified into two main branches known as innate and adaptive immunity, which are distinguished by their speed of response, specificity against pathogens, and ability to generate immunological memory¹¹. Despite these differences, the innate and adaptive immune systems work in a synergistic manner to coordinate a broad range of effects. Improper functioning of these systems can lead to immunological pathologies such as autoimmunity, inflammatory diseases, and cancer¹².

1.2.1 Innate Immunity

The innate immune system serves as the first line of defense by carrying out pro-inflammatory responses within seconds or minutes of an antigen's presence in the body¹³. Its primary function is to recruit immune cells to the source of infection through the production of chemical messengers such as cytokines¹⁴. Other key functions include the clearance of dead cells and activation of the adaptive immune response through antigen presentation¹³. Innate immune cells recognize microbial pathogens through pattern-recognition receptors (PRRs) that detect conserved pathogen-associated molecular patterns (PAMPs)¹⁵. Examples of PAMPs

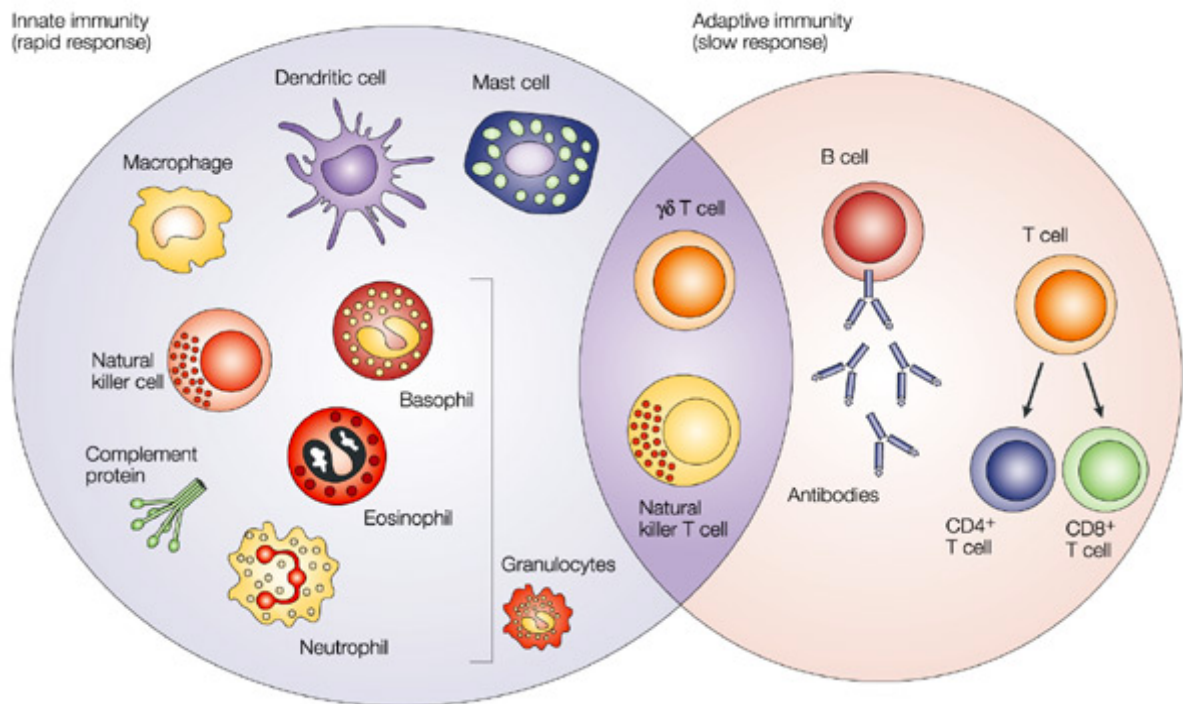
include components of microbial membranes, cell walls and DNA¹³. Important cellular components of the innate immune system include tissue-specific macrophages, neutrophils, natural killer cells, mast cells, and dendritic cells. Cells of the innate immune system, however, cannot eliminate all infectious agents or recognize certain pathogens¹⁶. Thus, the adaptive immune system has evolved to provide the body additional protection.

1.2.2 Adaptive Immunity

Adaptive immunity evolved much later than innate immunity and is only found in cartilaginous fish and higher vertebrates¹⁷. In contrast to the innate immune system, the adaptive immune system involves a more complicated process taking days to carry out antigen-specific responses. The main functions of the adaptive immune system include the recognition of specific “non-self” antigens in the presence of “self” antigens, the generation of effector pathways that eliminate specific pathogens or infected cells, and the development of immunological memory that can help eliminate a pathogen more efficiently during future encounters^{18,19}. The ability of this system to generate long-term immunological memory is the basis of vaccination²⁰. Cellular components of the adaptive immune system include naïve B cells and T cells that may be differentiated to generate a wide range of adaptive immune responses.

The adaptive immune system carries out two types of responses: humoral immunity, involving antibodies produced by B cells, and cell-mediated immunity, carried out by T cells. T cells and B cells originate from the bone marrow but undergo different developmental routes. T cells, which are the focus of this thesis, mature in the thymus and recognize specific peptides displayed by antigen-presenting cells (APCs). Cell-mediated immunity involves two main types of T cells: T_H cells and cytotoxic T cells, which are distinguished by the expression of

cell surface glycoproteins CD4 and CD8, respectively. The main role of T_H cells is to generate chemical signals such as cytokines to direct other T cells, phagocytes and B cells during an immune response¹⁸. Cytotoxic T cells, on the other hand, directly kill cells infected by viruses and pathogens. The components of the adaptive immune system generate a more potent and specialized response against specific microbial pathogens in comparison to the responses carried out by the innate immune system. However, it must be emphasized that the adaptive immune system cannot function without communication and activation from the innate immune system. This is done through the formation of immunological synapses between APCs of the innate immune system and T cells of the adaptive immune system²¹.



Nature Reviews | Cancer

Figure 1.1 Components of the innate and adaptive immune systems.

Reprinted from “Cytokines in cancer pathogenesis and cancer therapy,” by G Dranoff, 2004. *Nat Rev Cancer*. **4**: 11-22. Copyright (2004) by Nature Publishing Group. Reprinted with permission.

1.2.3 Antigen Presentation Process

Similar to how neurons communicate with each other at neuronal synapses, innate immune cells can transmit signals to T cells at what are called immunological synapses^{19,22}. Here, resting T cells are activated by APCs displaying a major histocompatibility complex (MHC). An MHC complex contains specialized molecules capable of presenting peptide fragments to T cells at the T cell receptor (TCR). There are two major classes of MHCs, each targeting a different type of T cell. The first kind are MHC class I molecules, which are found ubiquitously in all healthy cells in the body and display peptide antigens within the cytoplasm of cells. MHC I molecules report intracellular events such as viral infections and cellular transformation to cytotoxic T cells²³. In contrast, MHC class II molecules are restricted to “professional” APCs such as macrophages, dendritic cells, and B cells. These molecules display antigens from endocytic vesicles in cells; therefore, exogenous antigens are presented to T cells on MHC II complexes. MHC II molecules target T_H cells^{22,23}. Effective activation of T_H cells also requires a secondary signal from APCs to ligate CD28, which is a co-receptor to the TCR²⁴. If proper co-stimulation is absent, T_H cells go into a state of anergy where they cannot respond to re-stimulation. Dendritic cells are the most important type of APCs due to the expression of co-stimulatory molecules such as the B7 family of proteins, which are crucial for proper T cell co-stimulation^{25,26}.

When foreign pathogens are detected by APCs, they are ingested and degraded before assembly and presentation on the cell surface as an MHC II. Only part of the foreign microbe, such as the bacterial cell wall, is presented to T cells. Once TCRs are activated by MHC II complexes, a signaling cascade resulting in Ca²⁺ influx is initiated¹⁶. While T cells require activation from APCs, T cells can also regulate APC function through the release of specific

cytokines. For example, macrophage polarization is regulated by cytokines released by effector T_H cells. This reflects the complementary relationship between innate and adaptive immunity.

1.2.4 G-Protein Coupled Receptors

In addition to activation mediated by antigenic TCR stimulation, T cells are also under the influence of soluble factors in the microenvironment, which usually act upon G-protein coupled receptors (GPCRs) spanning across the T cell membrane. T cells express various types of GPCRs such as chemokine and muscarinic receptors^{28,29}. While the roles of T cell muscarinic receptors are still being investigated, chemokine receptors are well characterized and are known to play important roles in T cell homeostasis²⁸. Chemokines are soluble proteins that regulate T cell migration and activation through GPCR-binding; these molecules are differentially expressed in various T_H cell subsets³⁰. Binding of ligands to GPCRs activates the G-protein α -subunit, which goes on to activate phospholipase C and induce Ca^{2+} entry (explained in subsequent sections).

1.2.5 CRTh2 Receptor

Chemokine receptor homologous molecule expressed on T helper type 2 cells (CRTh2) is a unique type of GPCR expressed in T_H2 cells. It is activated by prostaglandin D2 (PGD2), an arachidonic acid metabolite known to be released by activated mast cells and dendritic cells^{31,32}. Activation of CRTh2 has been shown to exacerbate asthmatic symptoms through recruitment of eosinophils and T_H2 cells, as well as the induction of T_H2 cytokine synthesis^{33,34}. A selective CRTh2 agonist enhanced asthmatic symptoms in a mouse model of the disease³⁵. CRTh2 has also been suggested to be the most reliable marker of circulating T_H2 cells³⁶.

Taken together, there is strong evidence that this receptor plays a critical role in regulating and maintaining T_H2 cell functions.

1.3 Store Operated Calcium Entry (SOCE)

Calcium ions (Ca²⁺) are an important secondary messenger in all eukaryotic cells. In T cells, store-operated Ca²⁺ entry (SOCE) is the main signaling mechanism to increase intracellular Ca²⁺ concentrations³⁷. This type of Ca²⁺ signaling is dependent on the active refilling of intraluminal Ca²⁺ in the endoplasmic reticulum (ER) by sarco-endoplasmic reticulum Ca²⁺-ATPases (SERCAs)³⁸. Once the ER Ca²⁺ stores are released, large amounts of extracellular Ca²⁺ enter the cell to activate gene transcription. The elevation of intracellular Ca²⁺ levels is crucial for triggering T cell activation by antigens and other stimuli such as mitogens that cross-link the T cell receptor (TCR)^{39,40}.

1.3.1 TCR Signaling Cascade

When TCRs are stimulated, a signaling cascade is initiated and eventually results in the activation of Ca²⁺ release-activated Ca²⁺ (CRAC) channels (summarized in **Figure 1.2**). First, the TCR activates phospholipase C (PLC), which hydrolyzes phosphatidylinositol 4,5-bisphosphate (PIP₂) into secondary messengers diacylglycerol (DAG) and 1,4,5-inositol trisphosphate (IP₃). IP₃ opens Ca²⁺ channels on the endoplasmic reticulum (ER) to release Ca²⁺ into the cell cytosol, resulting in a drop in ER Ca²⁺ concentrations. This facilitates the rapid influx of extracellular Ca²⁺ through CRAC channels⁴¹. Ca²⁺ entering the cytosol binds to the regulatory protein calmodulin, which activates the phosphatase calcineurin. Calcineurin dephosphorylates nuclear factor of activated T cells (NFAT) in the cytosol, which can then translocate to the nucleus in its active, dephosphorylated form to modulate gene transcription¹⁸.

In a parallel pathway, DAG, the other product of PIP₂ hydrolysis, activates protein kinase C (PKC), which activates the transcription factor nuclear factor κ B (NF- κ B), another critical transcription factor in T cell activation⁴². The coordinated actions of various transcription factors induce the expression of numerous genes important for the function of activated T cells. The long-term functions of Ca²⁺ signaling also include cell proliferation, effector functions such as the production of cytokines and chemokines, and the differentiation of naïve T cells into various effector or memory T cells⁴³. The amplitude, duration, and kinetics of SOCE influence the specificity of gene activation events that help instruct T cells on which differentiation pathway to take⁴⁴.

1.3.2 CRAC Channels

CRAC channels are located on the T cell plasma membrane and are distinguished by an extremely high selectivity for Ca²⁺ ions⁴⁵. The exact composition and activation mechanism of this channel were unknown until the discovery of its two protein components: Ca²⁺ sensor protein stromal interaction molecule 1 (STIM1) and channel pore protein Orai1⁴⁶⁻⁴⁹. STIM1 proteins are located on the ER membrane and are usually present as monomers containing Ca²⁺ ions in their Ca²⁺-binding sites near the protein's N-terminal. Following a drop-in ER Ca²⁺ stores, Ca²⁺ falls off the protein and STIM1 monomers begin to form oligomers^{50,51}. Interaction between STIM1 oligomers and a cytosolic domain in Orai1 activates the CRAC channel, allowing large amounts of extracellular Ca²⁺ into the T cell cytosol⁵².

It has been demonstrated that STIM1 proteins are crucial for CRAC channel function and adaptive immunity; knockdown of STIM1 in mammalian cells and *Drosophila* S2 cells results in suppressed CRAC channel conductance^{46,47}. Homozygous nonsense mutations in the STIM1 gene produce symptoms of severe immunodeficiency, autoimmune disease, and

myopathy in human patients⁵³. These symptoms are similar to those observed in patients with Orai1 mutations, highlighting the critical role of CRAC channels and SOCE in immune function and host defense^{54,55}.

1.3.3 SOCE Regulation

The magnitude and rate of Ca^{2+} entry through CRAC channels is dependent on endogenous regulators of CRAC channels as well as the membrane potential of cells⁴⁴. For example, several types of potassium (K^+) channels can modulate the rate of Ca^{2+} entry by hyperpolarizing the membrane, which increases the driving force for Ca^{2+} entry^{56,57}. Studies have demonstrated that K^+ -channel blockers could potentially be immunosuppressant^{58,59}. Therefore, modulators of T cell membrane potential could have significant effects on T cell functions through their influence on SOCE. This concept is important in understanding the results of this project.

1.3.4 Thapsigargin-induced SOCE

As mentioned previously, SOCE is a process mediated by active sequestration of intracellular Ca^{2+} in endoplasmic reticulum stores by SERCAs³⁸. Exogenous compounds that inhibit SERCAs are useful in the study of Ca^{2+} signaling mechanisms. Among these, thapsigargin is the most widely used SERCA inhibitor due to its high potency and specificity. This guaianolide compound is isolated from the Mediterranean plant *Thapsia garganica* L. It works by counterbalancing the passive Ca^{2+} leak from ER stores in the cytosol. During *in vitro* settings such as Ca^{2+} imaging and electrophysiology studies, thapsigargin can be applied to induce an immediate but transient increase in cytosolic Ca^{2+} levels at concentrations in the micromolar range⁶⁰.

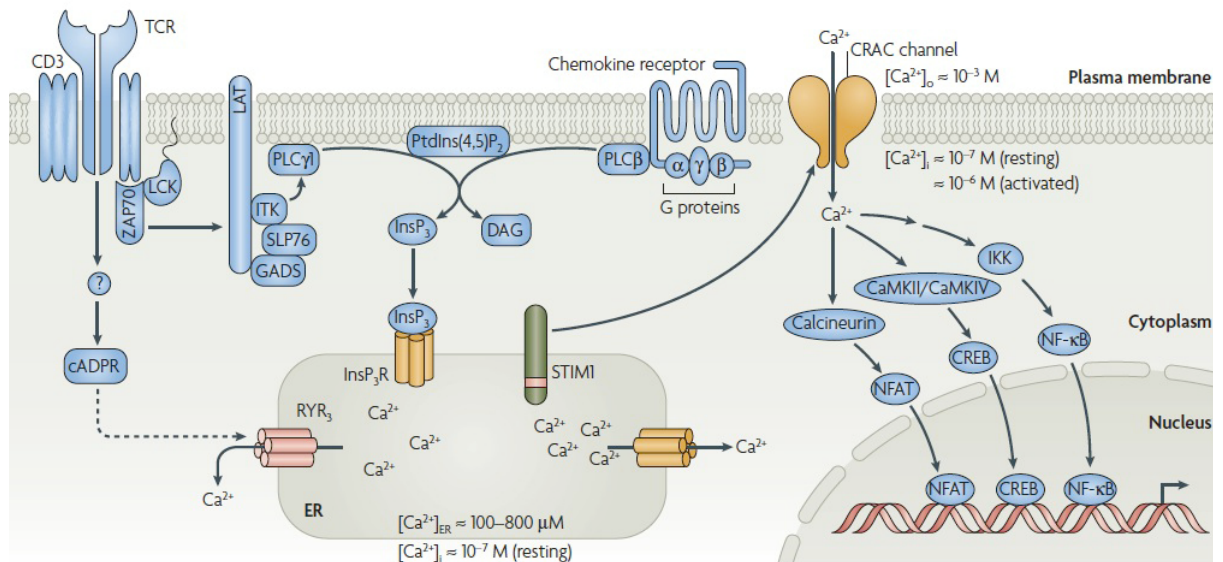


Figure 1.2 Store-operated Calcium entry in T lymphocytes.

Reprinted from “Calcium signaling in lymphocyte activation and disease,” by S Feske. 2007. *Nat Rev Immunol.* **7**: 690-702. Copyright (2007) by Nature Publishing Group. Reprinted with permission.

1.4 T cell Development

T cell development is an intricate process occurring in the thymus; it involves the maturation of lymphoid progenitor cells into mature CD4⁺ or CD8⁺ T cells that are then released from the thymus to peripheral tissues⁶¹. Lymphoid progenitor cells originate from haematopoietic stem cells in the bone marrow and enter the thymus through the circulation⁶². Once they populate the thymus, progenitor cells lose the potential for B cell and natural killer cell development and become committed to the T cell lineage^{63,64}. These cells then expand by cell division to generate a large population of immature thymocytes⁶⁵⁻⁶⁷. Thymocytes undergo a series of developmental checkpoints to become mature T cells; this includes TCR β -chain rearrangement followed by positive and negative selection^{68,69}. These processes occur in different areas of the thymus that have different microenvironments to support T cell development. About 98% of thymocytes die during the development process in the thymus by failing positive selection or negative selection⁷⁰. This is to ensure that T cells function properly in the peripheries. The thymus contributes fewer cells as a person ages, and eventually becomes useless in older individuals where tissue expansion of immature T cells is the main source of T cell generation⁷¹.

In general, the goal of T cell development is to produce T cells that have functional $\alpha\beta$ -TCRs and can bind to self-antigens with a moderate affinity. Early progenitor cells lack the expression of CD4 and CD8 and are termed double negative (DN) cells. DN thymocytes are subdivided into four stages of differentiation identified by the expression of cell surface markers CD44 and CD25⁷². DN1 cells (CD44⁺ CD25⁻) can give rise to several types of cells including T cells, NK cells, dendritic cells, macrophages, and B cells. After specification to the T cell lineage, DN2 cells (CD44⁺ CD25⁺) begin TCR gene arrangements. DN3 cells (CD44⁻ CD25⁺) have fully rearranged their TCR β -chain and associate with an invariant pre-TCR

α -chain and CD3 signaling molecules to form the pre-TCR complex⁷³. DN4 cells (CD44⁺ CD25⁻) upregulate expression of CD4 and CD8 to produce double-positive cells. The progression through these stages is called the β -selection checkpoint. This process is crucial in the generation of unique TCR sequences through gene rearrangement^{74,75}. Following β -selection, double positive (DP) cells undergo positive and negative selection^{76,77}.

During positive selection, DP thymocytes are presented with self-antigens expressed by thymic cortical epithelial cells on MHC I or MHC II molecules. Only thymocytes that interact with MHC I or MHC II at moderate affinities will survive. This is to ensure that selected T cells will have an MHC affinity that can serve useful functions in the body⁷⁸. Moreover, a thymocyte's fate is determined by positive selection; DP cells that interact well with MHC II molecules will eventually become CD4⁺ cells whereas those that interact with MHC I molecules will become CD8⁺ cells⁷⁹. Following positive selection, T cells undergo negative selection where they bind to macrophages or dendritic cells expressing Class I or Class II MHC containing "self" peptides. The goal of negative selection is the removal of thymocytes that strongly bind with "self" MHC peptides. This prevents the formation of self-reactive T cells capable of causing autoimmune diseases⁸⁰. After surviving positive and negative selection, mature, singly positive T cells exit the thymus into peripheral systems where they can be activated and further differentiated by APCs. The T cell developmental process is summarized in **Figure 1.3** –the locations of each developmental point in the thymus are illustrated.

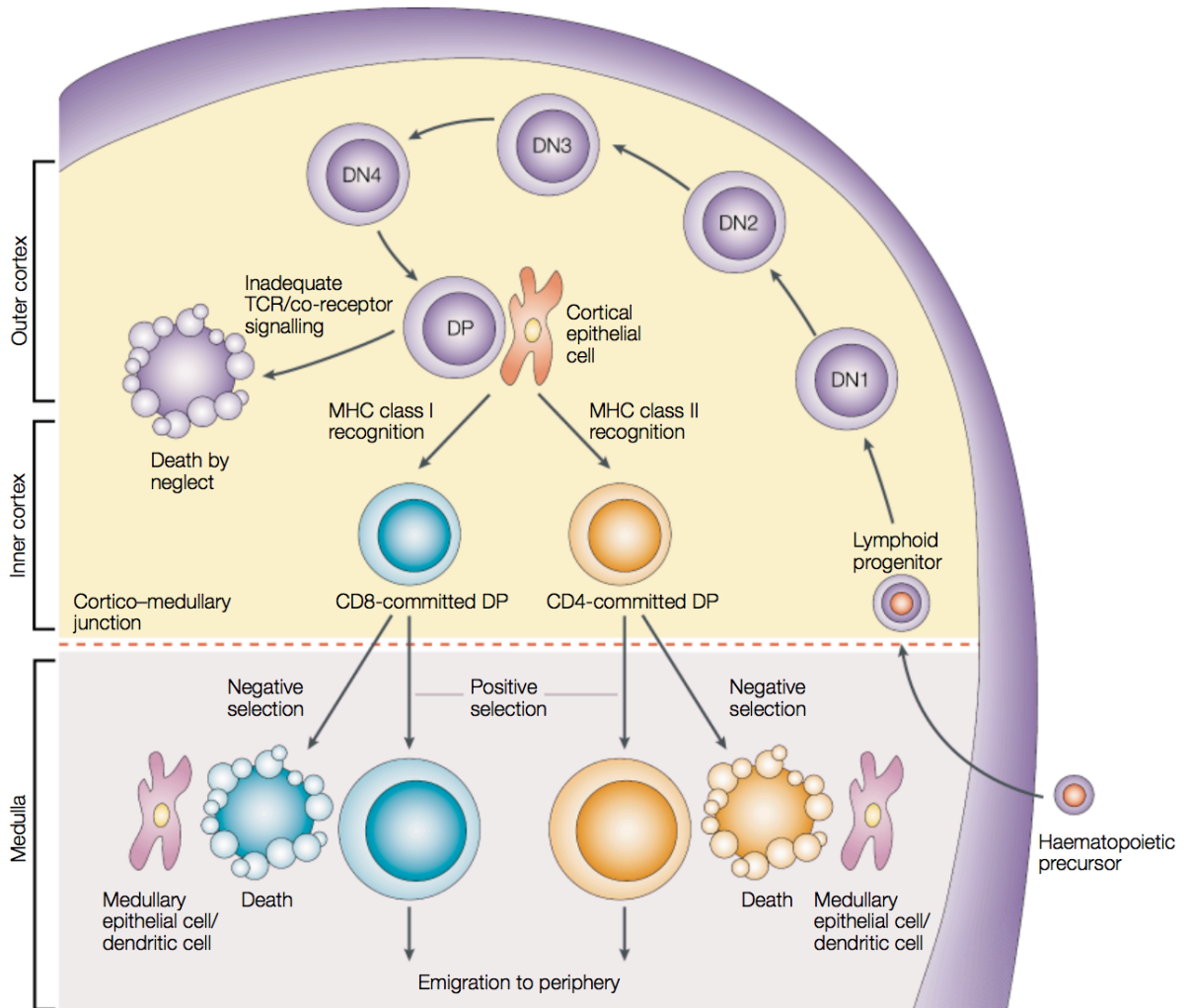


Figure 1.3 T cell development in the thymus.

Reprinted from “T-cell development and the CD4-CD8 lineage decision,” by RN Germain. 2002. *Nat Rev Immunol.* **2**: 309-322. Copyright (2007) by Nature Publishing Group. Reprinted with permission.

1.4.1 T_H Cell Differentiation

During TCR activation in the presence of certain soluble factors in the immediate environment, naïve CD4⁺ T cells may differentiate into one of several lineages of T_H cells, including T_H1, T_H2, T_H17, and T_{reg}, as defined by their pattern of cytokine production and function⁸¹ (**Figure 1.4**). The exact factors and mechanism behind their differentiation *in vivo* is still not well understood. However, previous literature have suggested that both the nature of the presented antigen and the surrounding cytokine profile influence the differentiation of naïve CD4⁺ T cells into specific subtypes^{1,82}. The initial steps of naïve CD4⁺ T cell differentiation involve stimulation of the TCR and CD4 co-receptor with MHC II complexes from APCs. The specific stimulatory conditions influence transcription factor expression, which determines the differentiation route that the CD4⁺ T cell will follow.

The first two subtypes of T_H cells were long recognized as the T_H1 and T_H2 cells. T_H1 and T_H2 development routes appear to be antagonistic, thus giving rise to a dichotomy paradigm in T_H cell differentiation⁸³. However, several recent studies have shown more complex patterns of cytokine interaction and the discovery of T_H17 cells further suggests that T_H differentiation is not a simple dichotomy but rather, a spectrum^{1,81}. During *in vitro* settings, various cytokines can induce naïve T_H cells to differentiate into a certain lineage⁸⁴.

T_H1 cells function to eliminate intracellular pathogens and play a role in organ-specific autoimmunity and inflammation⁸⁵. They produce IFN- γ as their signature cytokine and produce IL-2 and TNF- α as well. IFN- γ is important for the activation of macrophages and microglial cells, both mediators of phagocytic activity⁸⁶. IL-2 promotes proliferation of CD8⁺ cytotoxic T cells and is also a growth factor for T_H cells⁸⁷. The master regulator for differentiation of the T_H1 cells is the T-box transcription factor (T-bet). Not only can it activate sets of genes to promote T_H1 differentiation, it can also suppress the development of opposing

cell lineages^{88,89}. Naïve T_H cells could be induced to differentiate into T_H1 cells by the addition of IL-12 and IFN- γ *in vitro*⁹⁰.

T_H2 cells mediate immune responses to extracellular parasites and play a major role in the pathophysiology of allergic disease^{85,91}. They produce IL-4, IL-5, and IL-13 as their signature cytokines. IL-4 is involved in antibody secretion by B cells and is important in allergic inflammation⁹². IL-13 activates eosinophils, enhances mucus secretion and airway hyperresponsivity in allergic asthma⁹³. IL-5 is also involved in the activation of eosinophils⁹⁴. The master regulator involved in the differentiation of T_H2 cells is GATA-binding protein (GATA3)⁹⁵. GATA3 enhances T_H2 cytokine production, T_H2 cell proliferation, and inhibits T_H1 differentiation through its interactions with T-bet⁹⁶. Naïve T_H cells could be induced to differentiate into T_H2 cells through the addition of IL-4 and IL-2 into the culture medium *in vitro*.

The classic T_H1/T_H2 model of CD4⁺ T_H cell has been significantly modified in recent years with the addition of other types of CD4⁺ subsets. Among these is the T_H17 subset that was established as a true distinct CD4⁺ lineage in 2005⁹⁷. T_H17 cells produce the cytokines IL-17A, IL-17F and IL-22, and are thought to play a role in autoimmunity and inflammation. Naïve T_H cells could be induced to differentiate into T_H17 cells by the addition of TGF- β and IL-6 *in vitro*⁹⁸. Another important T_H subset are the T_{reg} cells, which play a role in immune tolerance and regulation of other T_H subsets. They produce IL-10, IL-35, and TGF- β . Naïve T_H cells can be induced to differentiate into T_{reg} by the addition of TGF- β and IL-2 *in vitro*⁹⁹.

Given the time restrictions on this project, we chose to focus on the T_H1 and T_H2 cell phenotypes. We acknowledge that T_H differentiation involves many different subtypes and that by only focusing on T_H1 and T_H2, we may be oversimplifying T_H cell physiology. However, considering that they are the two most well-established subtypes with clearly defined

characteristics and roles in immune pathologies, this was a good place to start our investigation. Moreover, the purpose of this project was to investigate GABA signaling in two *unique* types of T_H cell types. Future studies should involve the exploration of other phenotypes of T_H cells.

1.4.2 T_H Cell Regulation of Macrophage Polarization

Although macrophages can direct T_H cell differentiation through antigen presentation, cytokines released from effector T_H cells can also drive macrophage polarization towards pro-inflammatory (M1) and anti-inflammatory (M2) phenotypes¹⁰⁰. M1 macrophages differentiate under the influence of T_{H1} cytokine IFN- γ and bacterial lipopolysaccharide (LPS)¹⁰¹. These macrophages are characterized by high microbicidal activity and the secretion of pro-inflammatory cytokines, reactive oxygen species (ROS), and iNOS. Conversely, M2 macrophages are differentiated under the influence of T_{H2} cytokines IL-4 and IL-13. This phenotype is characterized by the selective expression of arginase-1 and mediate anti-inflammatory responses^{102,103}. The M1/M2 nomenclature was derived as an extension of the T_{H1}/T_{H2} system, reflecting their analogous relationship. It is important to note that macrophage polarization is a very complex process and may not be a clear-cut dichotomy. Macrophages can polarize into a continuum of pro-inflammatory and anti-inflammatory phenotypes.

Previous studies in our lab found that the expression levels of autocrine GABA signaling proteins in macrophages are downregulated during M1 polarization and upregulated during M2 polarization. Moreover, activation of GABA_AR signaling in macrophages restrained M1 activation but enhanced M2 responses. Considering the specific roles of T_{H1} and T_{H2} cells in the regulation of M1 and M2 polarization, it is possible that GABA also plays different roles in T_{H1} and T_{H2} cells.

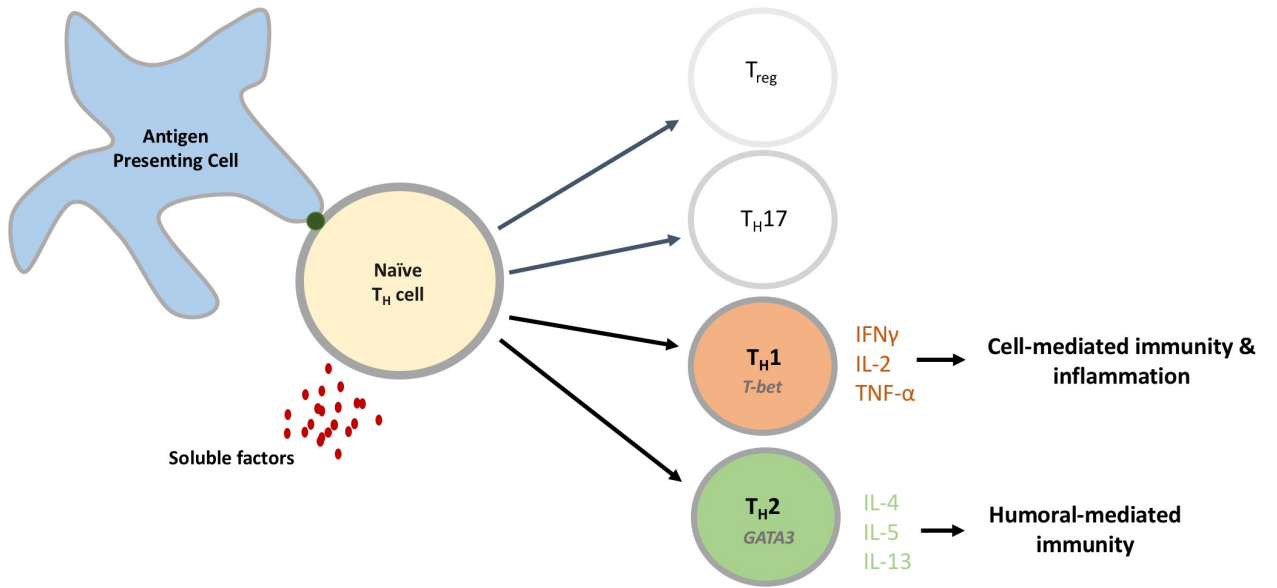


Figure 1.4 Differentiation of naïve T_H cells into various effector subtypes.

1.4.3 Unique CD4⁺ Cell Lines

Many studies on T cell signaling mechanisms to date have been conducted using transformed T cell lines. Among them, the best-known and most widely-used T cell model is the Jurkat line, which was derived from human leukemic T cells¹⁰⁴. Jurkat cells were first established in 1977 from the peripheral blood of a 14-year-old boy and were crucial in the discovery of the TCR activation pathway¹⁰⁵. These cells express $\alpha\beta$ -TCRs and the CD4 glycoprotein, a marker of T_H cells. Upon stimulation with lectins or monoclonal antibodies against the TCR, intracellular Ca²⁺ levels are increased and high levels of IL-2 are produced¹⁰⁶. Maximal production of IL-2 requires two synergistic signals: one from TCR activation and the other by a phorbol ester such as phorbol myristate acetate (PMA)¹⁰⁷.

Another unique T cell line is CCRF-CEM, which was established in 1964 from the peripheral blood buffy coat of a 4-year-old girl¹⁰⁸. These cells are not as well studied or characterized as the Jurkat cells. However, they also express $\alpha\beta$ -TCRs and CD4 exclusively. Preliminary results from our collaborator Dr. Lisa Cameron's lab in Department of Pathology and Laboratory Medicine suggest that Jurkat and CCRF-CEM cells contain phenotypic traits of T_{H1} and T_{H2} cells, respectively. When compared to each other, Jurkat cells contain approximately double the amount of mRNA for IFN- γ , a classic T_{H1} cytokine, while CCRF-CEM cells contain approximately five times the mRNA levels for IL-13, a classic T_{H2} cytokine. In addition, CCRF-CEM cells contain about six times the amount of mRNA for CRTh2, a GPCR found in T_{H2} cells, and double the mRNA of GATA3, a T_{H2} transcription factor. These results imply that Jurkat and CCRF-CEM cells contain certain features of T_{H1} and T_{H2} cells, respectively (**Figure 1.5**).

Although there are obvious limitations to using cell lines in research, they are often used in place of primary cells because they also offer several advantages: they are cost

effective, easy to use, easy to culture, and bypass certain ethical concerns. Cell lines also provide a relatively pure population of cells, which is important since it provides consistent samples and reproducible results¹⁰⁹. Cultured T cell lines may be used in conjunction with *in vivo* studies to provide a more thorough understanding of T_H cell physiology.

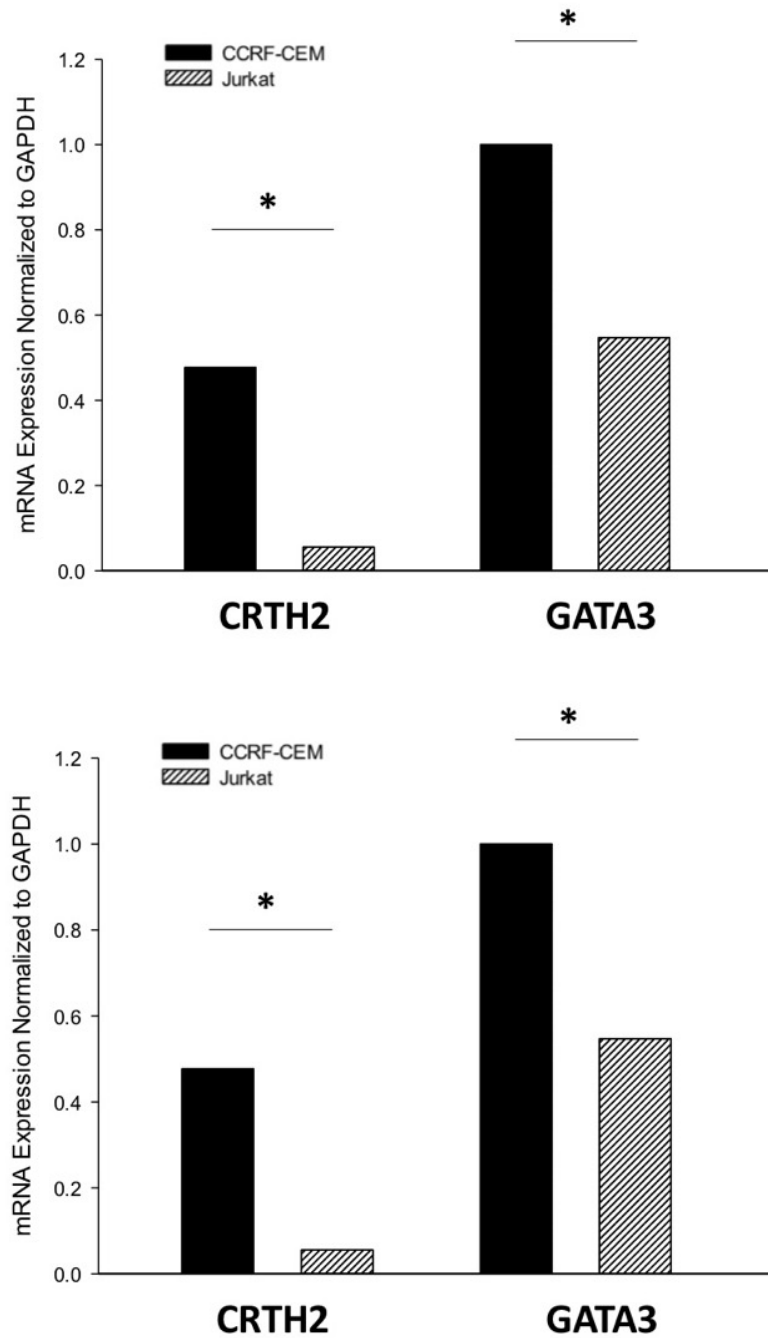


Figure 1.5 Comparison of mRNA levels of T_H1 and T_H2 markers in Jurkat and CCRF-CEM cells.

1.5 Gamma-Aminobutyric Acid

Gamma-aminobutyric acid (GABA) is widely known as the main inhibitory neurotransmitter in the mammalian central nervous system (CNS). It works alongside the main excitatory neurotransmitter glutamate to modulate inhibitory and excitatory balance for proper brain functions^{110,111}. GABA is involved in a variety of CNS responses and diseases involving anxiety-related behavior, cognitive processing, and the discrimination of information¹¹². For example, changes in GABA signaling may contribute to the generation and spreading of seizures in epilepsy¹¹³. Interestingly, it is becoming increasingly clear that the effects of GABA on human physiology extend far beyond the CNS.

GABA is produced through the decarboxylation of glutamate by the enzyme glutamic acid decarboxylase (GAD). In mammals, GAD exists in two isoforms: GAD65 and GAD67, which are encoded by *GAD1* and *GAD2*, respectively¹¹⁴. These two isoforms differ in molecular weight (65 and 67 kDa), function, and localization. In neurons, GAD67 is spread evenly throughout the cell body and synthesizes GABA for development and normal cell function. GAD65 is generally localized to nerve terminals and is involved with GABA synthesis for neurotransmission¹¹⁵.

GABA is degraded by the enzyme GABA transaminase (GABA-T) into succinate. GABA-T inhibitors such as vigabatrin produce a significant increase in GABA in the brain *in vivo*¹¹⁶. Another important component of the GABA signaling system are the GABA transporters (GATs). These transporters remove GABA from the intercellular space after synaptic transmission to prevent tonic activation of GABA receptors¹¹⁷. GABA acts on two different types of receptors: ionotropic GABA-A receptors (GABA_ARs), which are chloride channels, and metabotropic GABA-B receptors (GABA_BRs), which are GPCRs. Both types of receptors are located in the plasma membrane of cells. In the adult brain, GABA mainly acts

through activation of the fast hyperpolarizing GABA_ARs. When GABA binds to these receptors, the ion channel opens and Cl⁻ diffuses into the neuronal cell along its concentration gradient¹¹⁸. On the other hand, GABA_BRs are responsible for the later and slower component of inhibitory transmission¹¹⁹. Activation of these receptors initiates a GPCR-mediated pathway that activates postsynaptic K⁺ channels or inhibition of presynaptic Ca²⁺ channels. In the brain, approximately 20% of neurons are GABAergic and most of the physiological activities of GABA are generated through GABA_ARs¹²⁰. The focus of this thesis is on GABA signaling mediated through GABA_ARs.

1.5.1 GABA_AR Structure

GABA_ARs are formed by the assembly of five heterogeneous subunits. Each subunit contains four transmembrane regions, an extracellular N-terminal, and an intracellular C-terminal. 19 different mammalian GABA_AR subunits have been cloned (α 1-6, β 1-3, γ 1-3, δ , ϵ , π , θ , and ρ 1-3) thus far¹²¹. However, most of the physiologically relevant receptor compositions are formed by two α , two β , and one other subunit, most frequently the γ subunit¹²² (**Figure 1.6**). Both the α and β GABA_AR subunits are critical for GABA_AR activation¹²³. The diversity of the subunit combinations is dictated by the GABA_AR subunits that assemble from their component subunits in the endoplasmic reticulum (ER). Subunits that are not used are retained in the ER and degraded by ubiquitylation^{124,125}. However, what determines these unique subunit combinations is still a subject of investigation. The α 1 β 2 γ 2-containing GABA_ARs are the most abundant subtype of GABA_AR in the brain¹²⁶. The molecular weights of individual GABA_AR subunits range from 43-66 kDa and the estimated molecular weight of the entire GABA_AR complex is approximately 300 kDa.

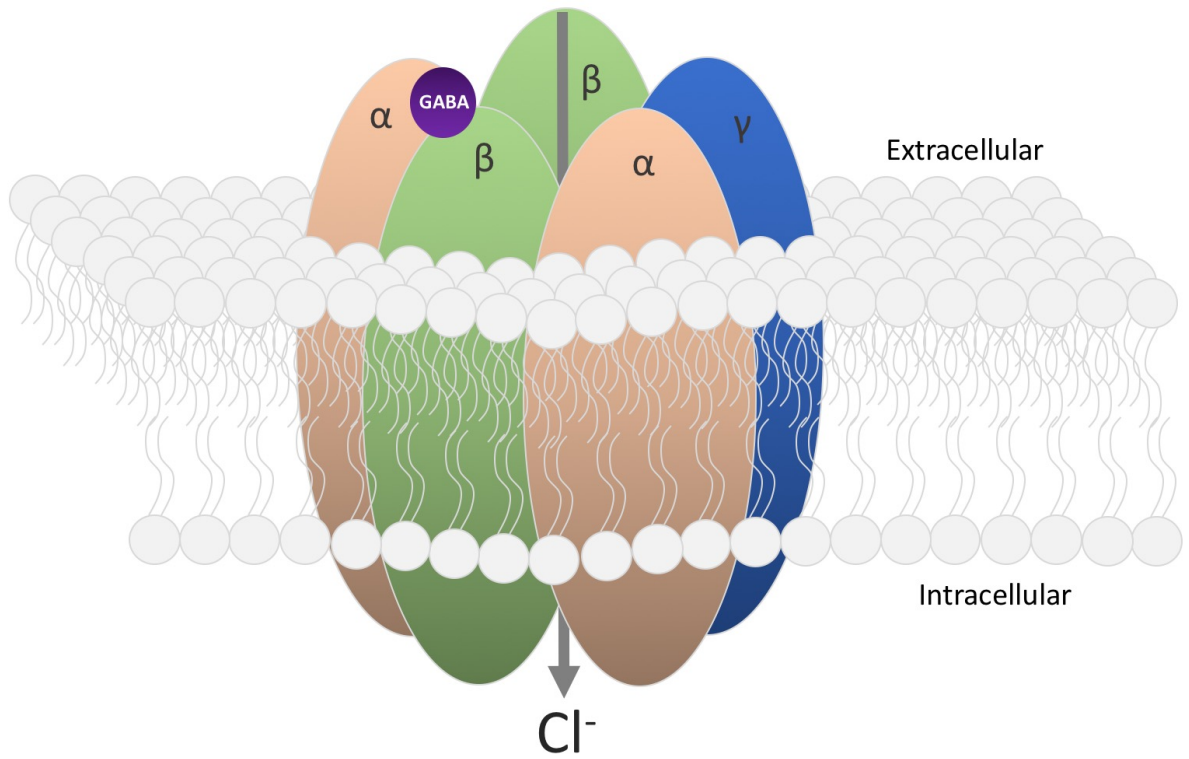


Figure 1.6 Illustration of a GABA_AR formed from two α , two β , and one γ subunit.

The GABA_AR is a pentameric Cl⁻ channel that opens upon the binding of GABA and the selective agonist muscimol. The competitive antagonists bicuculline and SR-95531 compete for the GABA binding site to decrease GABA_AR conductance. As Cl⁻ channels, GABA_ARs can mediate Cl⁻ currents into or out of cells depending on the resting membrane potential and the equilibrium potential for Cl⁻. The latter is governed by the expression and activity of Cl⁻ transporters in neuronal cells¹²⁷.

1.5.2 Chloride Transporters

In mature neurons, activation of GABA_ARs generally results in hyperpolarization of the cell and thus inhibition of neuronal activity¹²⁸. This is because the equilibrium potential for Cl⁻ is below (more negative) the neuronal resting membrane potential so Cl⁻ enters the cells during GABA_AR activation. However, GABA plays an excitatory role in immature neurons because they contain higher intracellular Cl⁻ levels, resulting in Cl⁻ efflux and depolarization of the cell upon GABA_AR activation¹²⁹. The intracellular Cl⁻ of neurons is predominantly regulated by two Cl⁻ transporters, NKCC1 and KCC2. NKCC1 increases intracellular Cl⁻ levels by internalizing one Na⁺, one K⁺ and two Cl⁻ ions to maintain electroneutral levels¹³⁰. Immature neurons express high levels of NKCC1 to maintain high intracellular Cl⁻. On the other hand, KCC2 decreases intracellular Cl⁻ levels by extruding K⁺ and Cl⁻ using the electrochemical gradient of K⁺. KCC2 is expressed at higher levels in mature neurons to maintain low intracellular Cl⁻ concentrations¹²⁷. NKCC1 is expressed ubiquitously in the body while KCC2 is only expressed in neurons. Therefore, the expression and activity levels of NKCC and KCC transporters in different cell types control the intracellular Cl⁻ concentrations and determine the direction of Cl⁻ currents.

1.5.3 GABA Signaling Outside of the CNS

A majority of studies on GABA signaling to date have been in the context of the CNS. However, components of the GABA signaling system have also been identified in several non-neuronal tissues including the pancreatic islets, testis and immune cells¹³¹⁻¹³³. GABA appears to play important regulatory roles in many cell types. In the pancreas, GABA originating from β -cells can act on GABA_ARs on α -cells to cause membrane hyperpolarization and suppression of glucagon secretion^{134,135}. Recently, an autocrine GABA signaling system was found in pancreatic β -cells and have been shown to promote β -cell regeneration¹³⁶. GABA produces membrane depolarization and activation of growth and survival pathways in β -cells. In animal models of Type I Diabetes (T1D), GABA prevents and reverses the disease by enhancing β -cell growth and survival¹³⁶. Therefore, GABA can play opposing roles in the two main cell types of the pancreas by hyperpolarizing α -cells while depolarizing β -cells.

GABA has also been demonstrated to play a role in testicular physiology by regulating steroid synthesis by Leydig cells. GABA signaling proteins including GAD65/67, VGAT, and GABA_AR subunits were detected in rodent and human testis¹³⁷. In a mouse cell line of Leydig cells called TM3, GABA agonists increased the proliferation of the cells¹³⁸. These data suggest that an autocrine GABAergic system can play regulatory roles in many different endocrine cell types. However, studies on GABAergic regulation of immune cells have only emerged in the last decade or so.

1.5.4 GABA in the Immune System

APCs: Components of the GABA signaling system have been detected in APCs including dendritic cells and macrophages¹³⁹. GAD65 was detected in dendritic cells and macrophages from encephalomyelitis (EAE) mice while GAD67 was found in human

peripheral monocytes¹⁴⁰. GABA-T has also been detected in macrophages and human monocytes^{139,141}. In murine macrophages, GABA_AR α 1, α 2, β 3 and δ subunits were detected¹⁴². Human peripheral monocytes express the α 1, α 3, β 2 and the δ subunits¹⁴³. So far, dendritic cells have not been reported to express GABA_ARs.

Anaesthetics that act through GABA_ARs severely compromise the immune system of patients. Functional GABA_ARs are present in monocytes and inhibit normal monocyte behaviour, which could contribute to the development of infections¹⁴⁴. On the other hand, this effect could be beneficial during inflammatory conditions. GABA has also been shown to inhibit pro-inflammatory cytokine secretion in dendritic cells and macrophages from wildtype and EAE mice^{139,142}.

As previously introduced, studies in our lab have shown that GABA_AR signaling could regulate macrophage polarization by promoting cells toward an M2 phenotype and inhibiting M1 development. Moreover, when naïve macrophages were polarized towards the M1 phenotype, GABA_ARs were downregulated. The opposite was observed in macrophages polarized towards the M2 phenotype, which had an upregulation of GABA_ARs¹⁴⁵. This suggests that the GABA signaling system plays critical roles in macrophage function and polarization and that GABA_AR expression is dependent on the phenotypic state of cells.

T cells: Many of the necessary components of the GABA signaling system have been reported in T cells from different species. GAD and GABA-T have been identified in CD4⁺ T cells from mice and in human T cells^{141,146}. Mendu and colleagues conducted a comprehensive study of mRNA expression of all 19 GABA_AR subunits in human, mouse and rat CD4⁺ and CD8⁺ T cells¹⁴⁷. In rat T cells, α 1, α 2, α 3, α 4, α 6, β 2, β 3, γ 1, θ , π , ρ 1, ρ 2, and ρ 3 subunits were detected. In mouse T cells, α 2, α 3, α 5, β 2, β 3, γ 1, and δ subunits were detected. In human

T cells, $\alpha 1$, $\alpha 5$, $\beta 1$, π , and $\rho 2$ subunits were detected. Lastly, in human Jurkat cells, $\alpha 1$, $\alpha 3$, $\alpha 5$, $\alpha 6$, $\beta 1$, $\beta 2$, $\beta 3$, π , and $\rho 1$ subunits were detected¹⁴⁷.

GABA has been shown to inhibit the activity of T cells from various species. GABA and selective GABA_AR agonist muscimol inhibited anti-CD3 mediated murine T_H cell proliferation *in vitro*; this effect was not seen with GABA_BR agonist baclofen, suggesting that GABA's effects are mediated through GABA_ARs¹⁴⁸. GABA and muscimol were shown to inhibit proliferation in human T cells as well¹⁴¹.

The various T_H cell subsets exhibit different properties including cytokine production patterns, regulatory mechanisms, and Ca²⁺ signaling kinetics^{149,150}. Studies on the role of GABA in T cells have generally been in the context of naïve T_H cells or in autoimmune disease models. Given that these are considered T_H1-mediated responses, it would be interesting to investigate whether GABA can play a different role in T_H2 cells. T_H1 and T_H2 cell development and functions are considered to oppose each other. GABA can play opposite roles in mature and immature neurons, as well as in the pancreatic α and β cells. Whether GABA differentially regulates T_H cell subsets is largely unknown and our study aimed to add insight into this topic.

1.5.5 GABA in Autoimmune Diseases

Numerous studies have provided evidence for an immunomodulatory role of GABA in diseased states. A few of these will be highlighted in this section. It has been shown that GABA inhibits pro-inflammatory CD4⁺ T cell responses and inhibit T cell autoimmunity in a mouse model of Type 1 diabetes^{142,143,151,152}. Oral GABA treatment downregulated inflammatory responses in a mouse model of rheumatoid arthritis and in a mouse model of obesity¹⁵³. Dysregulation of GABA metabolism lead to autoimmunity in children who later

had T1D¹⁵⁴. Interestingly, pancreatic β cells widely express GAD65/67, which is targeted by T cells during autoimmune destruction of β cells. In general, GABA appears to play a largely inhibitory role in T_H1-inflammatory and autoimmune disorders.

1.6 Rationale

CD4⁺ T cell differentiation is initiated by antigen presentation at the TCR and influenced by cytokines in the cell microenvironment which act on GPCRs. On the other hand, T cells have been shown to contain the necessary components of an autocrine GABA_AR signaling system. It is well known that the development and differentiation of many cell types are under the influence of GABA_ARs. For example, autocrine GABA_AR signaling promotes neuro-progenitor cell differentiation¹⁵⁵ and controls the phenotypic and functional trans-differentiation of pancreatic α and β cells¹⁵⁶. Studies in our lab have also demonstrated that GABA_AR activation inhibited M1 phenotype development while facilitating M2 development. M1 phenotype is driven by T_H1 cytokines while M2 phenotype is driven by T_H2 cytokines. Moreover, the M1/T_H1 line of development drives autoimmune and inflammatory responses. Therefore, this thesis sought to examine whether GABA can also play different regulatory roles in T_H cell phenotypes.

Another focus of this project was to investigate the underlying mechanism by which GABA_ARs affect T cell functions. Given the importance of the membrane potential in driving SOCE during T cell activation, we hypothesized that GABA_ARs mediate their effects by changing the membrane potential of cells, hence modulating SOCE (illustrated in **Figure 1.7**).

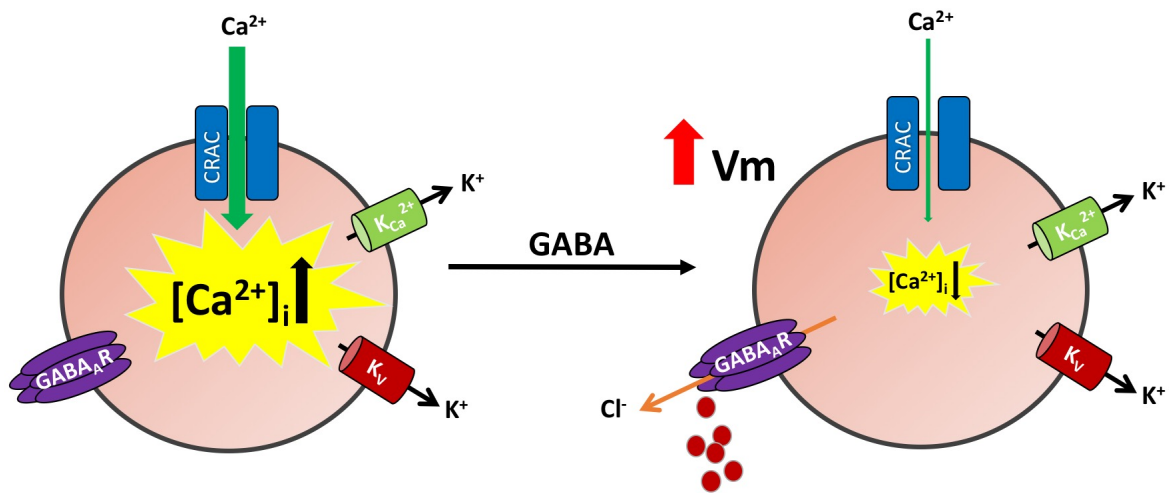


Figure 1.7 Proposed mechanism of GABA_AR signaling in T lymphocytes.

1.7 General Hypothesis

GABA_AR-mediated autocrine signaling differentially regulates the activity and functions of different T_H cell types through indirect modulation of SOCE.

1.8 Objectives

This thesis sought to examine the role of GABA_AR signaling in two T_H cell lines to establish proof of concept that GABA can play heterogeneous roles in different T_H cell types.

Aim 1 – Characterize Jurkat and CCRF-CEM T Lymphocyte Lines

Since Jurkat and CCRF-CEM cells contain different profiles of transcription factors and cytokines, the first aim was to further characterize the phenotypic and functional differences between these two cell lines. Specifically, we examined cell proliferation rate, cell size, and SOCE in response to thapsigargin stimulation.

Aim 2 –Examine the Expression of GABA Signaling Molecules

The composition of GABA_ARs varies between different species and even between different cell types in an individual. Given the importance of subunit expression on receptor pharmacological properties, we investigated which specific GABA_AR subunits are expressed in the two T_H cell lines. We also examined whether stimulation of these cells could affect GABA_AR expression.

Aim 3 – Determine the Effects of GABA_AR Agonists and Antagonists on Cell Function

GABA inhibits T_H1 cell functions and T_H1-mediated autoimmune diseases. To understand the mechanism(s) by which it does this and whether GABA has the same effect on all T_H subtypes, we examined the effects of GABA_AR agonist and antagonist on Ca²⁺ entry, nuclear NFAT expression, metabolic activity, and cell surface protein expression in the two T_H lines.

Chapter 2: Materials and Methods

2.1 Cell Cultures

Jurkat cells (obtained from ATCC; Manassas, VA) were thawed in a 37 °C water bath and transferred to a 100 mm culture dish containing 10 ml of RPMI-1640 medium (ThermoFisher; Waltham, MA) supplemented with 10% fetal bovine serum (FBS; ThermoFisher) and 100U/100 µg/mL penicillin/streptomycin (P/S; ThermoFisher). Cells were grown in suspension and incubated at 37 °C with 95% O₂ and 5% CO₂. They were sub-cultured every three days by diluting in fresh culture medium at a 1:10 split ratio. Cells were maintained at a density between 2 x 10⁵ and 2 x 10⁶ cells/mL as recommended by the supplier. Jurkat cells used in this study were maintained from passages 1 through 30.

CCRF-CEM cells were obtained from Dr. Lisa Cameron's lab at passage 2 and like Jurkat cells, were cultured in 100 mm dishes containing 10 mL of RPMI-1640 (ThermoFisher) medium supplemented with 10% FBS (ThermoFisher) and P/S (100U/100 µg/mL; ThermoFisher). Cells were grown in suspension and incubated at 37 °C with 95% O₂ and 5% CO₂. They were sub-cultured every three days by diluting in fresh culture medium at a 1:10 split ratio. Cells were maintained at a density between 2 x 10⁵ and 2 x 10⁶ cells/mL. CCRF-CEM cells used in this study were maintained from passages 1 through 30.

2.2 Cell Proliferation

The relative proliferative rates of the two cell lines were determined by counting and plating 1 mL of cells (in triplicates) at an equal density (2 x 10⁵ cells/mL) in a 12-well plate. Cells were grown in regular culture medium (RPMI-1640 with 10% FBS and 100X P/S)

over a period of 72 h. Live and dead cells were counted using trypan blue (1:1) (Sigma) on a haemocytometer the day after plating (Day 1) as well as 72 h after plating (Day 3). The average cell density for each cell line on each day were calculated from the triplicate wells.

2.3 MTT Assay

An MTT assay was used to test the effects of GABA and selective GABA_AR antagonist bicuculline on cell metabolic activity. A 96-well plate was coated with 10 µg/mL poly-D-lysine (PDL; Sigma-Aldrich; Oakville, ON) at 37 °C overnight. The following day, the wells were washed twice with PBS to remove unbound PDL. Jurkat and CCRF-CEM cells were counted and 100 µL of cells were plated (5×10^5 cells/mL) and incubated for 30 min in serum-free media to allow for attachment to the bottom of the wells. Following this period, the serum-free media was aspirated and cells were washed twice with PBS. Fresh RPMI-medium (10% FBS) were added into the wells. Cells were left untreated (control) or treated with GABA (100 µM; Sigma) or bicuculline (100 µM; Sigma) for 24 h at 37 °C.

Following the 24 h treatment period, 10 µL of MTT solution (5 mg/mL; Sigma) was added into each well using a multi-channel pipet. The plate was incubated at 37 °C for 4 h. Following incubation, the media was aspirated and 100 µL of DMSO was added into each well and mixed thoroughly to break down the formazan crystals. The plate was read within 10 min of DMSO addition using a Benchmark Microplate Reader (BioRad) at a wavelength of 570 nm. The experiment was conducted in quadruplet wells. Four wells containing only MTT and DMSO were used to get a baseline reading; the average baseline reading was subtracted from the readings from experimental wells. Values from each treatment were averaged among the four replicates and normalized to control values (Control CCRF-CEM).

2.4 Immunocytochemistry

Immunocytochemistry was used to determine the presence and localization of certain proteins in fixed cells. Prior to staining, glass coverslips were placed in 12-well plates and coated with 10 µg/mL PDL (Sigma-Aldrich) at 37 °C overnight. Coverslips were washed twice with PBS the following day to remove unbound PDL. Cells were counted and plated at 5×10^5 cells per well for 30 min in serum-free media to allow for attachment to coverslips. Following this period, the media was aspirated and cells were washed twice with PBS to remove cells that did not attach to coverslips. Cells were fixed for 10 min in 4% paraformaldehyde (PFA; Electron Microscopy Science; Hatfield, PA) solution diluted in PBS. Cells were then washed once with PBS containing 0.1M glycine (Sigma-Aldrich) for 5 min, 2 x 5 min with PBS, and then incubated at 4 °C overnight.

The following day, fixed cells were permeabilized using 0.1% Triton X-100 (Sigma-Aldrich) in PBS for 5 min, washed with PBS for 5 min, and then blocked with 5% Normal Donkey Serum (NDS; Jackson ImmunoResearch; West Grove, PA) diluted in PBS for 1 h to prevent non-specific staining. Primary antibody (see **Table 2.1** for list of primary antibodies) diluted in 1% NDS was added to each coverslip and incubated overnight at 4 °C. The following day, coverslips were washed with PBS for 3 x 5 min, followed by addition of secondary antibody (see **Table 2.1** for list of secondary antibodies) diluted in 5% NDS for 1 h at room temperature to allow for conjugation to the primary antibody. Cells were then rinsed with PBS and incubated with the nucleus stain 4', 6-diamidino-2-phenylindole (DAPI; 1 mg/ml; Sigma-Aldrich) for 10 min. Following immunostaining, coverslips were mounted on glass slides (ThermoFisher) using Fluoromount GT (Electron Microscopy Sciences) and sealed with nail polish to prevent coverslips from detachment.

Cells were examined and imaged using the Olympus FV1000 microscope at the Confocal Microscopy Core Facility located at Robarts Research Institute, London ON. A 60X magnification was used for the experiments. The microscope settings were kept consistent between and within experiments.

Table 2.1 Primary and secondary antibodies used for immunocytochemistry:

Primary Antibody	Source	Dilution	Company
STIM1	Rabbit	1:200	Proteintech Group Inc.
GABA _A R- α 1	Rabbit	1:100	Upstate
GAD65/67	Rabbit	1:1000	Sigma-Aldrich
NFATc2	Mouse	1:500	ThermoFisher
NKCC1	Goat	1:100	Santa Cruz

Secondary Antibody	Source	Dilution	Company
Cy3 anti-rabbit IgG	Donkey	1:600	Jackson Immunoresearch Labs
Cy3 anti-mouse IgG	Donkey	1:600	Jackson Immunoresearch Labs
Alexa 488 anti-mouse IgG	Donkey	1:600	Jackson Immunoresearch Labs
Alexa 488 anti-rabbit IgG	Donkey	1:600	Jackson Immunoresearch Labs

2.5 Cell Size Analysis

Confocal imaging was also used to analyze the relative cell sizes of Jurkat and CCRF-CEM cells. Ten differential interference contrast (DIC) images of each cell line were analyzed using ImageJ software to obtain an average cell area for each cell type. The outline of each cell was automatically determined as a region of interest (ROI) by the software and the area within the ROI was calculated. Multiple images of cells in different groups were taken. Approximately 30-50 cells were in the field of view of each image.

2.6 Mitogenic Stimulation of Cells

T cell activation is normally triggered by the antigenic stimulation of TCRs along with a co-stimulatory signal to activate CD28. Stimulation of T cells with a mitogen such as phytohaemagglutinin (PHA) and co-stimulus from phorbol 12-myristate 13-acetate (PMA) can also induce cell activation and the production of cytokines (Sigma). PHA is a lectin that crosslinks TCRs leading to receptor activation, while PMA is a phorbol ester that mimics DAG and activates PKC.

For these experiments, a time course treatment was performed to examine the effects of cell activation on the expression of various proteins over time. Cells were counted and transferred to 15 mL tubes before centrifugation (1000 rpm, 4 °C, 5 min). The supernatants were removed and cells were re-suspended in fresh growth medium. Cells were then plated in 60 mm dishes at a density of 5×10^5 cells/mL. Four dishes were plated for each cell line (one each for control, 24 h, 48 h, 72 h treatments). Cells were treated with PHA-L (eBioscience) at 1 $\mu\text{g}/\text{mL}$ and PMA (Sigma-Aldrich) at 50 ng/mL . Cells were re-harvested for whole cell lysate collection at 24 h, 48 h, and 72 h after treatment.

2.7 Western Blot

Whole cell lysate collection and Bradford assay

Western blot analysis was used to determine the relative amount of protein present in cells at the time of whole cell lysate collection. Protein lysates of cells were collected using SDS-free RIPA buffer (1.0% TritonX-100, 0.5% deoxychloric acid, and 1X phosphate buffer) supplemented with 100 mM EDTA (pH 8.0), 10 µg/ml each of protease inhibitors Aprotinin and Leupeptin (Sigma-Aldrich), and 2 mM of phenylmethylsulfonyl fluoride (PMSF; Sigma). Samples were incubated on ice for 30 min prior to centrifugation at 13000 rpm for 5 min at 4 °C. The supernatants were collected and frozen at -80 °C for protein quantification and Western blot analysis. The total protein concentrations of cell lysates were determined using a Bradford assay. A protein standard from 0 to 25 µg/mL was prepared using bovine serum albumin (BSA). The standard curve and protein concentrations were measured using a spectrophotometer (Eppendorf Biophotometer Plus). The amount of protein loaded for gel electrophoresis was optimized for each primary antibody (40-100 µg).

Gel electrophoresis

Prior to gel electrophoresis, whole cell lysates were mixed with 2X SDS loading buffer containing 100 mM Tris HCl, 5% B-mercaptoethanol, 10% SDS, 20% Glycerol, and 0.1% Bromophenol Blue. The samples were loaded on 4% stacking and 8% resolving polyacrylamide gels and separated by gel electrophoresis. One lane was loaded with Pink Plus Pre-stained Protein ladder (FroggaBio) to indicate the molecular weight of bands. A constant voltage of 60 V was applied to samples to allow for migration through the stacking gel, followed by an increase to 100 V for approximately 2 h through the resolving gel at room temperature.

Gel to membrane transfer and immunoblotting

Following gel electrophoresis, individual gels were wet-transferred to nitrocellulose membranes (Bio-Rad) for 2 h at 80 V on ice using Tris-glycine transfer buffer (20 % methanol). Following this transfer period, membranes were blocked with 5% w/v skim milk powder diluted in TBS-T (10 mM Tris HCl pH 8.0, 150 mM NaCl and 0.1% Tween-20) for 1.5 h at room temperature. Membranes were then incubated with primary antibody (see **Table 2.2** for primary antibodies) diluted in 5% w/v skim milk overnight at 4 °C. The following day, membranes were washed with TBS-T (3 x 10 min) and incubated with secondary antibody (see **Table 2.2** for list of secondary antibodies) also diluted in 5% w/v skim milk for 1.5 h at room temperature, followed by another set of TBS-T washes (3 x 10 min). Western ECL substrate (BioRad) was used to detect the presence of secondary antibodies conjugated to HRP.

Imaging membranes

A VersaDoc Molecular Imager (Bio-Rad) was used to image the membranes. The exposure times of individual membranes were optimized depending on the primary antibody being detected. Several images of different exposure times were taken for each membrane. Following imaging, the membranes were stripped using Restore Western Blot Stripping Buffer (Thermo Scientific) for 10-15 min and blocked with 5% milk or 5% bovine serum albumin (BSA) in TBS-T prior to the addition of β -actin or GAPDH primary antibodies, respectively. These proteins were used as the loading controls for densitometry analysis of the bands. Densitometry analysis was performed using ImageJ software and the protein of interest was normalized to β -actin or GAPDH loading controls before further normalization to control groups.

Table 2.2 Primary and secondary antibodies used for Western Blot:

Primary Antibody	Source	Dilution	Company	Molecular Weight
STIM1	Rabbit	1:800	Proteintech Group Inc.	80-90 kDa
Orai1	Rabbit	1:400	ABCAM	50 kDa
GAD65/67	Rabbit	1:1000	Sigma-Aldrich	65, 67 kDa
GABA _A R- α 1	Guinea Pig	1:1000	Alomone Labs	51 kDa
GABA _A R- β 1	Rabbit	1:1000	ABR	55 kDa
GABA _A R- β 3	Mouse	1:300	Santa Cruz	56 kDa
NKCC1	Goat	1:300	Santa Cruz	131 kDa
NFATc2	Mouse	1:1000	ThermoFisher	120 kDa
β -actin	Mouse	1:5000	Sigma-Aldrich	42 kDa
GAPDH	Mouse	1:1000	ABCAM	37 kDa

Secondary Antibody	Source	Dilution	Company
HRP-conjugated anti-guinea pig	Donkey	1:5000	Chemicon
HRP-conjugated anti-goat IgG	Rabbit	1:10000	BioRad Laboratories

HRP-conjugated anti-rat IgG	Goat	1:5000	BioRad Laboratories
HRP-conjugated anti-rabbit IgG	Goat	1:10000	Jackson ImmunoResearch
HRP-conjugated anti-mouse IgG	Sheep	1:10000	Amersham Bioscience

2.8 Calcium-Dependent Fluorescence Imaging

Cell Preparation

Calcium-dependent fluorescence imaging was used to examine the effects of GABA_AR agonists and antagonists on Ca²⁺ entry in the two cell lines. Prior to imaging, cells were counted, centrifuged, and re-suspended in serum-free media before plating 1 mL at an equal density (5 x 10⁵ cells/mL) in PDL-coated glass bottom dishes (MatTek Corporation; Ashland, MA). Depending on the number of groups and trials being assessed, 6-8 dishes of cells were prepared for each experiment. Cells were incubated for 30 min at 37 °C to allow for attachment to the cover glass. Following attachment, cells were washed twice with extracellular solution (ECS contents: 130 mM NaCl, 5.0 mM KCl, 2.0 mM MgCl₂, 2.0 mM CaCl₂, 10 mM HEPES, 5.0 mM Glucose) to remove unbound cells. Cells were then incubated with 1 μM Rhod-4AM (AAT Bioquest; Sunnyvale, CA), a membrane-permeable Ca²⁺-dependent fluorescent indicator, for 45 min at 37 °C to allow for Rhod-4AM to load into the cells. Following this period, cells were gently rinsed with ECS three times and then brought to the imaging facility.

Rhod-4AM Fluorescence Imaging

Live cell imaging was performed using the Olympus FV1000 microscope at Robarts Research Institute. The microscope was set up for detection of the Rhod-4AM fluorophore

(excitation: 546 nm, emission: 560-620 nm) at 20X magnification. Once the dish was loaded onto the microscope stage, a field of view (FOV) would be randomly selected for imaging. Approximately 30-50 cells were in each FOV during these imaging experiments. The microscope was set to run a time lapse where one image was captured every 2.7 s. When imaging started, a baseline intensity of Rhod-4AM fluorescence was established by allowing the microscope to run for 30 frames without addition of any test substances to the cell culture dish. Following 30 images of baseline detection, specific test substances/drugs (1.0 μ M thapsigargin, 100 μ M GABA and 100 μ M bicuculline) were applied to the dish to examine their effects on Rhod-4AM fluorescence in the cells. The working concentration of each test substance was determined from examining the literature and from earlier optimization experiments. The stock solution of thapsigargin was prepared using ethanol. The final working concentration of ethanol was 0.05% and at this concentration, it had no vehicle effects on Rhod-4AM fluorescence in the cells. GABA and bicuculline were both diluted in water.

Rhod-4AM Fluorescence Analysis

In this assay, intracellular Ca^{2+} levels were inferred from the fluorescence intensity of Rhod-4AM. To analyze the relative levels of intracellular Ca^{2+} , the time-lapse images were uploaded into ImageJ software and converted to greyscale. The outlines of each cell were automatically selected as regions of interest (ROIs) by the software. Cells that shifted locations during the imaging time course were excluded from the analysis. The fluorescence intensity of each image at each time point was detected by the software and normalized to baseline fluorescence. The average Rhod-4AM fluorescence intensities calculated from individual cells in each ROI were plotted against the time point. Lastly, the average fluorescence intensities of Rhod-4AM were pooled from multiple trials of the same treatment group.

2.9 Flow Cytometry

Flow cytometry was used to examine the effects of GABA and antagonist bicuculline on cell surface expression of CRTh2. Cells were counted and plated at an equal volume and density (3 mL at 2×10^5 cells/ mL) in a 6 well-plate and were either left untreated (control), or treated with GABA (100 μ M) or bicuculline (100 μ M). The cells were incubated with the treatments for 24 h at 37 °C before preparation for flow cytometry analysis.

Following the 24 h treatments, 5×10^6 cells from each condition were collected into 15 mL tubes. Cells were washed with PBS FACS (3% FBS, 0.5% BSA, 0.1% sodium azide) and spun down at 900 RPM for 10 min at 4 °C. The cells were then re-suspended in fresh PBS FACS and incubated with primary blocking antibody (rat IgG; BioLegend; San Diego, CA) for 45 min at room temperature in the dark. Following the blocking step, anti-CRTh2 AlexaFluor 647 primary antibody (rat anti-human) or isotype control (both from BioLegend) were added to the tubes and incubated for 30 min on ice. Cells were then washed and fixed with 2% PFA prior to flow cytometry analysis. The experiments were conducted in duplicates. Flow cytometry was performed at the London Regional Flow Cytometry Facility using the BD LSR II Flow Cytometer and FloJo analysis software. The values of CRTh2 intensities were normalized to control CCRF-CEM cells.

2.10 Statistical Analyses

Results from all experiments were presented as a mean \pm SEM. To calculate statistical differences between experimental groups, a Student's T-test or two-way ANOVA followed by a post-hoc Tukey's test was used when appropriate. A P-value of less than 0.05 was considered statistically significant. GraphPad Prism was used to generate all graphs and run statistical analyses.

Chapter 3: Results

3.1 Characterization of Jurkat and CCRF-CEM Lines

Preliminary results from qPCR assays performed by Dr. Cameron's lab showed that Jurkat and CCRF-CEM cells contained certain features of T_H1 and T_H2 effector cells, respectively. To further characterize the differences between these two T_H cell lines, we examined basic phenotypic features including cell proliferation rate, cell size, expression levels of CRAC channel proteins, and SOCE in response to thapsigargin. The following results pertain to this first aim.

3.1.1 CCRF-CEM cells proliferate faster than Jurkat cells

We examined the relative rates at which each cell line proliferates by counting the number of live cells in culture. More specifically, cells were plated at an equal density in RPMI-1640 medium (10% FBS), and live cells were counted the day after plating (Day 1) and 3 days after plating (Day 3). On Day 1, the cell densities were almost identical between the two cells lines, confirming that an equal number of cells were plated the day before and that they have yet to divide. On Day 3, the density of CCRF-CEM cells ($1.15 \pm 0.0493 \times 10^6$ cells/mL) were significantly higher than that of Jurkat cells ($7.442 \pm 0.729 \times 10^5$ cells/mL) (**Figure 3.1**). Almost all of cells (> 99%) were still viable during the cell counts (data not shown). These results indicate that CCRF-CEM cells proliferate at a relatively faster rate than Jurkat cells under culture conditions.

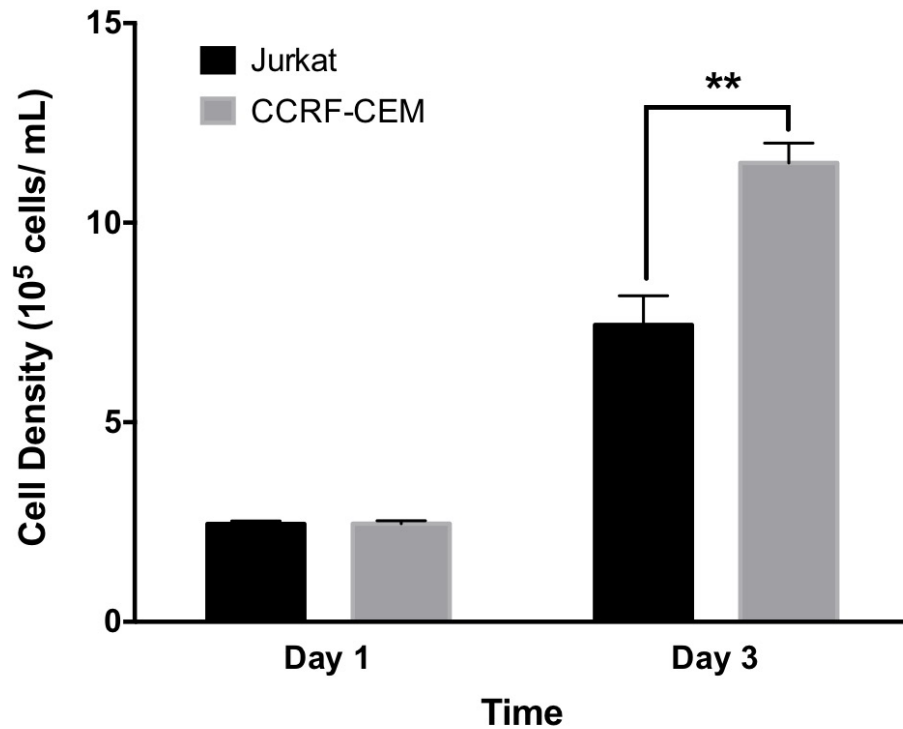


Figure 3.1 Proliferation of Jurkat and CCRF-CEM cells under culture conditions.

Jurkat and CCRF-CEM cells were cultured in 12-well plates at an equal density (2×10^5 cells/mL) in RPMI-1640 medium (10% FBS). Live cells were counted the day after plating (Day 1) and 3 days after plating (Day 3) while apoptotic cells were identified using trypan blue. Three wells per cell line were plated for the assay. The average densities of live cells on Day 1 and Day 3 are plotted in the graph. The values from the triplicate wells were analyzed using a two-way ANOVA followed by a post-hoc Tukey's test. Data are reported as a mean \pm SEM (n=3 technical replicates) (** indicates $P < 0.01$).

3.1.2 Jurkat cells are larger than CCRF-CEM cells

Another phenotypic trait that we examined were the relative cell sizes of the Jurkat and CCRF-CEM lines. We assessed this by analyzing DIC images of both cell types using ImageJ software. The average cell area obtained for Jurkat cells was $151 \pm 6.83 \mu\text{m}^2$, which was significantly larger than that of CCRF-CEM cells ($107 \pm 4.76 \mu\text{m}^2$) (**Figure 3.2A**). To confirm the result from image analysis, we also assessed the cell size using flow cytometry, a technique that can sort cells based on size and granularity. The forward scatter (x-axes) of a cell population on a flow cytometric plot indicates its relative cell size. According to the flow plots, the population of Jurkat cells on average had a larger forward scatter than CCRF-CEM cells, providing further evidence that Jurkat cells are larger in size than CCRF-CEM cells (**Figure 3.2B**).

Figure 3.2

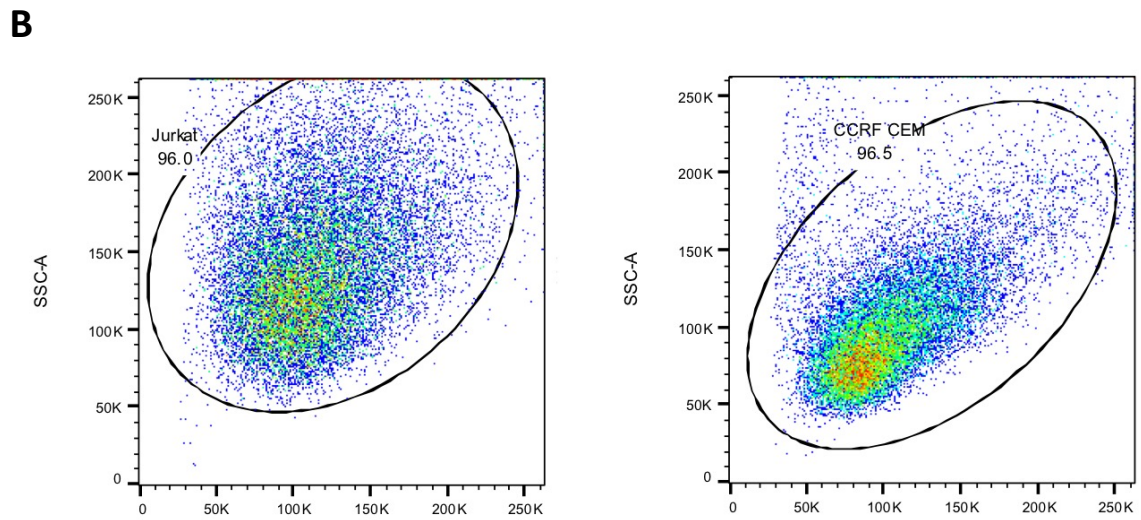
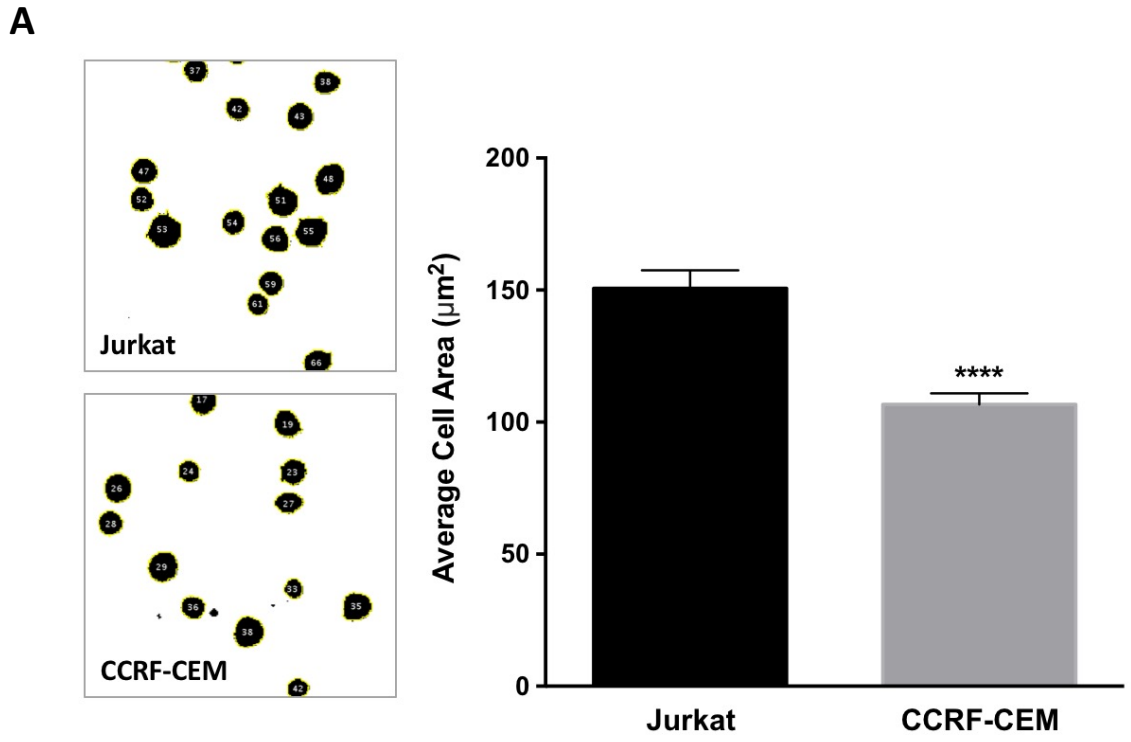


Figure 3.2 Analysis of average cell size of Jurkat and CCRF-CEM cells.

A) Analysis of cell size by confocal microscopy in combination with image analysis. Specifically, DIC images of both cell lines were taken with an Olympus confocal microscope at 20X magnification under the same microscope settings. The confocal images were analyzed using ImageJ software by converting into grayscale, outlining the outer membrane of each cell and obtaining the area within each outlined region of interest. Representative images in the left column are processed DIC images of Jurkat cells (upper panel) and CCRF-CEM cells (lower panel). The graph at the right summarizes the average area of all cells from ten images taken from each line. The average areas were analyzed using a two-way unpaired student's T-test. The data are reported as a mean \pm SEM. (**** indicates $P < 0.001$). **B)** Assessment of average cell size by flow cytometry. Shown are representative flow cytometry plots for each cell line. The circled area in each plot represents the population of Jurkat and CCRF-CEM cells, respectively. Forward scatter (x-axes) indicates relative cell size while side scatter (y-axes) represents cell granularity.

3.1.3 Both cell lines express CRAC channel components

Using Western blot, we examined whether Jurkat and CCRF-CEM cells express the protein components of CRAC channels: ER Ca^{2+} -sensor protein STIM1 and the channel forming protein Orai1, both of which are required for SOCE mechanisms in T_H cells. Western blot analysis detected STIM1 as a single band at ~85 kDa while Orai1 was detected as a single band at ~50 kDa in both cell lines (**Figure 3.3**). There were no observable differences in the expression levels of STIM1 and Orai1 between the two cell lines. Nevertheless, these results confirmed the expression of CRAC channel proteins by Jurkat and CCRF-CEM cells, suggesting that they are capable of generating SOCE. Previous immunocytochemistry experiments also detected STIM1 in Jurkat and RAW 264.7 cell co-cultures and in primary murine splenocytes (Appendix **Figure 6.1**).

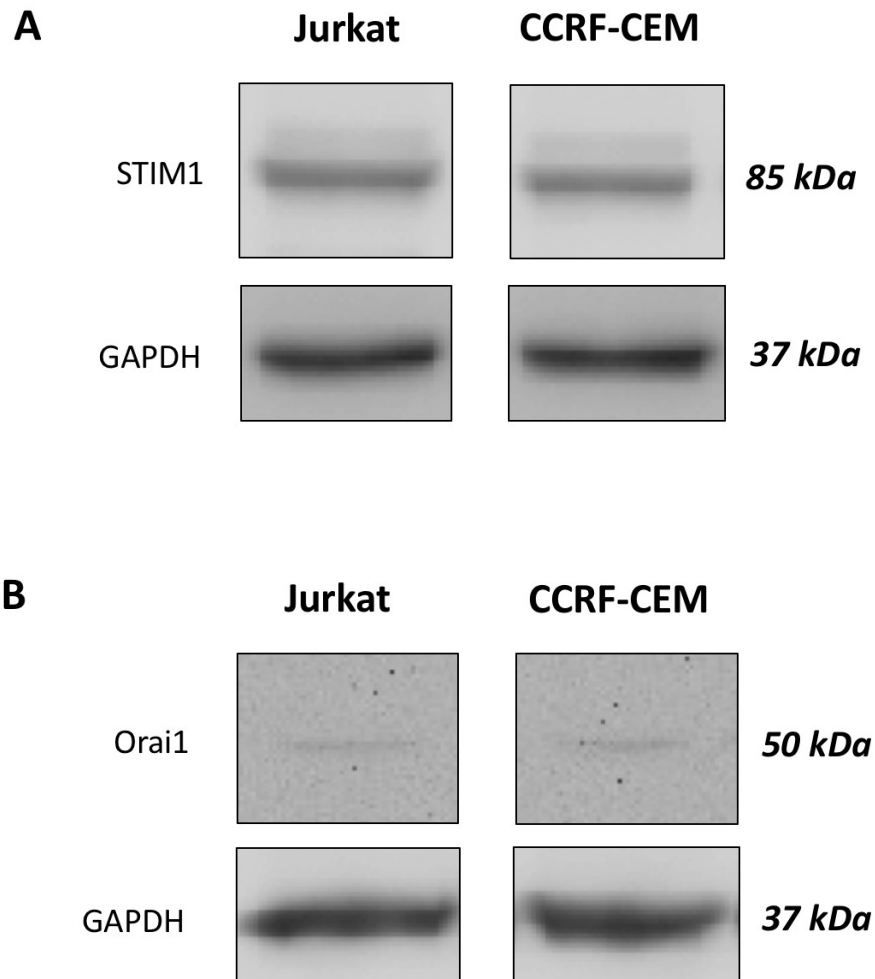


Figure 3.3 Protein expression of STIM1 and Orai1 in Jurkat and CCRF-CEM cells.

Representative Western blot images of **A)** STIM1 and **B)** Orai1 from whole cell lysates of Jurkat and CCRF-CEM cells. 50 μg and 100 μg of protein were loaded for the detection of STIM1 and Orai1, respectively. GAPDH was used as a loading control. Note that the densities of the STIM1 and Orai1 bands of Jurkat cells are similar to that of CCRF-CEM cells.

3.1.4 Larger SOCE magnitude observed in Jurkat cells in response to thapsigargin

Thapsigargin is a compound commonly used to induce SOCE in cells under various experimental settings. Since Jurkat and CCRF-CEM cells expressed relatively equal levels of CRAC channel proteins (**Figure 3.3**), we wanted to examine whether their Ca^{2+} response to thapsigargin would also be similar. It has been reported that different phenotypes of T_H cells contain unique Ca^{2+} signaling patterns, magnitude and rates^{157,158}.

Using Ca^{2+} -based fluorescence imaging and a specific Ca^{2+} indicator Rhod-4AM, indirect measurements of intracellular Ca^{2+} levels were recorded. Under control conditions (without the addition of any test substances), Rhod-4AM intensity appeared to be higher in Jurkat than in CCRF-CEM cells. There was also a greater variability in the intensity of Rhod-4AM fluorescence among Jurkat cells within a dish compared to CCRF-CEM cells (**Figure 3.4A**). Once 1 μM thapsigargin was applied to the cells, Rhod-4AM fluorescence increased dramatically in both cell lines (**Figure 3.4B**). The changes in Rhod-4AM fluorescence intensity over time were normalized to baseline fluorescence intensity to obtain relative fold-changes in Rhod-4AM fluorescence within each dish. The peak fluorescence levels were obtained from each trace and compared between the cell lines. The relative intensity changes in Rhod-4AM following thapsigargin addition was significantly larger in Jurkat cells (2.097 ± 0.04887 , $n=4$) than in CCRF-CEM cells (1.759 ± 0.06665 , $n=4$) ($P < 0.05$). This suggests that Jurkat cells flux relatively larger amounts of Ca^{2+} once SOCE is initiated by thapsigargin (**Figure 3.4C**).

Figure 3.4

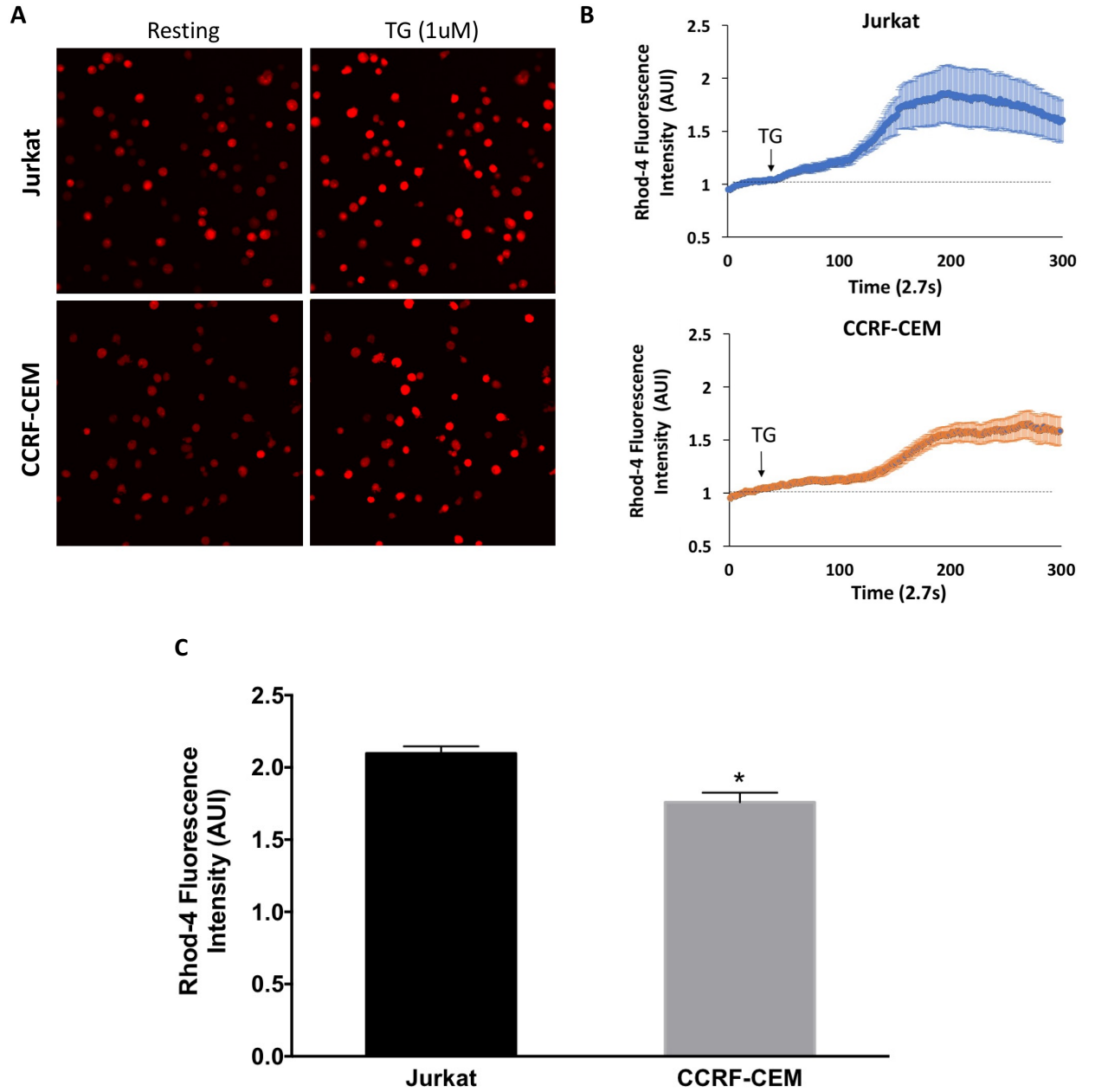


Figure 3.4 Thapsigargin-induced Ca^{2+} influx in Jurkat and CCRF-CEM cells.

Ca^{2+} -based fluorescence imaging was used to examine the effects of thapsigargin on intracellular Ca^{2+} levels in Jurkat and CCRF-CEM cells. Cells were plated and loaded with Rhod-4AM Ca^{2+} indicator prior to imaging. **A)** Representative images of a field of view for Ca^{2+} imaging. The baseline Rhod-4AM fluorescence is shown on the left panels and the rise in fluorescence following thapsigargin addition is shown in the right panels. **B)** Representative traces of Rhod-4AM fluorescence, measured in arbitrary units of intensity (AUI), normalized to baseline. The time point where thapsigargin was added into the dish is indicated by an arrow. Each trace represents the average fluorescence intensity in a field of view containing 30-40 cells. **C)** The average peak Rhod-4AM fluorescence intensities for each cell line were compared over several trials using an unpaired student's T-test. Data are represented as a mean \pm SEM (n=4) (* indicates $P < 0.05$).

3.2 Expression of GABA Signaling Proteins

To address the second aim, we examined the protein expression profiles of GABA signaling proteins including GAD and various GABA_AR subunits. A functional GABA_AR pentameric channel is composed of 2 α , 2 β , and one other subunit out of 19 possible types. Considering the importance of α and β subunits for the formation of GABA_ARs and that Jurkat cells express $\alpha 1$ and $\beta 1-3$ subunits mRNA¹⁴⁷, we decided to examine the $\alpha 1$, $\beta 1$, and $\beta 3$ subunits of GABA_ARs.

3.2.1 Glutamic acid decarboxylase is expressed in both cell lines

GABA is synthesized from glutamate by the enzyme glutamic acid decarboxylase (GAD). This enzyme exists in two isoforms – GAD65 and GAD67, weighing 65 kDa and 67 kDa, respectively. Using a primary antibody that detects both isoforms, expression of GAD65 and GAD67 in Jurkat and CCRF-CEM cells were examined by Western blot. GAD was detected as a double band at 65 kDa and 67 kDa in both cell lines (**Fig 3.5A**), while immunocytochemistry detected the expression of GAD65/67 localized throughout the cell cytoplasm. This indicates that both cell lines express GAD65/67, enabling them to produce their own GABA.

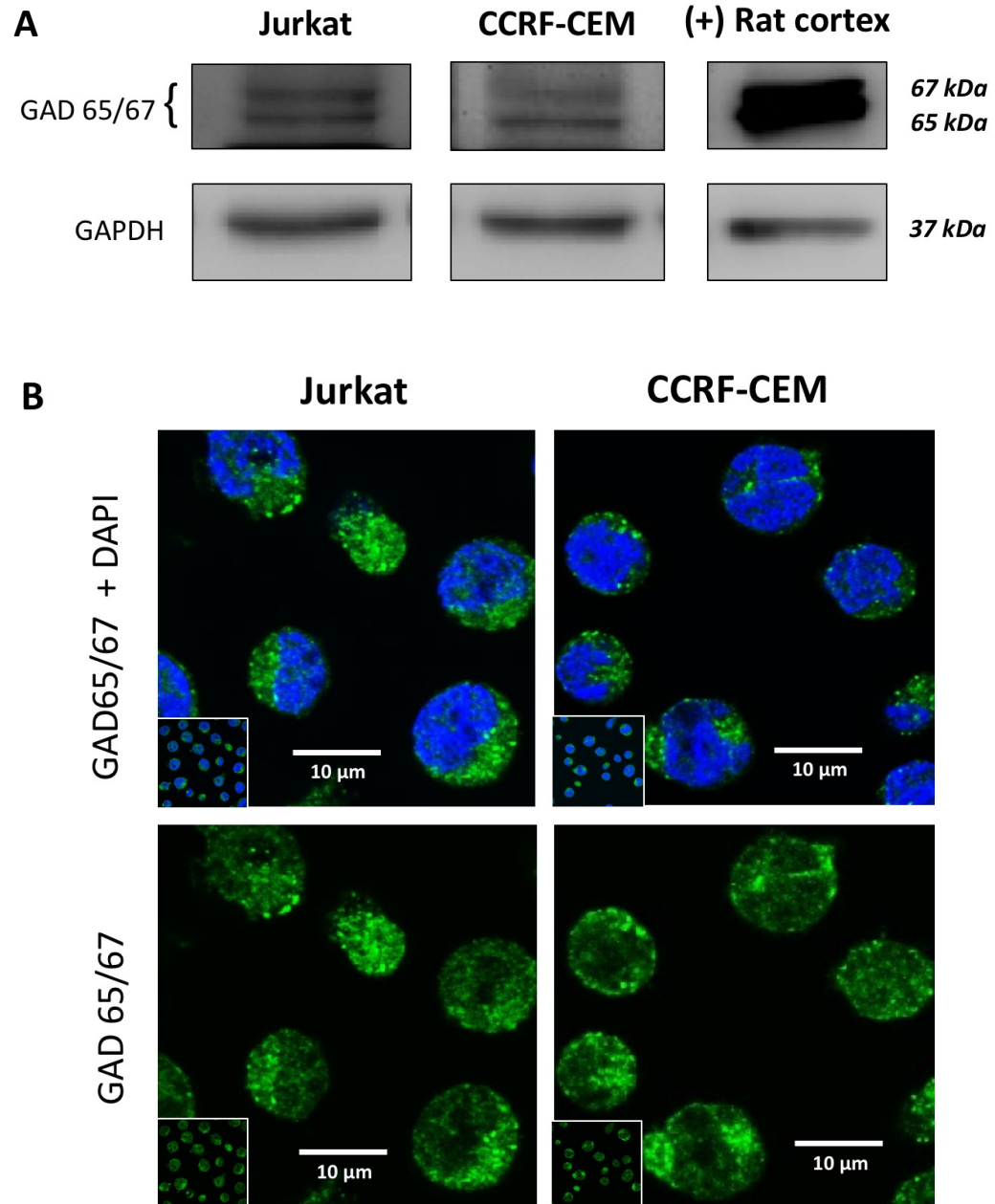


Figure 3.5 Protein expression and localization of glutamic acid decarboxylase (GAD) in Jurkat and CCRF-CEM cells with rat cortex as a positive control.

Western blot and Immunocytochemistry were used to detect the expression and localization of GAD65/67 in the two cell lines. **A)** Representative Western blot images of GAD65/67 and GAPDH loading control in whole cell lysates of Jurkat and CCRF-CEM. 50 μ g of protein was loaded for GAD 65/67 detection. **B)** Representative immunofluorescence images of Jurkat and CCRF-CEM cells stained with anti-GAD65/67 (Alexa 488, Green) and DAPI for nuclei (Blue).

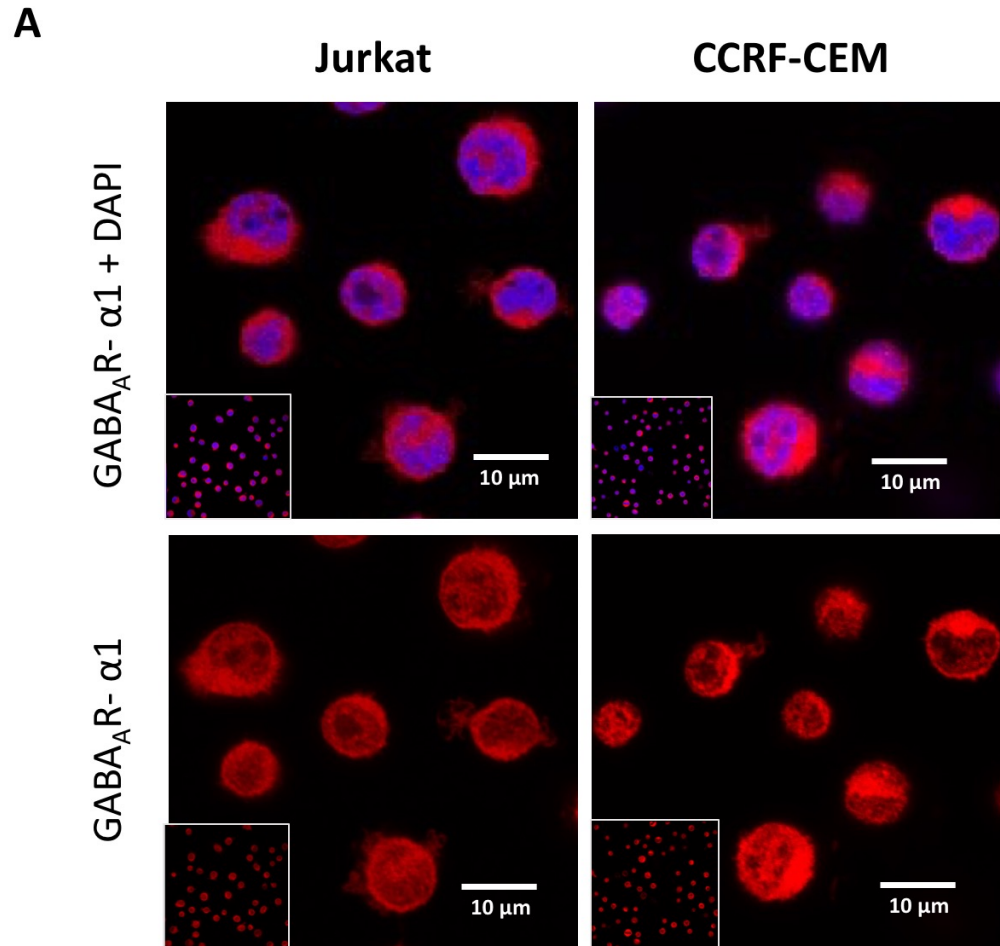
3.2.2 Various GABA_AR subunits are expressed in both cell lines

Next, we examined whether Jurkat and CCRF-CEM cells express different GABA_AR subunits and whether the expression levels would differ between the cell lines. The first subunit we looked at was GABA_AR- α 1, which is one of the most widely expressed subunits in the mammalian brain¹⁵⁹. Using immunocytochemistry, α 1 was detected in both cell lines localized throughout the cell cytosol and plasma membrane (**Figure 3.6A**).

After confirming the expression of α 1 through immunocytochemistry, we used a more quantitative technique to compare the expression levels of the α 1 subunit between the two cell lines. Our Western blot analysis detected α 1 as a single band at approximately 51 kDa. After normalizing these bands to GAPDH, it was determined that CCRF-CEM expressed significantly higher levels of GABA_AR- α 1 compared to Jurkat cells ($P < 0.01$).

Two other GABA_AR subunits were examined in this study, GABA_AR- β 1 and GABA_AR- β 3. Previous studies have reported high mRNA and protein expression levels of the β 3 subunit in Jurkat cells¹⁴⁷. Thus, we wanted to examine whether CCRF-CEM cells also expressed this subunit. Due to the nature of the primary antibody for β 3, immunocytochemistry was not a viable option. However, using Western blot, β 3 was detected as a single band at approximately 56 kDa in both cell lines. Following normalization to GAPDH, it was determined that Jurkat cells expressed significantly higher levels of β 3 protein than CCRF-CEM cells ($P < 0.05$). Lastly, the β 1 subunit was also examined in both cell lines using Western Blot. A single band at approximately 52 kDa was detected in both cell lines. There were no significant differences in the expression of this subunit between Jurkat and CCRF-CEM cells ($P > 0.05$).

Figure 3.6



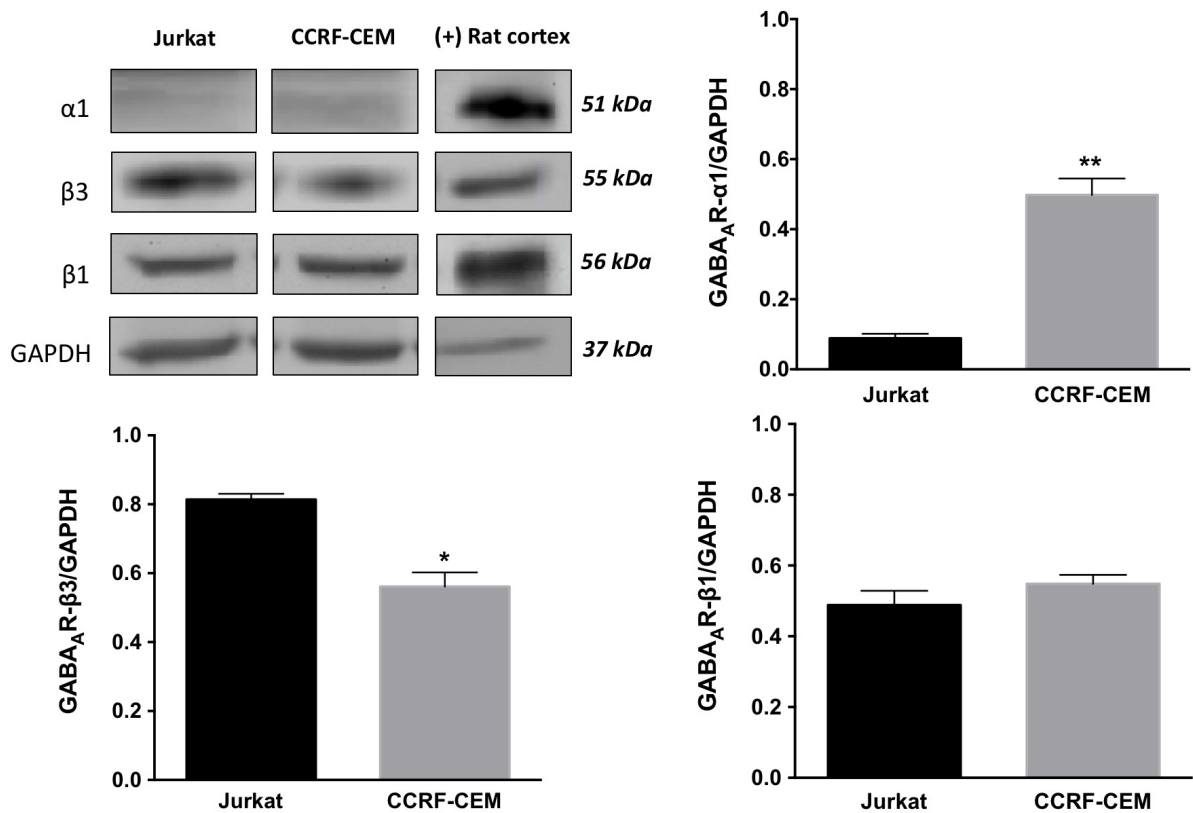


Figure 3.6 Protein expression of GABA_AR-α1, β1, and β3 subunits in cell lines.

Immunocytochemistry and Western blot were used to detect the protein expression levels of various GABA_AR subunits in the two cell lines. **A)** Representative immunofluorescence images of Jurkat and CCRF-CEM cells stained with anti-GABA_AR-α1 (Cy3, Red) and DAPI for nuclei (Blue). **B)** Representative Western blot images of GABA_AR-α1, β1, and β3 in whole cell lysates of Jurkat and CCRF-CEM. 100 μg of protein was loaded for GABA_AR-α1 and β1 detection while 60 μg for β3 detection. Densitometry was performed using GAPDH as a loading control. The normalized protein expression levels of GABA_AR-α1, β1, and β3 were averaged over several trials and analyzed using an unpaired student's T-test. Data are represented as a mean ± SEM (n=3). Each graph represents data for a different subunit. (* indicates P < 0.05, ** indicates P < 0.01).

3.3 Effects of GABA_AR Signaling and Blockade on Functions of Jurkat and CCRF-CEM Lines

The third aim of this thesis was to examine the effects of GABA_AR activation and blockade on the activities and functions of the two cell lines. Specifically, we examined the effects of GABA_AR signaling on cell metabolic activity, surface expression of CRTh2, NFATc2 expression, and SOCE magnitude. Lastly, we stimulated the cells with PHA and PMA to see whether cell activation could affect the expression levels of GABA_ARs. The results of this aim are presented in this following section.

3.3.1 GABA_AR blockade enhances cell metabolic activity in Jurkat cells

An MTT assay was conducted on Jurkat and CCRF-CEM cells following treatment with GABA (100 μ M) or the selective GABA_AR antagonist bicuculline (100 μ M) for 24 h. GABA treatment did not affect the metabolic activity in either cell lines. On the other hand, bicuculline significantly enhanced metabolic activity in Jurkat cells ($P < 0.001$) while having no effect on CCRF-CEM cells (**Figure 3.7**). This suggests that under normal conditions, GABA_AR signaling plays a role in regulating cell metabolic activity in Jurkat cells.

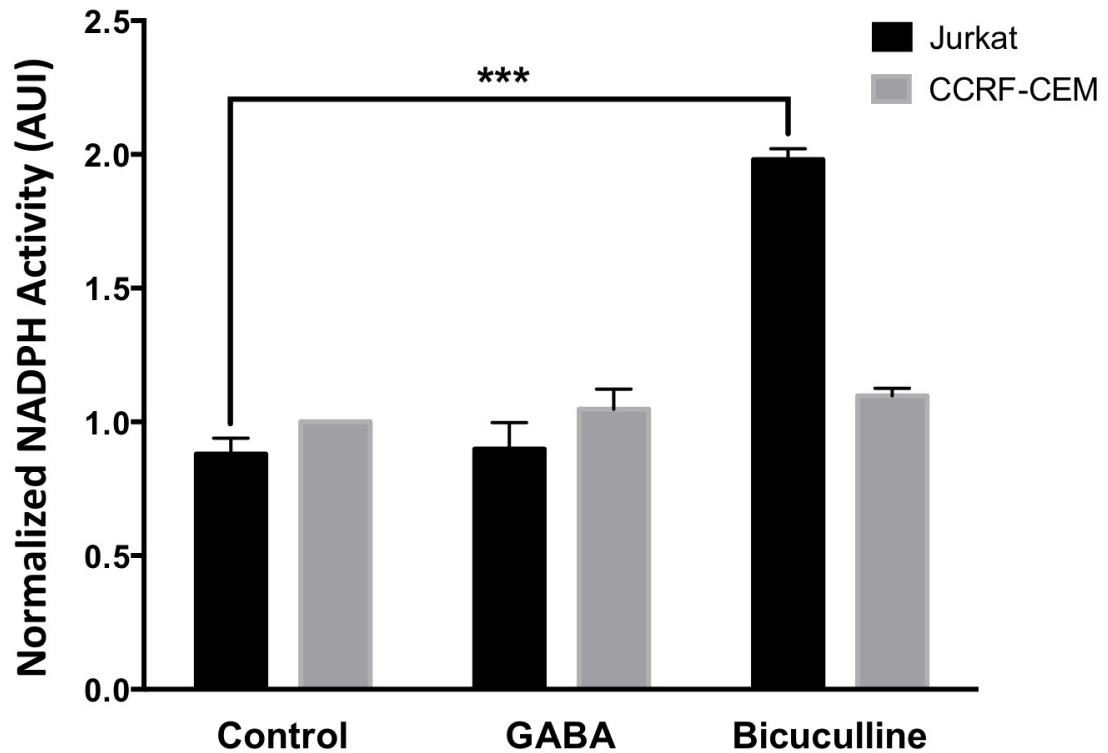


Figure 3.7 Effects of GABA and bicuculline on cell metabolic activity.

MTT readout for Jurkat and CCRF-CEM cells treated without (control) or with GABA (100 μ M) or bicuculline (100 μ M) for 24 h. The data is represented as a fold change from the average metabolic activity of control CCRF-CEM cells. The values from each treatment were analyzed by Two-Way ANOVA followed by a post-hoc Tukey's test to compare the cell lines and treatments within each cell line. The data are presented as a mean \pm SEM. (***) indicates $P < 0.001$)

3.3.2 GABA_AR blockade enhances CRTh2 surface expression in CCRF-CEM cells

CRTh2 is a GPCR expressed on the surface of T_H2 cells. It can be activated by prostaglandins and is critical for the survival and activity of T_H2 cells. With assistance from Meerah Vijeyakumaran in Dr. Lisa Cameron's lab, flow cytometry was performed to analyze the surface expression of this receptor following GABA (100 μM) or bicuculline (100 μM) treatment for 24 h. Firstly, CCRF-CEM cells expressed significantly higher levels of CRTh2 in comparison to Jurkat cells ($P < 0.001$; **Figures 3.8A** and **3.8B**). GABA had no effect on surface CRTh2 expression in either cell line while bicuculline significantly enhanced CRTh2 surface expression in the CCRF-CEM cells. This suggests that under control conditions, GABA_AR signaling mechanisms could be playing a regulatory or suppressive role in CRTh2 surface expression in the CCRF-CEM cells.

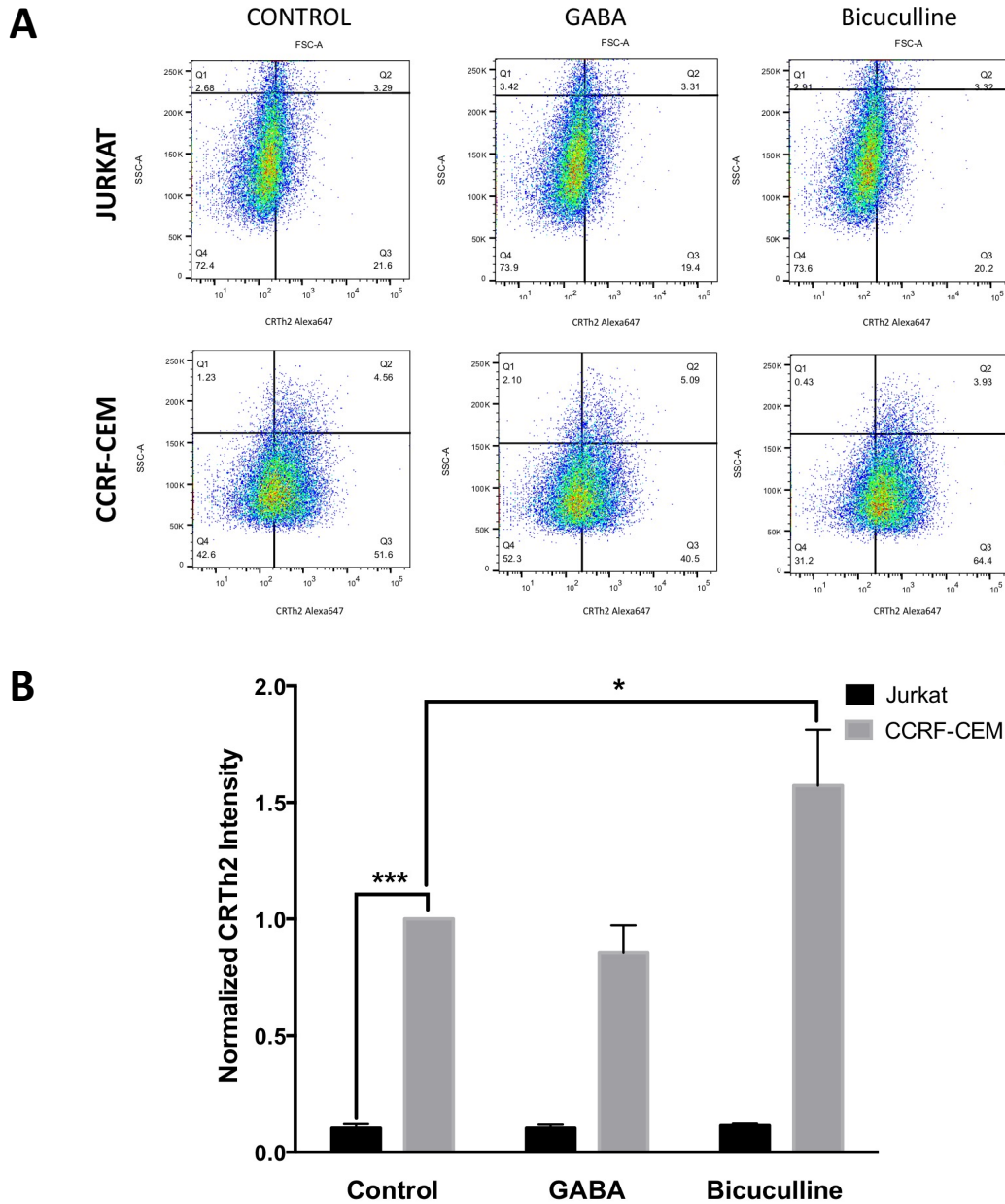


Figure 3.8 Flow cytometric analysis of surface CRTh2 receptor expression.

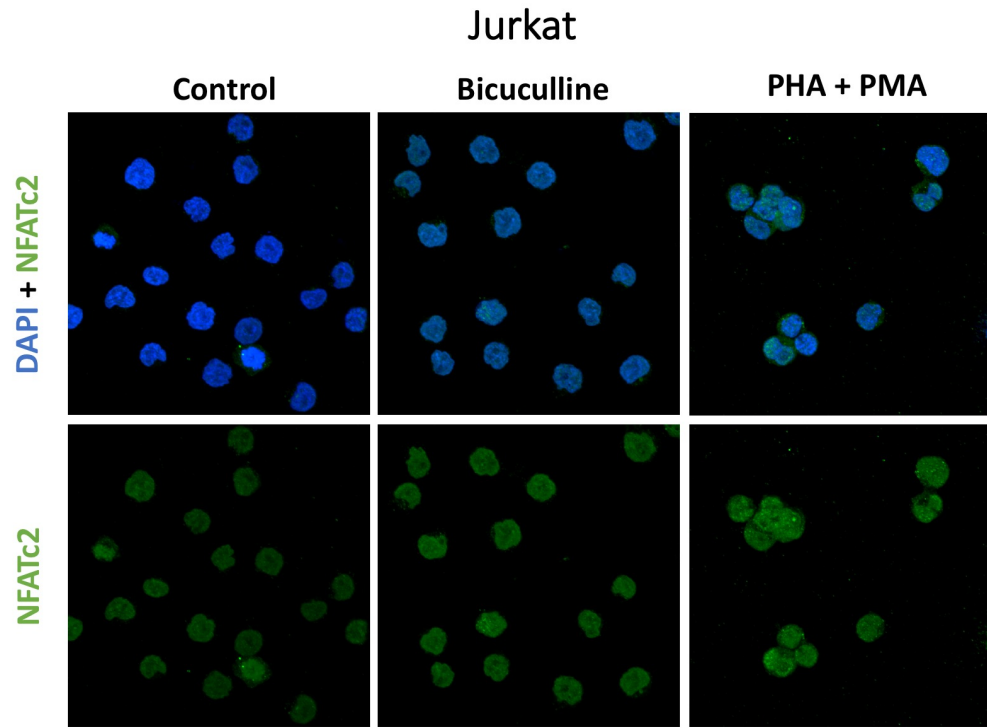
A) Representative flow cytometric plots for surface CRTh2 expression in Jurkat and CCRF-CEM cells. The x-axes represent the population of CRTh2-expressing cells and the y-axes represent side scatter. **B)** The intensity of CRTh2 detection was normalized to that of control CCRF-CEM cells. The average values from each treatment were analyzed by Two-Way ANOVA followed by a Tukey's Test to compare the cell lines and treatments within each cell line. The data are presented as a mean \pm SEM. (* indicates $P < 0.05$, *** indicates $P < 0.001$, both relative to the control CCRF-CEM group).

3.3.3 GABA_AR blockade increases nuclear NFATc2 expression in Jurkat cells

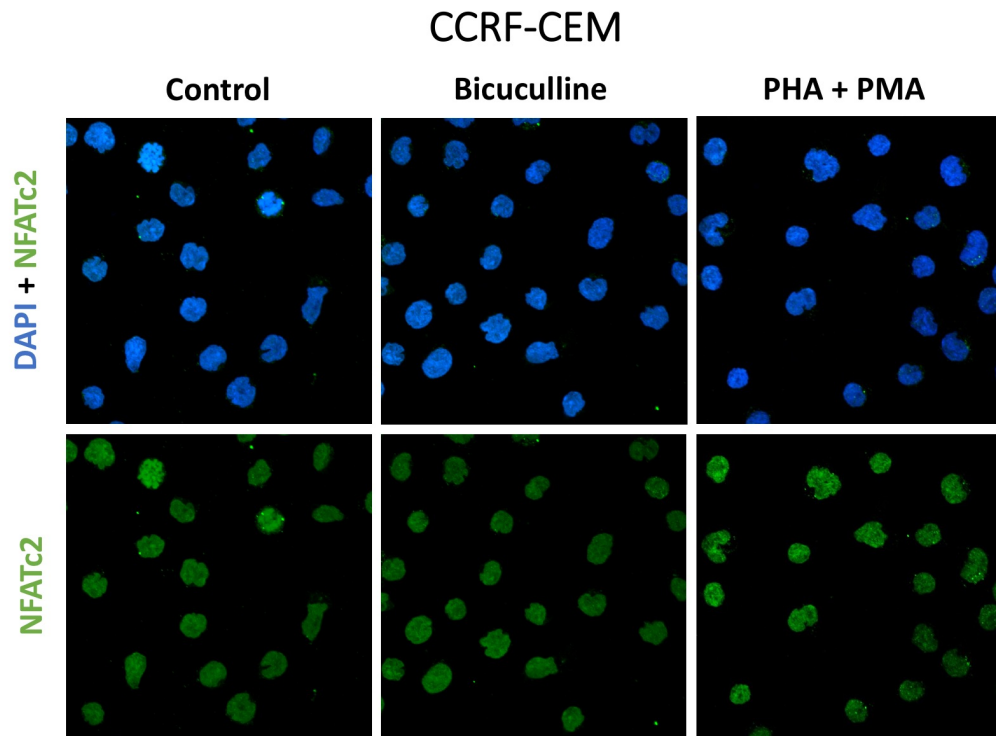
NFAT is a key transcription factor present in the cytoplasm of resting T cells. When T cells are activated, NFAT translocates into the nucleus to promote the transcription of genes required for T cell functions¹⁶⁰. We examined the nuclear expression levels of NFATc2 in Jurkat and CCRF-CEM using immunocytochemistry and Western Blot. Interestingly, NFATc2 expression was co-localized with DAPI (nucleus marker) in all conditions (**Figures 3.9A and 3.9B**), suggesting that these cell lines are activated and Ca²⁺ signaling occurs even without any stimulation.

Using Western blot, we found that the selective GABA_AR antagonist bicuculline significantly increased NFATc2 expression in Jurkat cells ($P < 0.05$) while having no effect on CCRF-CEM cells (**Figure 3.9C**). GABA treatment had no effect on NFATc2 expression in either cell line (data not shown). This suggests that under control conditions, GABA_AR signaling plays an active role in suppressing NFATc2 expression in Jurkat cells. Moreover, CCRF-CEM cells contain higher levels of NFATc2 under control conditions. It could be possible that we did not see an effect of bicuculline in the CCRF-CEM cells due to saturation in the levels of NFATc2.

A



B



C

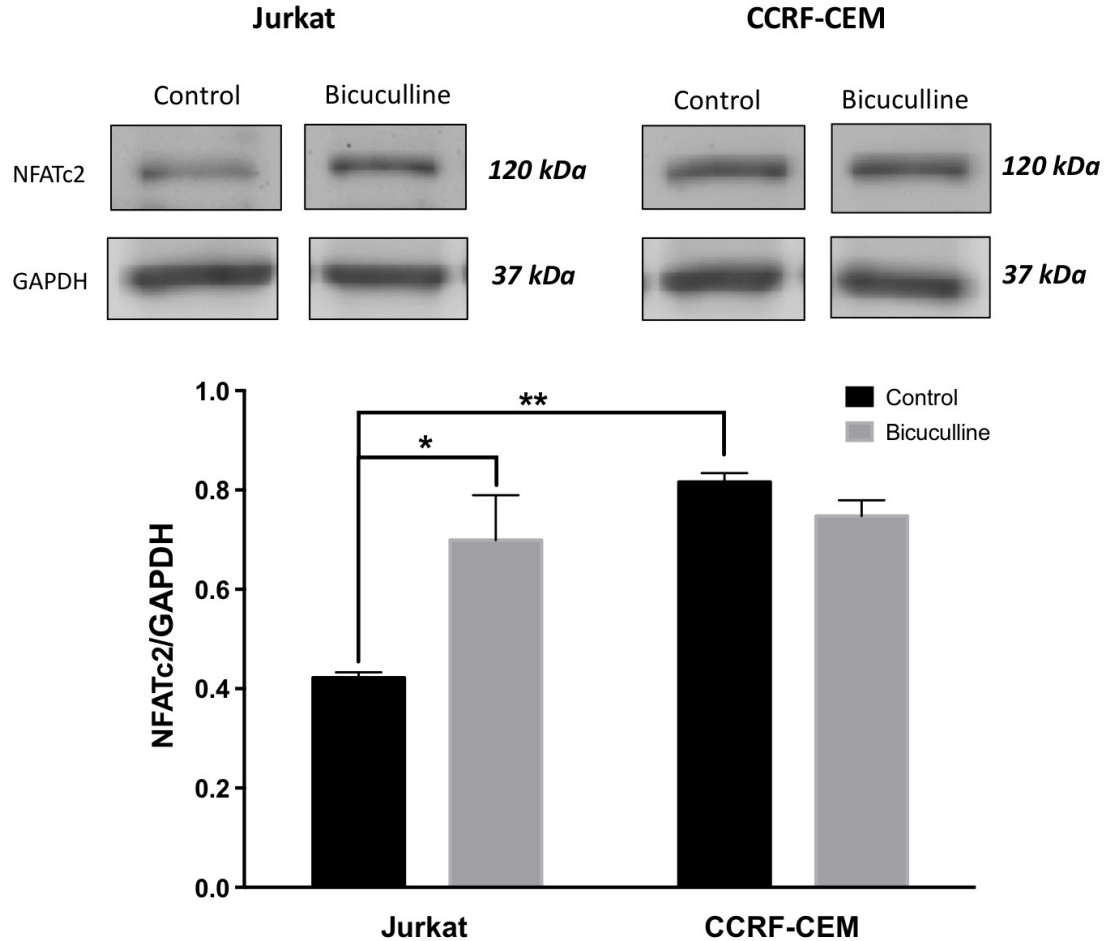


Figure 3.9 Protein expression of nuclear NFATc2 in Jurkat and CCRF-CEM cells.

Expression levels of nuclear NFATc2 under control, bicuculline, and PHA/PMA conditions were examined. **A)** Representative immunofluorescence images of NFATc2 (Alexa488; Green) and DAPI (Blue) staining in Jurkat and CCRF-CEM cells under various conditions. The top panels show an overlay of NFATc2 and DAPI while the bottom panels show NFATc2 alone. **B)** Western Blot of NFATc2 and GAPDH in whole cell lysates of Jurkat and CCRF-CEM cells treated with or without bicuculline for 24 h. The average values from each treatment were analyzed by Two-Way ANOVA to compare the cell lines and treatments within each cell line. The data are presented as a mean \pm SEM. (* indicates $P < 0.05$; ** indicates $P < 0.01$, both relative to control Jurkat cells).

3.3.4 GABA_AR blockade differentially regulates SOCE in the two cell lines

Store-operated Ca²⁺ entry (SOCE) is a critical process in T cells following cell activation. We proposed that GABA_AR signaling affects downstream activities in the two cell lines by modulating SOCE through its effects on membrane potential. Using Ca²⁺ based-fluorescence imaging in control, GABA pretreated, and bicuculline pretreated cells, the magnitudes of SOCE following thapsigargin addition were compared. The addition of thapsigargin alone resulted in a rise in Rhod-4AM fluorescence intensity in both cell lines. In GABA pretreated cells, there were no significant effects on the magnitude of SOCE in either cell line (**Figures 3.10A and 3.10B**). However, in cells pretreated with bicuculline, Ca²⁺ entry was enhanced in Jurkat cells and reduced in CCRF-CEM cells. Interestingly, bicuculline treatment alone also caused an enhancement in Rhod-4AM fluorescence in the Jurkat cells (**Figure 3.10C**).

The traces from several trials were averaged to construct a summary plot of SOCE responses for each cell line (**Figures 3.10E and 3.10F**). GABA pre-treatment had no significant effect on TG-induced SOCE in either cell line. Bicuculline caused a significant enhancement in Ca²⁺ entry in Jurkat cells starting at 8 min. In CCRF-CEM cells, bicuculline significantly reduced Ca²⁺ entry starting at 12 min. These data suggest that GABA_AR blockade differentially modulates SOCE magnitude in both cell lines.

Figure 3.10

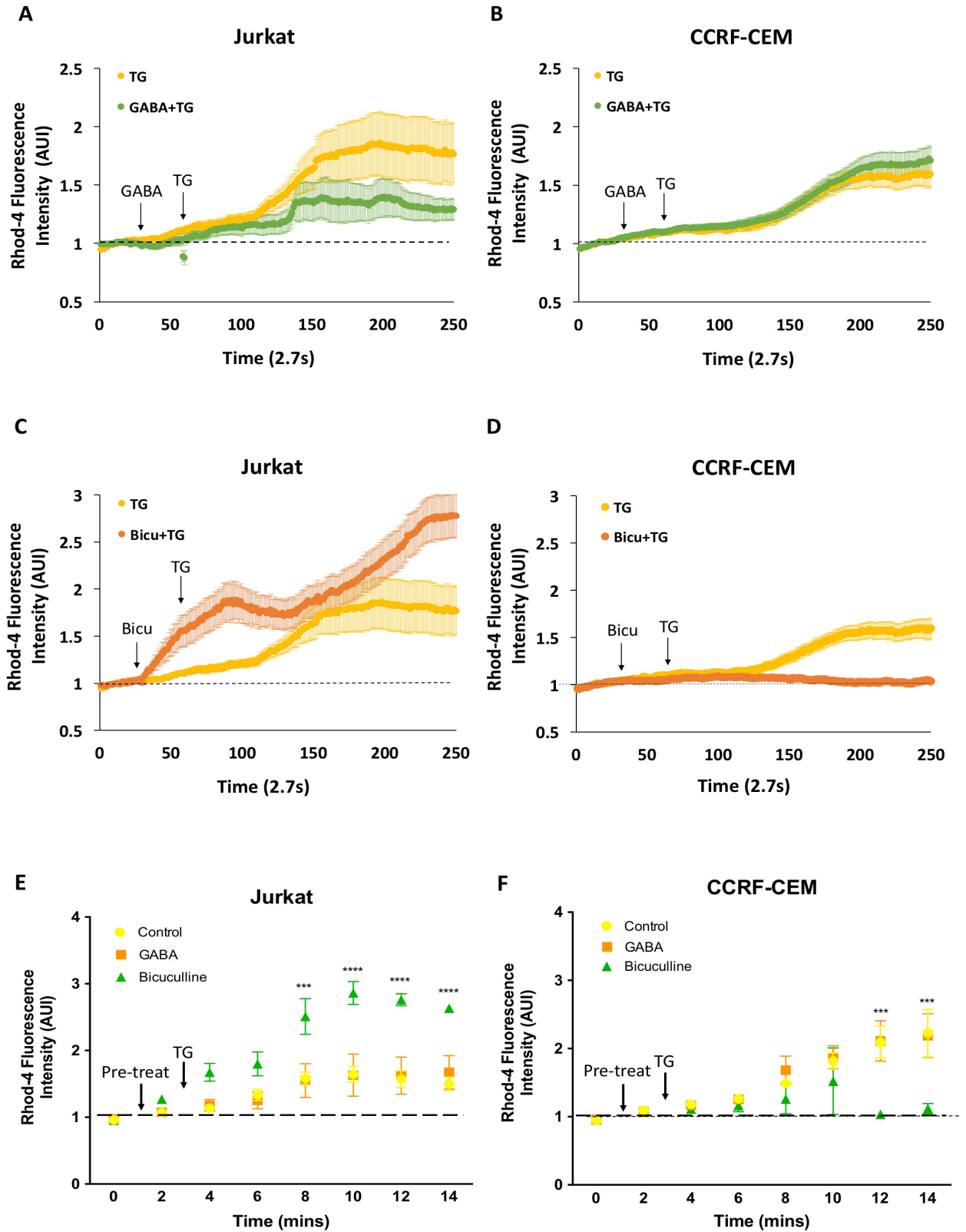


Figure 3.10 Effects of GABA and bicuculline pre-treatment on TG-induced Ca²⁺ entry.

Ca²⁺-based fluorescence imaging was used to examine the effects of GABA and bicuculline pre-treatment on thapsigargin-induced Ca²⁺ entry in Jurkat and CCRF-CEM cells. Representative traces of **A)** Rhod-4AM fluorescence in thapsigargin only (yellow) and GABA pre-treatment (green) conditions in Jurkat cells, **B)** Rhod-4AM fluorescence in thapsigargin only (yellow) and GABA pre-treatment (green) conditions in CCRF-CEM cells, **C)** Rhod-4AM fluorescence in thapsigargin only (yellow) and bicuculline pre-treatment (orange) conditions in Jurkat cells, and **D)** Rhod-4AM fluorescence in thapsigargin only (yellow) and bicuculline (orange) pre-treatment conditions in CCRF-CEM cells.

The average Rhod-4AM fluorescence intensity at each time point was taken for several traces under the same experimental conditions and analyzed using a Two-Way ANOVA. **E)** Average Rhod-4AM fluorescence values for thapsigargin, GABA pre-treatment, and bicuculline pre-treatment in Jurkat cells. **F)** Average Rhod-4AM fluorescence values for thapsigargin, GABA pre-treatment, and bicuculline pre-treatment in CCRF-CEM cells. Data are represented as a mean \pm SEM (n=3). (***) indicates $P < 0.001$; (****) indicates $P < 0.0001$.

3.3.5 GABA_AR subunit expression changes following mitogenic stimulation

Physiologically, T cells require antigen presentation at the TCR and a co-stimulus to induce SOCE and cell activation. However, many researchers use other methods to stimulate T cells. Phytohaemagglutinin is a lectin that can crosslink TCRs and cause receptor activation. When used in conjunction with PMA, a PKC activator, the combination can induce strong activation of T cells¹⁶¹. In this part of the project, we wanted to examine whether T cell stimulation would affect the expression levels of GABA_AR subunits. It is well known that the activation state of T cells can affect gene expression and T cells in activated states can behave differently than those at rest. Since this project was conducted on resting Jurkat and CCRF-CEM cells, this experiment would provide information on how these cells regulate GABA_AR expression in response to stimulation. Both cell lines were stimulated with PHA (1 µg/mL) and PMA (50 ng/mL) over a period of 24 h, 48 h, and 72 h and the protein levels of GABA_ARs were then examined by western blot.

Stimulation of Jurkat cells did not result in any changes in GABA_AR-β3 expression (**Figure 3.11A**) throughout the time course. Stimulation of CCRF-CEM cells significantly reduced GABA_AR-β3 expression by 48 h ($p < 0.05$), and further reduced at 72 h (**Figure 3.11B**; $P < 0.01$). The expression levels of another subunit, GABA_AR-β1 was also examined. Stimulation of Jurkat cells did not result in any changes in GABA_AR-β1 expression (**Figure 3.12A**) throughout the time course. Stimulation of CCRF-CEM cells did not significantly affect GABA_AR-β1 expression either; however, there was a general upward trend associated with stimulation (**Figure 3.12B**).

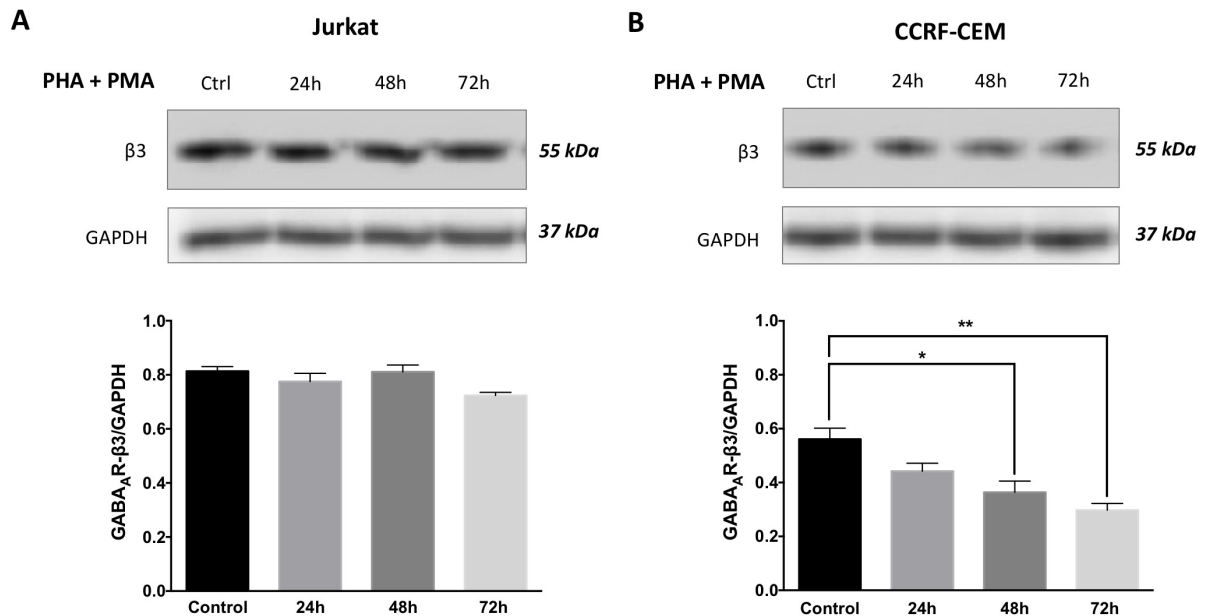


Figure 3.11 Effect of PHA/PMA stimulation on GABA_AR- $\beta 3$ expression in the cell lines.

A) Representative Western blot of GABA_AR- $\beta 3$ in Jurkat cells stimulated with PHA/PMA (1 $\mu\text{g}/\text{mL}$; 50 ng/mL) for 24 h, 48 h, or 72 h. The bands were normalized to a GAPDH loading control and plotted in a histogram. **B)** Representative Western blot of GABA_AR- $\beta 3$ in CCRF-CEM cells stimulated with PHA/PMA for 24 h, 48 h, or 72 h. The bands were normalized to a GAPDH loading control and plotted on a histogram. The average values of $\beta 3$ expression were obtained from several trials and analyzed using a One-way ANOVA followed by a Tukey's Test to determine statistical significance. Data are presented as a mean \pm SEM (n=4). (* indicates $P < 0.05$; ** indicates $P < 0.01$).

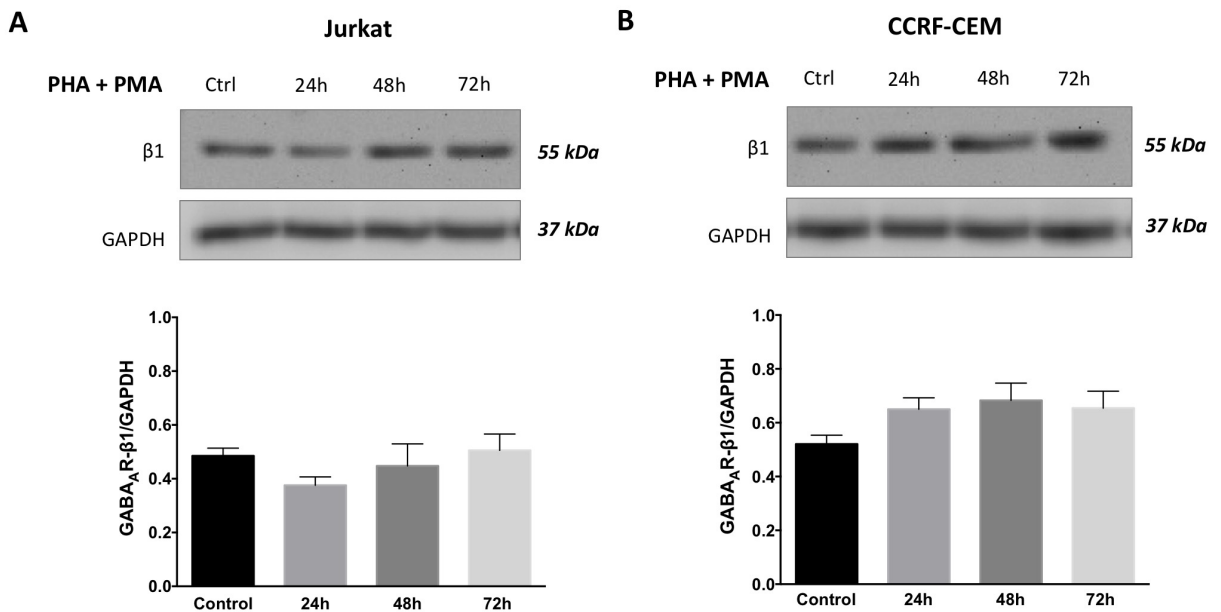


Figure 3.12 Effect of PHA/PMA stimulation on GABA_AR- β 1 expression in the cell lines.

A) Representative Western blot of GABA_AR- β 1 in Jurkat cells stimulated with PHA/PMA (1 μ g/mL; 50 ng/mL) for 24 h, 48 h, and 72 h. The bands were normalized to a GAPDH loading control and plotted in a histogram. **B)** Representative Western blot of GABA_AR- β 1 in CCRF-CEM cells stimulated with PHA/PMA for 24 h, 48 h, and 72 h. The bands were normalized to a GAPDH loading control and plotted on a histogram. The average values of β 1 expression were obtained from several trials and analyzed using a One-way ANOVA followed by a Tukey's Test to determine statistical significance. Data are presented as a mean \pm SEM (n=4).

Chapter 4: Discussion

4.1 Summary of results

In the present study, we first demonstrated that the human T_H cell lines Jurkat and CCRF-CEM bear similarities to T_H1 and T_H2 cells, respectively, and that both cell lines express GAD and GABA_AR subunits. Next, we found that GABA_AR blockade differentially affected the metabolic activity and surface expression of CRTh2 in the cell lines. Lastly, we showed that selective blockade of GABA_ARs increased intracellular Ca²⁺ levels and the expression of active NFATc2 in Jurkat cells but not in CCRF-CEM cells. These results demonstrated for the first time that GABA_AR-mediated autocrine signaling differentially regulates the functions of different T_H effector cell subtypes by modulating SOCE.

4.2 Unique features of Jurkat and CCRF-CEM cells

The cell lines used for this study were the Jurkat and CCRF-CEM cells, both of which were derived from human cancerous T lymphomas. There were two main reasons for why we chose to work with cell lines rather than primary cells. First, the aim of this thesis was to determine whether autocrine GABA signaling can play unique regulatory roles in different T_H cells types. Since this was a relatively novel proposal, the goal was to first establish proof of concept for this topic. Second, we were under a strict time restraint due to the nature of the accelerated graduate program and by using cell lines, we were able to obtain a sufficient number of cells for experiments. In other words, we simply wanted to select two unique cell lines to study the effects of GABA_AR signaling in different T_H phenotypes.

We selected the Jurkat line because it is the most widely used T cell model in the study of T_H cell signaling¹⁶² and our results showed that they contain some features of T_H1 cells. The

CCRF-CEM line was chosen following a recommendation from Dr. Lisa Cameron, who at the time was investigating this cell line as a T_H2 cell model due to high expression levels of CRTh2. As introduced previously, CRTh2 is a GPCR that plays important roles in the development and function of T_H2 cells, and has been called the most reliable marker for detecting T_H2 cells³⁶.

Dr. Lisa Cameron's lab demonstrated that Jurkat and CCRF-CEM cells differed greatly in the mRNA levels of T_H1 and T_H2 markers. Preliminary qPCR data showed that CCRF-CEM cells contained significantly higher levels of mRNA for CRTh2 than Jurkat cells. Moreover, CCRF-CEM cells also contained higher mRNA levels of GATA3 and IL-13, both of which are markers of T_H2 cells. On the other hand, Jurkat cells contained higher mRNA levels of IFN- γ , a T_H1 signature cytokine¹⁶³, suggesting that they more closely resemble T_H1 cells. It should be emphasized that physiologically, the boundaries between T_H1 and T_H2 cells are not black and white and additional T_H subtypes exist. In the present study, we simply propose that Jurkat cells and CCRF-CEM cells bear features of T_H1 and T_H2 cells, respectively. To further determine whether they were appropriate cellular models of T_H subtypes, we characterized differences in proliferation and morphology as well as SOCE and NFATc2 levels.

4.2.1 Cell size, proliferation and metabolism

The relationship between the cell size and proliferation rate of multicellular organisms is not well understood¹⁶⁴. It has been proposed that there is an indirect relationship between these two factors because cells must grow to a certain size before undergoing mitosis and cell division¹⁶⁵. Our analysis showed that relative to CCRF-CEM cells, Jurkat cells were larger in size with a slower proliferation rate (**Figures 3.1 and 3.2**). A possible explanation for this difference in cell size could be that the faster proliferative rate of CCRF-CEM cells led to a

larger proportion of smaller, freshly divided cells at any given time. However, the proliferation of cancerous lines is dependent on many other factors that we did not explore.

Cellular metabolism is required for sustaining cell growth and proliferation¹⁶⁶. Cells that are metabolically active convert MTT, a tetrazolium compound, into formazan by NAD(P)H-dependent oxidoreductases, producing a purple colour. The readout of this type of assay is in the form of a colorimetric value from which cell metabolic activity is deduced. Although statistically insignificant, there was a trend towards a higher resting metabolic activity in CCRF-CEM cells when compared to Jurkat cells (**Figure 3.7**). This would be consistent with the higher proliferation rate observed in CCRF-CEM cells because cell metabolic activity directly fuels mitotic activity¹⁶⁷. Further studies need to be done to confirm whether there are differences in resting cell metabolic activity.

4.2.2 CRAC channels and SOCE

Considering that SOCE mediated through CRAC channels is critical for gene expression and downstream activities in T_H cells, we examined the expression levels of CRAC channel proteins in the two cell lines using a Western blot. Our results showed that both Jurkat and CCRF-CEM cells express Orai1 and STIM1 (**Figure 3.3**), the key protein components of CRAC channels¹⁶⁸. The expression levels of Orai1 and STIM1 were high in both cell lines, suggesting that CRAC channels are critical for the function of these cells.

It has been reported that different phenotypes of T_H cells contain unique Ca²⁺ signaling patterns, magnitude, and rates¹⁶⁹. Following analysis of CRAC channel proteins, we examined the activity of CRAC channels by using thapsigargin to pharmacologically evoke SOCE. This compound is commonly used to induce cellular SOCE in experimental settings by blocking SERCA pumps, which are responsible for actively transporting cytosolic Ca²⁺ back into the

ER to maintain Ca^{2+} stores. When SERCA pumps are inhibited, intraluminal Ca^{2+} levels in the ER immediately decrease and SOCE is induced without the need for physiological stimulation of receptors.

In our analyses, the magnitude of SOCE was inferred from the fluorescence intensity of Ca^{2+} indicator Rhod-4AM. Since this technique only allowed for the measurement of relative changes in Ca^{2+} and not actual Ca^{2+} concentrations, we could not quantitatively compare the resting/basal levels of intracellular concentration of Ca^{2+} between the two cell lines. Future studies should involve using quantitative measures of intracellular Ca^{2+} to compare basal levels of Ca^{2+} in these cells. When thapsigargin (1 μM) was applied to each cell line, the average magnitude of change in Rhod-4AM fluorescence was significantly higher in the Jurkat cells than in the CCRF-CEM cells (**Figure 3.4C**). This reflected a relatively larger SOCE magnitude in the Jurkat cells when CRAC channels were activated.

Differences in Ca^{2+} signaling patterns have been observed in subsets of T_H cell types. One study using flow cytometry to observe Ca^{2+} levels in primary T_{H1} and T_{H2} cells following PHA stimulation reported that T_{H2} cells underwent a lower level of Ca^{2+} flux upon stimulation¹⁶⁹. The authors of this paper proposed that differences in Ca^{2+} flux of T_{H1} and T_{H2} cells may contribute to distinct cytokine production patterns by these subsets. Another study using Fura-2 Ca^{2+} indicator and thapsigargin as a stimulus found similar results¹⁷⁰. They proposed that the combination of a faster Ca^{2+} clearance mechanism and weaker Ca^{2+} -activated K^+ currents in T_{H2} cells accounted for the lower Ca^{2+} response of T_{H2} cells. These data are in line with what we found in our study, in which the CCRF-CEM (our T_{H2} -like model) showed a smaller magnitude of SOCE compared to the Jurkat cells. It is possible that CCRF-CEM cells contain higher resting levels of Ca^{2+} , thereby reducing the chemical gradient and driving force for Ca^{2+} entry during SOCE.

4.2.3 Active form of NFAT

Nuclear factor of activated T cells (NFAT) is a family of transcription factors known to play crucial roles in regulating the immune system. NFAT is a key regulator of T cell development, differentiation, and activation. There are five types of NFAT proteins: NFATc1, NFATc2, NFATc3, NFATc4, and NFAT5, with NFATc1 through NFATc4 being regulated by Ca^{2+} signaling¹⁶⁰. During TCR activation, intracellular Ca^{2+} levels rise and activate the Ca^{2+} sensor protein calmodulin, which in turn activates the serine/threonine phosphatase calcineurin. The activated calcineurin dephosphorylates serine-rich domains in the amino terminal of NFAT proteins, resulting in conformational changes to NFAT and translocation into the nucleus where it regulates gene expression. It is thought that different Ca^{2+} signaling patterns activate different sets of NFAT proteins to modulate unique gene transcription profiles¹⁷¹. We studied the activity levels of NFAT2c in the two cell lines, because NFATc2 is critical for both T_H1 and T_H2 responses¹⁷².

In our experiments, we used a monoclonal antibody that detects NFATc2 in the nucleus¹⁷³. Our immunocytochemistry assays detected NFATc2 completely co-localized with nuclear DAPI staining, further supporting that this antibody detects NFATc2 in the nucleus (**Figure 3.9A** and **3.9B**). Interestingly, this antibody also detected the nuclear localization of NFATc2 in resting, non-stimulated cells, suggesting that Ca^{2+} signaling occurs in these cells even under resting conditions, thereby facilitating nuclear localization of NFATc2. This would also explain why these cells proliferate without the need for external stimulation. Using Western blot, we found that CCRF-CEM cells expressed higher levels of NFATc2 under control conditions (**Figure 3.9C**). Future studies should focus on examining other forms of NFAT proteins. Given that NFAT activity is associated with cell proliferation, this may reflect the difference in proliferation rate between the two cell lines.

4.2.4 Autocrine GABA signaling system

Autocrine signaling occurs when a cell produces and secretes chemical messengers that act upon receptors on the same cell, leading to biological changes. Almost all cells types are under the influence of autocrine signaling mechanisms. In the case of T cells, chemokine and purinergic receptors are expressed on the cell surface and are activated by factors secreted by the same cells^{7,174}. We examined whether the two T_H cell lines differ in the level of autocrine GABA signaling-related proteins. Specifically, we looked at the expression of three different GABA_AR subunits in both cell lines. These were the GABA_AR- α 1, β 1 and β 3 subunits (**Figure 3.6**). Jurkat cells expressed higher levels of the β 3 subunit, CCRF-CEM cells expressed higher levels of the α 1 subunit, and no differences were observed in the levels of β 1 expression. Our results in the Jurkat cells were consistent with a previous study that found β 3 to be the most highly expressed GABA_AR-subunit in Jurkat cells while α 1 subunits were expressed at significantly lower levels¹⁴⁷. The same study also found drastic differences among GABA_AR subunit expression between naïve CD4⁺ cells isolated from rat, mice and humans. Clearly, the expression levels of different GABA_AR subunits vary quite dramatically between different cell types and species. What dictates this unique composition of GABA_AR subunits in different cell types remains unclear. What is known, however, is that both the α - and the β -subunits are required for GABA_AR activation¹⁷⁵. GABA_ARs have two GABA binding sites located at the interface between α and the β subunits^{126,176}. Both Jurkat and CCRF-CEM cells expressed at least one type of α subunit and one type of β subunit, suggesting that these cells contain functional GABA_ARs.

Our immunocytochemistry and Western blot assays showed that both cell lines expressed the two isoforms of GAD (GAD65/67), suggesting that these cells produce and secrete GABA molecules (**Figure 3.5**). In this regard, a previous study conducted by Bhat and

colleagues detected GABA in the culture media of naïve T_H cells¹⁴⁶. These results suggest that both Jurkat and CCRF-CEM cells could be equipped with a constitutively active autocrine GABA signaling system.

In summary, the results discussed thus far showed that Jurkat and CCRF-CEM cells contain T_H1-like and T_H2-like properties and that both cell lines express GAD and GABA_ARs, likely possessing an autocrine GABA signaling system. Therefore, they are suitable cell lines for the study of GABA_AR signaling in different T_H cell types.

4.3 GABA signaling in Jurkat and CCRF-CEM Cells

In the last decade, numerous studies have established GABA as an immunomodulatory molecule^{9,140}. Many of them have found GABA to be immunosuppressive and protective against autoimmune and inflammatory conditions. In the context of adaptive immunity, autoimmunity and related inflammation are generally considered to be mediated by T_H1 (and more recently, T_H17) cells and cytokines. However, there have not been many reports on how GABA affects T_H2 cells and T_H2-mediated diseases. We proposed that although GABA signaling inhibits T_H1 responses, it may not inhibit all subtypes of T_H cells. Instead, GABA signaling could potentially upregulate the activity/function of certain phenotypes of T_H cells. Using Jurkat and CCRF-CEM cells, two unique T_H cell lines, we tested this idea by examining the effects of GABA_AR activation and blockade on certain activities of these cells.

4.3.1 Role of GABA signaling on cell metabolism and receptor protein expression

We first assessed the effects of GABA_AR signaling on cell metabolic activity and CRTh2 surface expression in the two cell lines. As introduced previously, cell metabolic activity reflects the activation state of cells while CRTh2 expression is essential for T_H2 cell

function. We did not observe any effects on these two attributes from the addition of GABA itself. However, we did find that GABA_AR blockade with its selective antagonist bicuculline had unique effects in the two cell lines. Specifically, bicuculline treatment enhanced the surface expression of the CRTh2 receptor in CCRF-CEM cells but did not affect its cell metabolic activity (**Figures 3.7 and 3.8**). In Jurkat cells, bicuculline significantly enhanced cell metabolic activity but did not affect surface expression of CRTh2. These results suggest that under resting conditions, Jurkat cells are under the regulation of autocrine GABA signaling which restrains cellular metabolic activity, whilst in CCRF-CEM cells, autocrine GABA_AR signaling regulates the surface expression levels of CRTh2 receptors. When GABA_ARs are blocked with an antagonist, these cells are released from the regulatory effects of GABA, resulting in changes to cellular phenotype. Taken together, these results imply that autocrine GABA signaling distinctively regulates the function/activity of different T_H cells.

4.3.2 Effects of GABA signaling on SOCE and NFAT expression

To understand the potential mechanisms by which autocrine GABA_AR signaling regulates these T_H cell lines, we examined the effects of GABA and bicuculline on SOCE and NFAT expression. Our results showed that GABA had no significant effect on SOCE or NFAT expression in either cell line, which was consistent with what was reported in the MTT and CRTh2 flow cytometry experiments. Excitingly, GABA_AR blockade with bicuculline significantly enhanced nuclear NFATc2 expression and SOCE magnitude in Jurkat cells. This suggests that a constitutively active autocrine GABA signaling system restrains activation of this cell line by limiting SOCE and NFAT expression. In CCRF-CEM cells, bicuculline did not affect nuclear NFATc2 expression but significantly reduced SOCE magnitude. This suggests that under resting conditions, a constitutively active autocrine GABA signaling

system also exists in these cells to facilitate, rather than limit, SOCE. The results discussed thus far confirm that an autocrine GABA signaling system plays unique roles in each cell lines, and its actions are likely mediated through differential modulation of SOCE.

4.3.3 Potential mechanisms by which autocrine GABA signaling regulates SOCE

As introduced previously, SOCE is the primary route of Ca^{2+} influx during T_H cell activation and its magnitude is largely dependent on the electrochemical gradient of Cl^- across the cell membrane. The negative resting membrane potential of cells is the main driving force of transmembrane Ca^{2+} movement. The membrane potential of a cell is primarily determined by K^+ and Cl^- conductance, which is in turn determined by the electrochemical gradients of K^+ and Cl^- across the cell membrane. The efflux of K^+ and influx of Cl^- would lead to a more negative membrane potential and hence increased Ca^{2+} influx. For example, in T cells, an increase in SOCE occurs when K^+ channels are activated and cause membrane hyperpolarization¹⁷⁷.

There have been quite a few different values and ranges reported for the resting membrane potential of T cells. One study using flow cytometry reported a value of -70 mV in mouse spleen cells and human T cells¹⁷⁸. Another study examined T cells from healthy and Ataxia Telangiectasia (AT) patients, and reported that T cells from AT patients had a RMP of -46 ± 9 mV, while normal T cells had a potential of -63 ± 4 mV¹⁷⁹. A more recent study found the membrane potential of $\text{CD3}^+/\text{CD45RO}^-$ T cells to be -58 ± 3.6 mV and $\text{CD3}^+/\text{CD45RO}^+$ (memory) T cells to be -37 ± 4.1 mV¹⁸⁰. Clearly, the membrane potential of T cells varies quite dramatically and can be influenced by diseased states and phenotype. This dramatic variation is likely due to differential expression of K^+ and Cl^- channels and/or transporters.

GABA_ARs are pentameric ligand-gated Cl⁻ channels. It is believed that the opening of GABA_ARs causes Cl⁻ efflux and hence depolarization of T cells due to high intracellular Cl⁻ concentrations (30-40 mM)^{181,182}. The Cl⁻ equilibrium potential of T cells has been reported to be around -33 mV¹⁸³. Therefore, activation of GABA_ARs in T cells results in membrane depolarization and decreased Ca²⁺ entry^{148,152}. One study reported that the intracellular Cl⁻ concentration of Jurkat cells was as high as 58 mM¹⁸⁴, suggesting that activation of Cl⁻ channels such as GABA_ARs would lead to strong Cl⁻ efflux and membrane depolarization in these cells. This could largely explain the results we observed in the Jurkat cell line: an enhancement in Ca²⁺ entry following GABA_AR blockade, which means that GABA normally has an inhibitory role on Ca²⁺ entry.

However, this mechanism does not account for our observations in the CCRF-CEM cell lines, where we observed a reduction in Ca²⁺ entry when GABA_ARs were blocked. This suggests that in contrast to Jurkat cells, autocrine GABA_AR signaling normally facilitates Ca²⁺ entry in CCRF-CEM cells. Previous studies in Dr. Lisa Cameron's lab demonstrated that the activation of T_H2 cells downregulates endogenous expression of CRTh2 through an NFAT-mediated pathway¹⁸⁵. This is consistent with our data because NFAT activation requires SOCE, and we found that GABA_AR blockade reduces SOCE in CCRF-CEM cells, thereby inhibiting NFAT signaling and releasing the inhibition to CRTh2 expression.

As simplified in **Figure 4.1**, we propose that Jurkat and CCRF-CEM cells possess different membrane potentials or Cl⁻ equilibrium potentials due to different expression/activity levels of K⁺ and Cl⁻ channels as well as transporters. Specifically, we propose that the Cl⁻ equilibrium potential is below the resting membrane potential in CCRF-CEM cells. Therefore, activation of GABA_ARs would result in Cl⁻ influx, membrane hyperpolarization and enhanced Ca²⁺ entry.

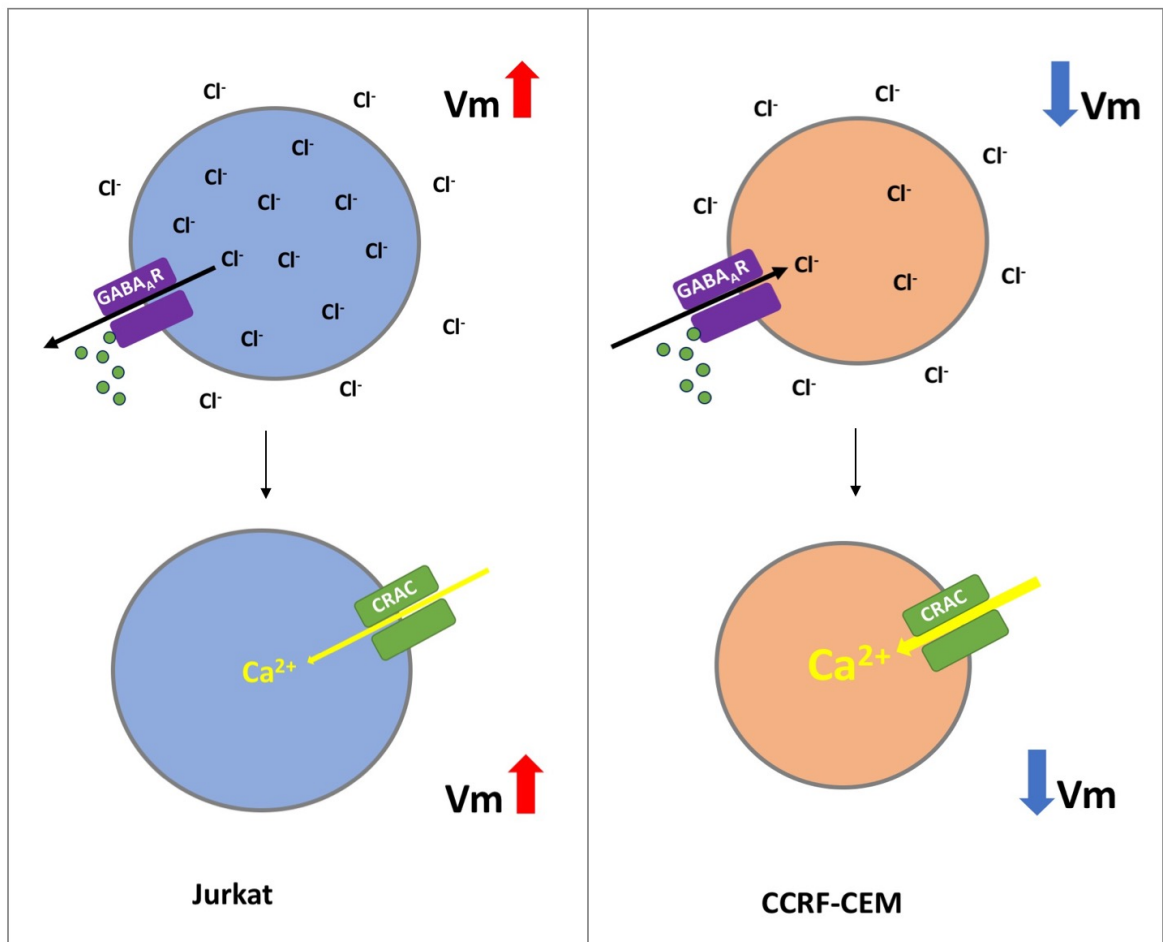


Figure 4.1 Proposed mechanism of how GABA_AR signaling differentially acts on Jurkat and CCRF-CEM cells.

4.3.4 KCC and NKCC

The Cl^- equilibrium potential of a given cell is determined by the transmembrane gradient of Cl^- . The chemical gradient of Cl^- in neurons of the CNS is maintained through the actions of two Cl^- transporters, NKCC and KCC, which intrude and extrude Cl^- , respectively. Immature neurons express higher levels of NKCC and contain relatively high concentrations of Cl^- , resulting in a more positive Cl^- equilibrium potential¹⁸⁶. Thus, activation of GABA_A Rs in immature neurons leads to Cl^- efflux and membrane depolarization. During neuronal development, the expression of KCC increases, resulting in lower intracellular Cl^- concentrations and a lower Cl^- equilibrium potential. Activation of GABA_A Rs in mature neurons leads to Cl^- influx and membrane hyperpolarization. Therefore, changes in the expression of these two Cl^- transporters can lead to opposite actions of GABA_A R signaling¹¹². It is largely unknown whether this reversal in Cl^- intrusion/extrusion transporter expression also occurs in effector T_H cells.

With this knowledge in mind and considering that the expression of Cl^- transporters in T cells have not been well studied, we made an effort to examine the expression of NKCC1, a ubiquitously expressed NKCC as well as KCC3 in the two cell lines. Surprisingly, we detected higher levels of NKCC1 in the CCRF-CEM cells than in Jurkat cells (**Figure 6.2**). This was unexpected because we had proposed that Jurkat cells would contain higher levels of NKCC1 that were responsible for higher levels of intracellular Cl^- . Unfortunately, we were unable to detect KCC3 in either of the cell lines. A possible explanation of this unexpected result is that CCRF-CEM cells express relatively higher levels of Cl^- extrusion transporters (such as KCCs) relative to Cl^- intrusion transporters (such as NKCCs) or that they express less K^+ channels, resulting in a more positive resting membrane potential.

4.4 GABA_AR plasticity during T_H cell activation

A few studies have demonstrated that pharmacological treatments and activation states can modulate the expression of GABA_AR subunits in T cells^{187,188}. We used the mitogen PHA and phorbol ester PMA to stimulate the cell lines. Stimulation of Jurkat cells with these compounds were shown to increase IL-2 production¹⁸⁹. We found that following stimulation over 24 h, 48 h, and 72 h, GABA_AR-β3 expression was reduced in the CCRF-CEM cells, while GABA_AR-β1 expression was trending towards an increase. PHA/PMA stimulation had no effect on GABA_AR-β1 expression in Jurkat cells (**Figures 3.10 and 3.11**). Further studies would help in figuring out what regulates the expression of GABA_ARs in specific T_H phenotypes. Nevertheless, we found that these T_H cell lines regulate GABA_ARs differently in response to the same stimuli. It would be worth examining the effect of GABAergic stimulation and blockade in activated T_H cells.

4.5 Roles of GABA signaling in T_H1 and T_H2 diseases

The literature surrounding GABA signaling in the immune system have painted it as an inhibitory molecule in many immune cell types. However, a vast majority of these studies were conducted in the context of T_H1/M1-mediated responses while the role of GABA in T_H2/M2 responses remain elusive. In short, we know that GABA signaling plays an inhibitory role in the proliferation and activity of macrophages and T cells from various species^{139,140,142,148,182}. Moreover, many studies have shown GABA to be protective against T_H1/M1 mediated-diseases such as EAE, T1D, rheumatoid arthritis, and collagen-induced arthritis^{139,152,190–192}.

Taken together, it is clear that GABA signaling plays an anti-inflammatory role in T_H1/M1 immune responses. Given the opposing roles that T_H1 and T_H2 cells play in adaptive

immunity, we propose that GABA should play either a neutral or excitatory role in T_H2 cells and responses. Although the T_H1 and T_H2 spectrums are not clear cut dichotomies, there is still good evidence to suggest that they are responsible for very different adaptive immune responses^{193,194}. Substances that facilitate T_H1 development and responses generally inhibit T_H2 development, and vice versa. The studies on GABAergic signaling in T_H2 responses gives us some insight into what GABA can do in T_H2 cells.

There have not been many reports on the effects of the GABAergic system in the context of T_H2 responses such as allergic asthma. It is unclear whether GABA also plays an inhibitory role in T_H2 and M2 cells, or whether it can be protective against T_H2 /M2 diseases. A study done by our lab examined the role of a GABAergic system in airway epithelial cells and found that GABA was essential for mucus overproduction in asthma¹⁹⁵. Moreover, this study found that IL-13 (T_H2 cytokine) administration caused an increased expression of GAD and GABA_ARs in the lung epithelial cells. Another study published in 2016 found that luteolin, a functional inhibitor of the GABAergic system, was able to suppress airway mucus overproduction in a mouse model induced by ovalbumin¹⁹⁶. Given the significance of T_H2 -mediated inflammation and IL-13 production in asthma pathology, it suggests that GABA_AR signaling plays an important activating role in the T_H2 /M2 system.

Previous studies in our lab also found that lung macrophages are equipped with a functional autocrine GABA signaling system, and blocking this system enhanced secretion of the M1 cytokine TNF- α . In both RAW 264.7 cells (a murine macrophage line) and primary lung macrophages, treatment with T_H1 cytokine IFN- γ and bacterial LPS reduced GAD and GABA_AR- $\alpha 2$ expression. Conversely, treatment with T_H2 cytokines IL-4 and IL-13 caused an increase in GAD and $\alpha 2$ expression¹⁴⁵. These findings suggested that the GABAergic system in macrophages tend to inhibit the M1 phenotype while facilitating the M2 response. The

results of this earlier project could be extended to our results, since the M1 phenotype is directly associated with T_H1 phenotype while M2 responses are associated with T_H2 responses.

4.6 Limitations and future studies

As with any scientific investigation, there are inevitably challenges and limitations involved, the most evident in our study was the use of cell lines rather than isolated primary cells to infer a physiological mechanism. Cell lines are transformed cells that may not reflect the true nature of primary T_H cells. Moreover, primary T_H cells contain unique cellular markers and traits that may not be fully represented by cell lines. Future studies should involve the use of primary T cells differentiated into T_H1 and T_H2 cells using *in vitro* techniques, followed by using *in vivo* models of T_H1 and T_H2 disease to examine GABAergic signaling. Other T_H subtypes, most notably the T_H17 and T_{reg} cells, should also be examined.

Although it is imperative to use primary cells to confirm our results obtained from the cell lines, further studies on these cell lines are also important in helping us gain a deeper understanding of our current results. For example, in the Jurkat and CCRF-CEM cells, we can examine the effects of GABA signaling on cytokine production and the expression of transcription factors and surface marker proteins unique to T_H1 and T_H2 cells. We can run an ELISA or Luminex assay on signature T_H1 and T_H2 cytokines following treatment with GABA agonists and antagonists. We can also run qPCR and flow cytometry experiments to examine T_H1 and T_H2 transcription factors and cell surface markers. Since the focus of this thesis was to study the cellular physiology of GABA_AR signaling in a non-CNS cell type, we did not place as much focus on the immunological aspects of T_H cells. Nonetheless, these are all important future directions to take for this project.

Another possible direction to take would be to use electrophysiological techniques to assess whether our proposed mechanism is true. Patch-clamp recordings can be used to examine the movement of Cl⁻ during GABA_AR stimulation. This would help confirm our proposal of the mechanism by which GABA acts. One of the main techniques used in this project was Ca²⁺-based fluorescence imaging. This technique is not a direct measure of intracellular Ca²⁺ levels and relies on the detection of a Ca²⁺ based fluorescent molecule. For this reason, we were unable to take absolute quantitative measures of intracellular Ca²⁺ levels. Thapsigargin is also not an endogenous inducer of SOCE and bypasses TCR engagement and its immediate downstream pathways. In future studies, a more physiological stimulus could be explored and we can use other Ca²⁺ indicators such as Fura-2 that enable quantitative detection of Ca²⁺. Lastly, the effects of GABA_BR activation and blockade could also be examined using selective GABA_BR agonists/antagonists.

4.7 Conclusions and significance

This project demonstrated that Jurkat and CCRF-CEM cells express components of the GABA_AR signaling system and that blockade of GABA_ARs results in changes to cellular phenotype and activity. These results suggest that autocrine GABA_AR signaling could differentially modulate T_H subtypes depending on its effects on SOCE. We propose that variations in membrane potential and Cl⁻ equilibrium potential contribute to whether GABA plays a depolarizing or hyperpolarizing role in T cells. Different phenotypes of T cells may have different Cl⁻ signaling mechanisms that result in distinct GABA_AR regulation. GABA may also have unique effects in different T_H subtypes in the body. Further studies need to be conducted on primary T_H1 and T_H2 cells, as well as in animal models of T_H2 disorders.

The results from this project have several implications in clinical settings. We have demonstrated proof of concept that GABA signaling could indeed play unique roles in different T_H cell types. Selective modulation of this system could be beneficial in different spectrums of adaptive immune diseases. For example, in T_H1 -dominant disorders, the GABAergic system signaling could be enhanced to facilitate inhibition of T_H1 cell activity. In T_H2 atopic disorders, we can selectively block GABAergic signaling to reduce the activity of T_H2 cells. The role of the mammalian GABAergic system extends far beyond the CNS, and we are just scratching the surface of its potential as a therapeutic target.

Chapter 5: References

1. Zhu, J., Yamane, H. & Paul, W. Differentiation of effector CD4 T cell populations. *Annu Rev Immunol.* **28**, 445–489 (2010).
2. Mazzarella, G., Bianco, A., Catena, E., De Palma, R. & Abbate, G. F. Th1/Th2 lymphocyte polarization in asthma. *Allergy* **55 Suppl 61**, 6–9 (2000).
3. Ngoc, P. L. *et al.* Cytokines, allergy, and asthma. *Curr. Opin. Allergy Clin. Immunol.* **5**, 161–6 (2005).
4. Hafler, D. A. & Astier, A. L. Editorial: T Cell Regulation by the Environment. *Front. Immunol.* **6**, 229 (2015).
5. Chen, J. *et al.* Autocrine/paracrine cytokine stimulation of leukemic cell proliferation in smoldering and chronic adult T-cell leukemia. *Blood* **116**, 5948–5956 (2010).
6. Kupper, T., Flood, P., Coleman, D. & Horowitz, M. Growth of an interleukin 2/interleukin 4-dependent T cell line induced by granulocyte-macrophage colony-stimulating factor (GM-CSF). *J. Immunol.* **138**, 4288–92 (1987).
7. Junger, W. G. Immune cell regulation by autocrine purinergic signalling. *Nat. Rev. Immunol.* **11**, 201–212 (2011).
8. Watanabe, M., Maemura, K., Kanbara, K., Tamayama, T. & Hayasaki, H. GABA and GABA receptors in the central nervous system and other organs. *Int. Rev. Cytol.* **213**, 1–47 (2002).
9. Barragan, A., Weidner, J. M., Jin, Z., Korpi, E. R. & Birnir, B. GABAergic signalling in the immune system. *Acta Physiol.* **213**, 819–827 (2015).
10. Tian, J. *et al.* Gamma-aminobutyric acid inhibits T cell autoimmunity and the development of inflammatory responses in a mouse type 1 diabetes model. *J. Immunol.* **173**, 5298–304 (2004).
11. Janeway, C. *Immunobiology 5 : the immune system in health and disease.* (Garland Pub, 2001).
12. O’Byrne, K. J. & Dalglish, A. G. Chronic immune activation and inflammation as the cause of malignancy. *Br. J. Cancer* **85**, 473–83 (2001).
13. Janeway, C. A. & Medzhitov, R. Innate immune recognition. *Annu. Rev. Immunol.* **20**, 197–216 (2002).

14. Turvey, S. E. & Broide, D. H. Innate immunity. *J. Allergy Clin. Immunol.* **125**, S24-32 (2010).
15. Janeway, C. A. Approaching the asymptote? Evolution and revolution in immunology. *Cold Spring Harb. Symp. Quant. Biol.* **54 Pt 1**, 1–13 (1989).
16. Charles A Janeway, J., Travers, P., Walport, M. & Shlomchik, M. J. Principles of innate and adaptive immunity. (2001).
17. Pancer, Z. & Cooper, M. D. The evolution of adaptive immunity. *Annu. Rev. Immunol.* **24**, 497–518 (2006).
18. Bonilla, F. A. & Oettgen, H. C. Adaptive immunity. *J. Allergy Clin. Immunol.* **125**, S33–S40 (2010).
19. Dempsey, P. W., Vaidya, S. A. & Cheng, G. The Art of War: Innate and adaptive immune responses. *Cell. Mol. Life Sci.* **60**, 2604–2621 (2003).
20. Clem, A. S. Fundamentals of vaccine immunology. *J. Glob. Infect. Dis.* **3**, 73–8 (2011).
21. Dustin, M. L. The immunological synapse. *Cancer Immunol. Res.* **2**, 1023–33 (2014).
22. Vyas, J. M., Van der Veen, A. G. & Ploegh, H. L. The known unknowns of antigen processing and presentation. *Nat. Rev. Immunol.* **8**, 607–618 (2008).
23. Jensen, P. E. Recent advances in antigen processing and presentation. *Nat. Immunol.* **8**, 1041–1048 (2007).
24. Allison, J. P. CD28-B7 interactions in T-cell activation. *Curr. Opin. Immunol.* **6**, 414–9 (1994).
25. Coyle, A. J. & Gutierrez-Ramos, J.-C. The expanding B7 superfamily: increasing complexity in costimulatory signals regulating T cell function. *Nat. Immunol.* **2**, 203–209 (2001).
26. Schwartz, J.-C. D., Zhang, X., Fedorov, A. A., Nathenson, S. G. & Almo, S. C. Structural basis for co-stimulation by the human CTLA-4/B7-2 complex. *Nature* **410**, 604–608 (2001).
27. Wang, M., Yin, B., Wang, H. Y. & Wang, R.-F. Current advances in T-cell-based cancer immunotherapy. *Immunotherapy* **6**, 1265–78 (2014).
28. Jones, D. *et al.* Expression pattern of T-cell-associated chemokine receptors and their chemokines correlates with specific subtypes of T-cell non-Hodgkin lymphoma. *Blood*

- 96, 685–90 (2000).
29. Kawashima, K., Fujii, T., Moriwaki, Y., Misawa, H. & Horiguchi, K. Non-neuronal cholinergic system in regulation of immune function with a focus on $\alpha 7$ nAChRs. *Int. Immunopharmacol.* **29**, 127–134 (2015).
 30. Piali, L. *et al.* The chemokine receptor CXCR3 mediates rapid and shear-resistant adhesion-induction of effector T lymphocytes by the chemokines IP10 and Mig. *Eur. J. Immunol.* **28**, 961–72 (1998).
 31. Lewis, R. A. *et al.* Prostaglandin D2 generation after activation of rat and human mast cells with anti-IgE. *J. Immunol.* **129**, 1627–31 (1982).
 32. Gosset, P. *et al.* Prostaglandin D2 affects the differentiation and functions of human dendritic cells: impact on the T cell response. *Eur. J. Immunol.* **35**, 1491–1500 (2005).
 33. Hirai, H. *et al.* Prostaglandin D2 selectively induces chemotaxis in T helper type 2 cells, eosinophils, and basophils via seven-transmembrane receptor CRTH2. *J. Exp. Med.* **193**, 255–61 (2001).
 34. Gervais, F. G. *et al.* Selective modulation of chemokinesis, degranulation, and apoptosis in eosinophils through the PGD2 receptors CRTH2 and DP. *J. Allergy Clin. Immunol.* **108**, 982–988 (2001).
 35. Sugimoto, H. *et al.* An Orally Bioavailable Small Molecule Antagonist of CRTH2, Ramatroban (BAY u3405), Inhibits Prostaglandin D2-Induced Eosinophil Migration in Vitro. *J. Pharmacol. Exp. Ther.* **305**, 347–352 (2003).
 36. Cosmi, L. *et al.* CRTH2 is the most reliable marker for the detection of circulating human type 2 Th and type 2 T cytotoxic cells in health and disease [In Process Citation]. *Eur J Immunol* **30**, 2972–2979 (2000).
 37. Pozzan, T., Rizzuto, R., Volpe, P. & Meldolesi, J. Molecular and cellular physiology of intracellular calcium stores. *Physiol. Rev.* **74**, 595–636 (1994).
 38. Burk, S. E., Lytton, J., MacLennan, D. H. & Shull, G. E. cDNA cloning, functional expression, and mRNA tissue distribution of a third organellar Ca²⁺ pump. *J. Biol. Chem.* **264**, 18561–8 (1989).
 39. Weiss, A. & Imboden, J. B. Cell surface molecules and early events involved in human T lymphocyte activation. *Adv. Immunol.* **41**, 1–38 (1987).
 40. Premack, B. A. & Gardner, P. Signal transduction by T-cell receptors: mobilization of Ca and regulation of Ca-dependent effector molecules. *Am. J. Physiol.* **263**, C1119–40 (1992).

41. Berridge, M. J. Capacitative calcium entry. *Biochem. J.* **312** (Pt 1), 1–11 (1995).
42. Vallabhapurapu, S. & Karin, M. Regulation and function of NF- κ B transcription factors in the immune system. *Annu. Rev. Immunol.* **27**, 693–733 (2009).
43. Hogan, P. G., Chen, L., Nardone, J. & Rao, A. Transcriptional regulation by calcium, calcineurin, and NFAT. *Genes Dev.* **17**, 2205–2232 (2003).
44. Lewis, R. S. Calcium signaling mechanisms in T lymphocytes. 497–521 (2001).
45. Parekh, A. B. & Putney, J. W. Store-operated calcium channels. *Physiol. Rev.* **85**, 757–810 (2005).
46. Roos, J. *et al.* STIM1, an essential and conserved component of store-operated Ca²⁺ channel function. *J. Cell Biol.* **169**, 435–445 (2005).
47. Liou, J. *et al.* STIM is a Ca²⁺ sensor essential for Ca²⁺-store-depletion-triggered Ca²⁺ influx. *Curr. Biol.* **15**, 1235–1241 (2005).
48. Prakriya, M. *et al.* Orai1 is an essential pore subunit of the CRAC channel. *Nature* **443**, 230–233 (2006).
49. Yeromin, A. V. *et al.* Molecular identification of the CRAC channel by altered ion selectivity in a mutant of Orai. *Nature* **443**, 226–229 (2006).
50. Lewis, R. S. The molecular choreography of a store-operated calcium channel. *Nature* **446**, 284–287 (2007).
51. Luik, R. M., Wang, B., Prakriya, M., Wu, M. M. & Lewis, R. S. Oligomerization of STIM1 couples ER calcium depletion to CRAC channel activation. *Nature* **454**, 538–42 (2008).
52. Park, C. Y. *et al.* STIM1 clusters and activates CRAC channels via direct binding of a cytosolic domain to Orai1. *Cell* **136**, 876–890 (2009).
53. Picard, C. *et al.* STIM1 mutation associated with a syndrome of immunodeficiency and autoimmunity. *N. Engl. J. Med.* **360**, 1971–1980 (2009).
54. Feske, S. *et al.* A mutation in Orai1 causes immune deficiency by abrogating CRAC channel function. *Nature* **441**, 179–185 (2006).
55. Le Deist, F. *et al.* A primary T-cell immunodeficiency associated with defective transmembrane calcium influx. *Blood* **85**, 1053–62 (1995).
56. Lewis, R. S. & Cahalan, M. D. Potassium and calcium channels in lymphocytes. *Annu.*

- Rev. Immunol.* **13**, 623–653 (1995).
57. Cahalan, M. D. & Chandy, K. G. Ion channels in the immune system as targets for immunosuppression. *Curr. Opin. Biotechnol.* **8**, 749–56 (1997).
 58. Leonard, R. J., Garcia, M. L., Slaughter, R. S. & Reuben, J. P. Selective blockers of voltage-gated K⁺ channels depolarize human T lymphocytes: mechanism of the antiproliferative effect of charybdotoxin. *Proc. Natl. Acad. Sci. U. S. A.* **89**, 10094–8 (1992).
 59. Lin, C. S. *et al.* Voltage-gated potassium channels regulate calcium-dependent pathways involved in human T lymphocyte activation. *J. Exp. Med.* **177**, 637–45 (1993).
 60. Treiman, M., Caspersen, C. & Christensen, S. B. A tool coming of age: thapsigargin as an inhibitor of sarco-endoplasmic reticulum Ca(2⁺)-ATPases. *Trends Pharmacol. Sci.* **19**, 131–5 (1998).
 61. Singer, A., Adoro, S. & Park, J.-H. Lineage fate and intense debate: myths, models and mechanisms of CD4- versus CD8-lineage choice. *Nat. Rev. Immunol.* **8**, 788–801 (2008).
 62. Zlotoff, D. A. & Bhandoola, A. Hematopoietic progenitor migration to the adult thymus. *Ann. N. Y. Acad. Sci.* **1217**, 122–38 (2011).
 63. Radtke, F. *et al.* Deficient T cell fate specification in mice with an induced inactivation of Notch1. *Immunity* **10**, 547–58 (1999).
 64. Wilson, A., MacDonald, H. R. & Radtke, F. Notch 1-deficient common lymphoid precursors adopt a B cell fate in the thymus. *J. Exp. Med.* **194**, 1003–12 (2001).
 65. Hedrick, S. M. Thymus lineage commitment: a single switch. *Immunity* **28**, 297–299 (2008).
 66. Jenkinson, E. J., Jenkinson, W. E., Rossi, S. W. & Anderson, G. The thymus and T-cell commitment: the right niche for Notch? *Nat. Rev. Immunol.* **6**, 551–555 (2006).
 67. Takahama, Y. Journey through the thymus: stromal guides for T-cell development and selection. *Nat. Rev. Immunol.* **6**, 127–135 (2006).
 68. Rothenberg, E. V., Moore, J. E. & Yui, M. A. Launching the T-cell-lineage developmental programme. *Nat. Rev. Immunol.* **8**, 9–21 (2008).
 69. Germain, R. N. T-cell development and the CD4-CD8 lineage decision. *Nat. Rev. Immunol.* **2**, 309–322 (2002).

70. Bevan, M. J. & Goldrath, A. W. Selecting and maintaining a diverse T-cell repertoire. *Nature* **402**, 255–262 (1999).
71. Palmer, D. B. The effect of age on thymic function. *Front. Immunol.* **4**, 316 (2013).
72. Koch, U. & Radtke, F. Mechanisms of T cell development and transformation. *Annu. Rev. Cell Dev. Biol.* **27**, 539–562 (2011).
73. Ciofani, M. & Zúñiga-Pflücker J.C. Determining $\gamma\delta$ versus $\alpha\beta$ T cell development. *Nat. Rev. Immunol.* **10**, 657–63 (2010).
74. Huang, C.Y., Sleckman, B. P. & Kanagawa, O. Revision of T cell receptor α chain genes is required for normal T lymphocyte development. *Proc. Natl. Acad. Sci.* **102**, 14356–14361 (2005).
75. Abbey, J. L. & O'Neill, H. C. Expression of T-cell receptor genes during early T-cell development. *Immunol. Cell Biol.* **86**, 166–174 (2008).
76. MacDonald, H. R., Lees, R. K., Schneider, R., Zinkernagel, R. M. & Hengartner, H. Positive selection of CD4⁺ thymocytes controlled by MHC class II gene products. *Nature* **336**, 471–473 (1988).
77. Klein, L., Kyewski, B., Allen, P. M. & Hogquist, K. A. Positive and negative selection of the T cell repertoire: what thymocytes see (and don't see). *Nat. Rev. Immunol.* **14**, 377–91 (2014).
78. Kisielow, P., Teh, H. S., Blüthmann H., & von Boehmer, H. Positive selection of antigen-specific T cells in thymus by restricting MHC molecules. *Nature* **335**, 730–733 (1988).
79. Jameson, S. C., Hogquist, K. A. & Bevan, M. J. Positive selection of thymocytes. *Annu. Rev. Immunol.* **13**, 93–126 (1995).
80. Robey, E. & Fowlkes, B. J. Selective events in T cell development. *Annu. Rev. Immunol.* **12**, 675–705 (1994).
81. Luckheeram, R. V., Zhou, R., Verma, A. D. & Xia, B. CD4⁺ T cells: differentiation and functions. *Clin. Dev. Immunol.* **2012**, 1–12 (2012).
82. Tao, X., Constant, S., Jorritsma, P. & Bottomly, K. Strength of TCR signal determines the costimulatory requirements for Th1 and Th2 CD4⁺ T cell differentiation. *J. Immunol.* **159**, 5956–63 (1997).
83. Mosmann, T. R., Cherwinski, H., Bond, M. W., Giedlin, M. A. & Coffman, R. L. Two types of murine helper T cell clone. I. Definition according to profiles of lymphokine

- activities and secreted proteins. *J. Immunol.* **136**, 2348–57 (1986).
84. Flaherty, S. & Reynolds, J. M. Mouse Naïve CD4+ T cell isolation and in vitro differentiation into T cell subsets. *J. Vis. Exp.* 1–8 (2015). doi:10.3791/52739
 85. Del Prete, G. Human Th1 and Th2 lymphocytes: their role in the pathophysiology of atopy. *Allergy* **47**, 450–5 (1992).
 86. Murray, H. W., Spitalny, G. L. & Nathan, C. F. Activation of mouse peritoneal macrophages in vitro and in vivo by interferon-gamma. *J. Immunol.* **134**, 1619–22 (1985).
 87. Bachmann, M. F. & Oxenius, A. Interleukin 2: from immunostimulation to immunoregulation and back again. *EMBO Rep.* **8**, 1142–1148 (2007).
 88. Afkarian, M. *et al.* T-bet is a STAT1-induced regulator of IL-12R expression in naïve CD4+ T cells. *Nat. Immunol.* **3**, 549–557 (2002).
 89. Lugo-Villarino, G., Maldonado-Lopez, R., Possemato, R., Penaranda, C. & Glimcher, L. H. T-bet is required for optimal production of IFN- γ and antigen-specific T cell activation by dendritic cells. *Proc. Natl. Acad. Sci.* **100**, 7749–7754 (2003).
 90. Trinchieri, G., Pflanz, S. & Kastelein, R. A. The IL-12 family of heterodimeric cytokines: new players in the regulation of T cell responses. *Immunity* **19**, 641–4 (2003).
 91. Sokol, C. L. *et al.* Basophils function as antigen-presenting cells for an allergen-induced T helper type 2 response. *Nat. Immunol.* **10**, 713–720 (2009).
 92. Steinke, J. W. & Borish, L. Th2 cytokines and asthma. Interleukin-4: its role in the pathogenesis of asthma, and targeting it for asthma treatment with interleukin-4 receptor antagonists. *Respir. Res.* **2**, 66–70 (2001).
 93. Wynn, T. A. IL-13 effector functions. *Annu. Rev. Immunol.* **21**, 425–456 (2003).
 94. Martinez-Moczygamba, M. & Huston, D. P. Biology of common beta receptor-signaling cytokines: IL-3, IL-5, and GM-CSF. *J. Allergy Clin. Immunol.* **112**, 653–65; quiz 666 (2003).
 95. Zheng, W. & Flavell, R. A. The transcription factor GATA-3 is necessary and sufficient for Th2 cytokine gene expression in CD4 T cells. *Cell* **89**, 587–96 (1997).
 96. Zhu, J., Yamane, H., Cote-Sierra, J., Guo, L. & Paul, W. E. GATA-3 promotes Th2 responses through three different mechanisms: induction of Th2 cytokine production, selective growth of Th2 cells and inhibition of Th1 cell-specific factors. *Cell Res.* **16**,

- 3–10 (2006).
97. Harrington, L. E. *et al.* Interleukin 17-producing CD4⁺ effector T cells develop via a lineage distinct from the T helper type 1 and 2 lineages. *Nat. Immunol.* **6**, 1123–1132 (2005).
 98. Mangan, P. R. *et al.* Transforming growth factor- β induces development of the TH17 lineage. *Nature* **441**, 231–234 (2006).
 99. Vignali, D. A. A., Collison, L. W. & Workman, C. J. How regulatory T cells work. *Nat. Rev. Immunol.* **8**, 523–32 (2008).
 100. Martinez, F. O. & Gordon, S. The M1 and M2 paradigm of macrophage activation: time for reassessment. *F1000Prime Rep.* **6**, 13 (2014).
 101. Murray, P. J. *et al.* Macrophage activation and polarization: nomenclature and experimental guidelines. *Immunity* **41**, 14–20 (2014).
 102. Muraille, E., Leo, O. & Moser, M. TH1/TH2 paradigm extended: macrophage polarization as an unappreciated pathogen-driven escape mechanism? *Front. Immunol.* **5**, 603 (2014).
 103. Lee, W. J. *et al.* M2 macrophage polarization mediates anti-inflammatory effects of endothelial nitric oxide signaling. *Diabetes* **64**, 2836–46 (2015).
 104. Abraham, R. T. & Weiss, A. Jurkat T cells and development of the T-cell receptor signalling paradigm. *Nat. Rev. Immunol.* **4**, 301–308 (2004).
 105. Schneider, U., Schwenk, H. U. & Bornkamm, G. Characterization of EBV-genome negative “null” and “T” cell lines derived from children with acute lymphoblastic leukemia and leukemic transformed non-Hodgkin lymphoma. *Int. J. cancer* **19**, 621–6 (1977).
 106. Gillis, S. & Watson, J. Biochemical and biological characterization of lymphocyte regulatory molecules. V. Identification of an interleukin 2-producing human leukemia T cell line. *J. Exp. Med.* **152**, 1709–19 (1980).
 107. Weiss, A., Imboden, J., Shoback, D. & Stobo, J. Role of T3 surface molecules in human T-cell activation: T3-dependent activation results in an increase in cytoplasmic free calcium. *Proc. Natl. Acad. Sci. U. S. A.* **81**, 4169–73 (1984).
 108. FOLEY, G. E. *et al.* Continuous culture of human lymphoblasts from peripheral blood of a child with acute leukemia. *Cancer* **18**, 522–9 (1965).
 109. Kaur, G. & Dufour, J. M. Cell lines. *Spermatogenesis* **2**, 1–5 (2012).

110. Xu, G. *et al.* Late development of the GABAergic system in the human cerebral cortex and white matter. *J. Neuropathol. Exp. Neurol.* **70**, 841–858 (2011).
111. Takesian, A. E. & Hensch, T. K. Balancing plasticity/stability across brain development. *Prog. Brain Res.* **207**, 3–34 (2013).
112. Wu, C. & Sun, D. GABA receptors in brain development, function, and injury. *Metab. Brain Dis.* **30**, 367–79 (2015).
113. Sherwin, A. L. Neuroactive amino acids in focally epileptic human brain: a review. *Neurochem. Res.* **24**, 1387–95 (1999).
114. Erlander, M. G., Tillakaratne, N. J., Feldblum, S., Patel, N. & Tobin, A. J. Two genes encode distinct glutamate decarboxylases. *Neuron* **7**, 91–100 (1991).
115. Pinal, C. S. & Tobin, A. J. Uniqueness and redundancy in GABA production. *Perspect. Dev. Neurobiol.* **5**, 109–18 (1998).
116. Sherif, F., Harro, J., el-Hwuegi, A. & Orelund, L. Anxiolytic-like effect of the GABA-transaminase inhibitor vigabatrin (gamma-vinyl GABA) on rat exploratory activity. *Pharmacol. Biochem. Behav.* **49**, 801–5 (1994).
117. Jin, X.-T., Galvan, A., Wichmann, T. & Smith, Y. Localization and function of GABA transporters GAT-1 and GAT-3 in the basal ganglia. *Front. Syst. Neurosci.* **5**, 63 (2011).
118. Luján, R., Shigemoto, R. & López-Bendito, G. Glutamate and GABA receptor signalling in the developing brain. *Neuroscience* **130**, 567–580 (2005).
119. Couve, A., Moss, S. J. & Pangalos, M. N. GABAB receptors: A new paradigm in G protein signaling. *Mol. Cell. Neurosci.* **16**, 296–312 (2000).
120. Sieghart, W. Structure, pharmacology, and function of GABAA receptor subtypes. *Adv. Pharmacol.* **54**, 231–63 (2006).
121. Olsen, R. W. & Sieghart, W. International Union of Pharmacology. LXX. Subtypes of gamma-aminobutyric acid(A) receptors: classification on the basis of subunit composition, pharmacology, and function. Update. *Pharmacol. Rev.* **60**, 243–260 (2008).
122. Sieghart, W. & Sperk, G. Subunit composition, distribution and function of GABA(A) receptor subtypes. *Curr. Top. Med. Chem.* **2**, 795–816 (2002).
123. Schofield, P. R. *et al.* Sequence and functional expression of the GABAA receptor shows a ligand-gated receptor super-family. *Nature* **328**, 221–227 (1987).

124. Kittler, J. T., McAinsh, K. & Moss, S. J. Mechanisms of GABAA receptor assembly and trafficking: implications for the modulation of inhibitory neurotransmission. *Mol. Neurobiol.* **26**, 251–268 (2002).
125. Jacob, T. C., Moss, S. J. & Jurd, R. GABA(A) receptor trafficking and its role in the dynamic modulation of neuronal inhibition. *Nat. Rev. Neurosci.* **9**, 331–43 (2008).
126. Olsen, R. W. & Sieghart, W. GABAA receptors: subtypes provide diversity of function and pharmacology. *Neuropharmacology* **56**, 141–148 (2009).
127. Delpire, E. Cation-chloride cotransporters in neuronal communication. *News Physiol. Sci.* **15**, 309–312 (2000).
128. Spitzer, N. C. How GABA generates depolarization. *J. Physiol.* **588**, 757–8 (2010).
129. Ben-Ari, Y., Gaiarsa, J.-L., Tyzio, R. & Khazipov, R. GABA: a pioneer transmitter that excites immature neurons and generates primitive oscillations. *Physiol. Rev.* **87**, 1215–1284 (2007).
130. Payne, J. A., Rivera, C., Voipio, J. & Kaila, K. Cation–chloride co-transporters in neuronal communication, development and trauma. *Trends Neurosci.* **26**, 199–206 (2003).
131. Erdö, S. L. & Wolff, J. R. gamma-Aminobutyric acid outside the mammalian brain. *J. Neurochem.* **54**, 363–72 (1990).
132. Gladkevich, A., Korf, J., Hakobyan, V. P. & Melkonyan, K. V. The peripheral GABAergic system as a target in endocrine disorders. *Auton. Neurosci.* **124**, 1–8 (2006).
133. Young, S. Z. & Bordey, A. GABA's control of stem and cancer cell proliferation in adult neural and peripheral niches. *Physiology* **24**, 171–185 (2009).
134. Rorsman, P. *et al.* Glucose-inhibition of glucagon secretion involves activation of GABAA-receptor chloride channels. *Nature* **341**, 233–236 (1989).
135. Xu, E. *et al.* Intra-islet insulin suppresses glucagon release via GABA-GABAA receptor system. *Cell Metab.* **3**, 47–58 (2006).
136. Soltani, N. *et al.* GABA exerts protective and regenerative effects on islet beta cells and reverses diabetes. *Proc. Natl. Acad. Sci.* **108**, 11692–11697 (2011).
137. Geigerseder, C. *et al.* Evidence for a GABAergic system in rodent and human testis: local GABA production and GABA receptors. *Neuroendocrinology* **77**, 314–23 (2003).

138. Geigerseder, C., Doepner, R. F. G., Thalhammer, A., Krieger, A. & Mayerhofer, A. Stimulation of TM3 Leydig cell proliferation via GABA(A) receptors: a new role for testicular GABA. *Reprod. Biol. Endocrinol.* **2**, 13 (2004).
139. Bhat, R. *et al.* Inhibitory role for GABA in autoimmune inflammation. *Proc. Natl. Acad. Sci.* **107**, 2580–2585 (2010).
140. Jin, Z., Mendu, S. K. & Birnir, B. GABA is an effective immunomodulatory molecule. *Amino Acids* **45**, 87–94 (2013).
141. Dionisio, L., José De Rosa, M., Bouzat, C. & Esandi, M. D. C. An intrinsic GABAergic system in human lymphocytes. *Neuropharmacology* **60**, 513–519 (2011).
142. Reyes-García M.G., Hernández-Hernández, F., Hernández-Téllez, B., García-Tamayo, F. GABA (A) receptor subunits RNA expression in mice peritoneal macrophages modulate their IL-6/IL-12 production. *J. Neuroimmunol.* **188**, 64–68 (2007).
143. Alam, S., Laughton, D. L., Walding, A. & Wolstenholme, A. J. Human peripheral blood mononuclear cells express GABAA receptor subunits. *Mol. Immunol.* **43**, 1432–1442 (2006).
144. Wheeler, D. W. *et al.* Anaesthetic impairment of immune function is mediated via GABA(A) receptors. *PLoS One* **6**, e17152 (2011).
145. Poirier, J. The role of GABA signalling in lung macrophage immune response. *Electron. Thesis Diss. Repos.* (2016).
146. Bhat, R. *et al.* Inhibitory role for GABA in autoimmune inflammation. *Proc. Natl. Acad. Sci. U. S. A.* **107**, 2580–2585 (2010).
147. Mendu, S. K., Bhandage, A., Jin, Z. & Birnir, B. Different subtypes of GABA-A receptors are expressed in human, mouse and rat T lymphocytes. *PLoS One* **7**, e42959 (2012).
148. Tian, J., Chau, C., Hales, T. G. & Kaufman, D. L. GABA(A) receptors mediate inhibition of T cell responses. *J Neuroimmunol* **96**, 21–28 (1999).
149. Toldi, G. *et al.* Human Th1 and Th2 lymphocytes are distinguished by calcium flux regulation during the first 10min of lymphocyte activation. *Immunobiology* **217**, 37–43 (2012).
150. Feske, S. Ca(2+) influx in T cells: how many ca(2+) channels? *Front. Immunol.* **4**, 99 (2013).
151. Bergeret, M. *et al.* GABA modulates cytotoxicity of immunocompetent cells

- expressing GABAA receptor subunits. *Biomed. Pharmacother.* **52**, 214–219 (1998).
152. Tian, J. *et al.* Gamma-aminobutyric acid inhibits T cell autoimmunity and the development of inflammatory responses in a mouse type 1 diabetes model. *J. Immunol.* **173**, 5298–304 (2004).
 153. Tian, J., Yong, J., Dang, H. O. A. & Kaufman, D. L. Oral GABA treatment downregulates inflammatory responses in a mouse model of rheumatoid arthritis. 1–6 (2011). doi:10.3109/08916934.2011.571223
 154. Oresic, M. *et al.* Dysregulation of lipid and amino acid metabolism precedes islet autoimmunity in children who later progress to type 1 diabetes. *J. Exp. Med.* (2008).
 155. Tozuka, Y., Fukuda, S., Namba, T., Seki, T. & Hisatsune, T. GABAergic excitation promotes neuronal differentiation in adult hippocampal progenitor cells. *Neuron* **47**, 803–815 (2005).
 156. Ben-Othman, N. *et al.* Long-term GABA administration induces alpha cell-mediated beta-like cell neogenesis. *Cell* **168**, 73–85.e11 (2017).
 157. Toldi, G. *et al.* Human Th1 and Th2 lymphocytes are distinguished by calcium flux regulation during the first 10min of lymphocyte activation. *Immunobiology* **217**, 37–43 (2012).
 158. Weber, K. S., Miller, M. J. & Allen, P. M. Th17 cells exhibit a distinct calcium profile from Th1 and Th2 cells and have Th1-like motility and NF-AT nuclear localization. *J. Immunol.* **180**, 1442–1450 (2008).
 159. Wisden, W., Laurie, D. J., Monyer, H. & Seeburg, P. H. The distribution of 13 GABAA receptor subunit mRNAs in the rat brain. I. Telencephalon, diencephalon, mesencephalon. *J. Neurosci.* **12**, 1040–62 (1992).
 160. Macian, F. NFAT proteins: key regulators of T-cell development and function. *Nat. Rev. Immunol.* **5**, 472–484 (2005).
 161. Ohtsuka, T., Kaziro, Y. & Satoh, T. Analysis of the T-cell activation signaling pathway mediated by tyrosine kinases, protein kinase C, and Ras protein, which is modulated by intracellular cyclic AMP. *Biochim. Biophys. Acta* **1310**, 223–32 (1996).
 162. Abraham, R. T. & Weiss, A. Jurkat T cells and development of the T-cell receptor signalling paradigm. *Nat. Rev. Immunol.* **4**, 301–308 (2004).
 163. Viallard, J. F. *et al.* Th1 (IL-2, interferon-gamma (IFN-gamma)) and Th2 (IL-10, IL-4) cytokine production by peripheral blood mononuclear cells (PBMC) from patients with systemic lupus erythematosus (SLE). *Clin. Exp. Immunol.* **115**, 189–95 (1999).

164. Coelho, C. M. & Leever, S. J. Do growth and cell division rates determine cell size in multicellular organisms? *J. Cell Sci.* **113 (Pt 17)**, 2927–34 (2000).
165. Baserga, R. Is Cell Size Important? *Cell Cycle* **6**, 814–816 (2007).
166. Keibler, M. A. *et al.* Metabolic requirements for cancer cell proliferation. *Cancer Metab.* **4**, 16 (2016).
167. DeBerardinis, R. J., Lum, J. J., Hatzivassiliou, G. & Thompson, C. B. The biology of cancer: metabolic reprogramming fuels cell growth and proliferation. *Cell Metab.* **7**, 11–20 (2008).
168. Park, C. Y. *et al.* STIM1 clusters and activates CRAC channels via direct binding of a cytosolic domain to Orai1. *Cell* **136**, 876–890 (2009).
169. Toldi, G. *et al.* Human Th1 and Th2 lymphocytes are distinguished by calcium flux regulation during the first 10min of lymphocyte activation. *Immunobiology* **217**, 37–43 (2012).
170. Fanger, C. M., Neben, a L. & Cahalan, M. D. Differential Ca²⁺ influx, K_{Ca} channel activity, and Ca²⁺ clearance distinguish Th1 and Th2 lymphocytes. *J. Immunol.* **164**, 1153–1160 (2000).
171. Arrol, H. P., Church, L. D., Bacon, P. A. & Young, S. P. Intracellular calcium signalling patterns reflect the differentiation status of human T cells. *Clin. Exp. Immunol.* **153**, 86–95 (2008).
172. Bécart, S. *et al.* SLAT regulates Th1 and Th2 inflammatory responses by controlling Ca²⁺/NFAT signaling. *J. Clin. Invest.* **117**, 2164–2175 (2007).
173. Zanotti, S., Smerdel-Ramoya, A. & Canalis, E. Nuclear factor of activated T-cells (NFAT)C2 inhibits Notch receptor signaling in osteoblasts. *J. Biol. Chem.* **288**, 624–632 (2013).
174. Menten, P. *et al.* Role of the autocrine chemokines MIP-1alpha and MIP-1beta in the metastatic behavior of murine T cell lymphoma. *J. Leukoc. Biol.* **72**, 780–9 (2002).
175. Schofield, P. R. *et al.* Sequence and functional expression of the GABA_A receptor shows a ligand-gated receptor super-family. *Nature* **328**, 221–227 (1987).
176. Sigel, E. & Steinmann, M. E. Structure, function, and modulation of GABA_A receptors. *J. Biol. Chem.* **287**, 40224–40231 (2012).
177. George Chandy, K. *et al.* K⁺ channels as targets for specific immunomodulation. *Trends Pharmacol. Sci.* **25**, 280–289 (2004).

178. Wilson, H. A. & Chused, T. M. Lymphocyte membrane potential and Ca²⁺-sensitive potassium channels described by oxonol dye fluorescence measurements. *J. Cell. Physiol.* **125**, 72–81 (1985).
179. Ozer, N. K., Bashford, C. L., Carter, N. D. & Pasternak, C. A. Plasma membrane potential of lymphocytes from ataxia telangiectasia patients. *Clin. Biochem.* **22**, 469–73 (1989).
180. Mello de Queiroz, F., Ponte, C. G., Bonomo, A., Vianna-Jorge, R. & Suarez-Kurtz, G. Study of membrane potential in T lymphocytes subpopulations using flow cytometry. *BMC Immunol.* **9**, 63 (2008).
181. Pilas, B. & Durack, G. A flow cytometric method for measurement of intracellular chloride concentration in lymphocytes using the halide-specific probe 6-methoxy-N-(3-sulfopropyl) quinolinium (SPQ). *Cytometry* **28**, 316–322 (1997).
182. Bjurström, H. *et al.* GABA, a natural immunomodulator of T lymphocytes. *J. Neuroimmunol.* **205**, 44–50 (2008).
183. Grinstein, S., Clarke, C. A., Dupre, A. & Rothstein, A. Volume-induced increase of anion permeability in human lymphocytes. *J. Gen. Physiol.* **80**, 801–23 (1982).
184. Heimlich, G. & Cidlowski, J. A. Selective role of intracellular chloride in the regulation of the intrinsic but not extrinsic pathway of apoptosis in Jurkat T-cells. *J. Biol. Chem.* **281**, 2232–2241 (2006).
185. MacLean, E. I. Molecular regulation and endogenous expression of CRTh2 in in vitro differentiated CRTh2+ Th2 cells. (2011). doi:10.7939/R3F981
186. Kaila, K., Price, T. J., Payne, J. A., Puskarjov, M. & Voipio, J. Cation-chloride cotransporters in neuronal development, plasticity and disease. *Nat. Rev. Neurosci.* **15**, 637–654 (2014).
187. Dionisio, L., De Rosa, M. J., Bouzat, C. & Esandi, M. del C. An intrinsic GABAergic system in human lymphocytes. *Neuropharmacology* **60**, 513–519 (2011).
188. Dionisio, L., Arias, V., Bouzat, C. & Esandi, M. D. C. GABAA receptor plasticity in Jurkat T cells. *Biochimie* **95**, 2376–2384 (2013).
189. Weiss, A., Wiskocil, R. L. & Stobo, J. D. The role of T3 surface molecules in the activation of human T cells: a two-stimulus requirement for IL 2 production reflects events occurring at a pre-translational level. *J. Immunol.* **133**, 123–8 (1984).
190. Demakova, E. V., Korobov, V. P. & Lemkina, L. M. Determination of gamma-aminobutyric acid concentration and activity of glutamate decarboxylase in blood

- serum of patients with multiple sclerosis. *Klin. Lab. Diagn.* 15–7 (2003).
191. Tian, J., Yong, J., Dang, H. & Kaufman, D. L. Oral GABA treatment downregulates inflammatory responses in a mouse model of rheumatoid arthritis. *Autoimmunity* **44**, 465–470 (2011).
 192. Prud'homme, G. J., Glinka, Y. & Wang, Q. Immunological GABAergic interactions and therapeutic applications in autoimmune diseases. *Autoimmun. Rev.* **14**, 1048–1056 (2015).
 193. Romagnani, S. T-cell subsets (Th1 versus Th2). *Ann. Allergy, Asthma Immunol.* **85**, 9–21 (2000).
 194. Kidd, P. Th1/Th2 balance: the hypothesis, its limitations, and implications for health and disease. *Altern. Med. Rev.* **8**, 223–46 (2003).
 195. Xiang, Y.-Y. *et al.* A GABAergic system in airway epithelium is essential for mucus overproduction in asthma. *Nat. Med.* **13**, 862–867 (2007).
 196. Shen, M.-L. *et al.* Luteolin attenuates airway mucus overproduction via inhibition of the GABAergic system. *Sci. Rep.* **6**, 32756 (2016).

Appendices

Appendix A: Supplementary Figures

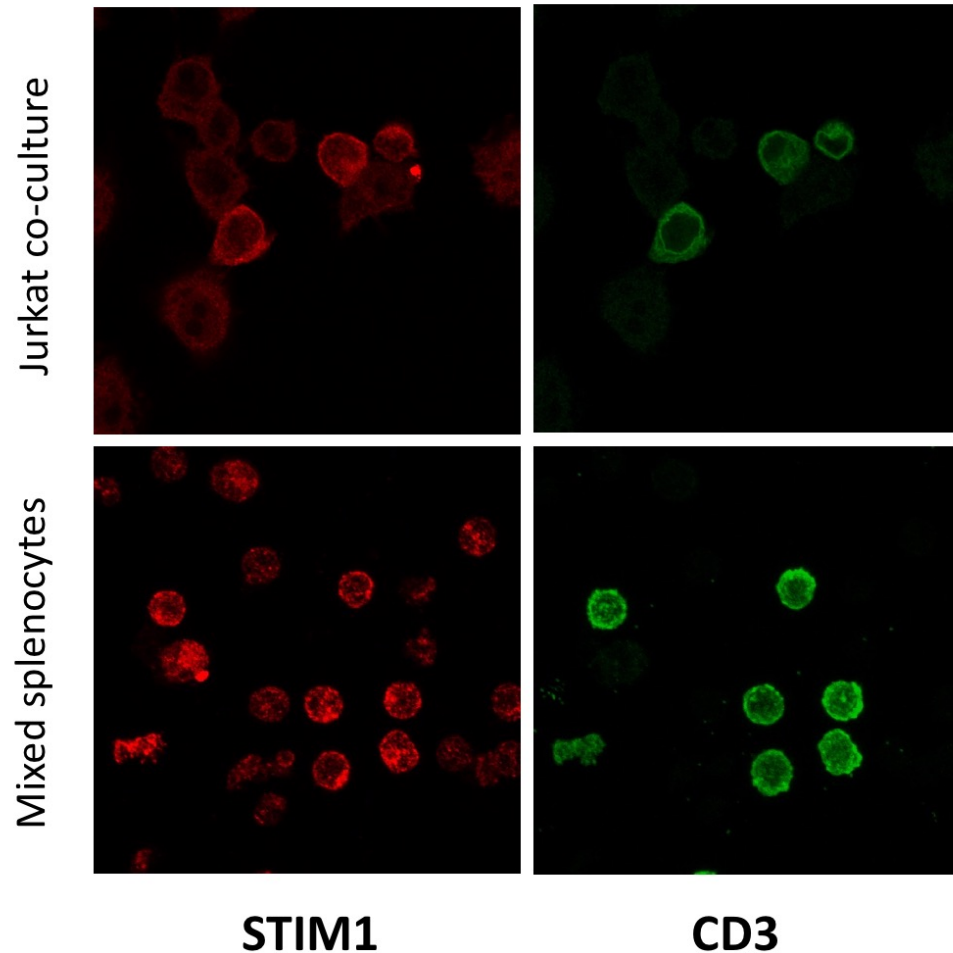


Figure 6.1 Protein expression and localization of STIM1 and CD3 in Jurkat cells co-cultured with RAW 264.7 cells and isolated primary mixed splenocytes.

Top: Representative immunofluorescence images of Jurkat and RAW 264.7 cells stained with anti-STIM1 (Cy3, Red) and anti-CD3 (Alexa488, Green). **Bottom:** Representative immunofluorescence images of mixed splenocytes isolated from mice and stained with anti-STIM1 (Cy3, Red) and anti-CD3 (Alexa488, Green). Note that CD3 is a marker for T cells.

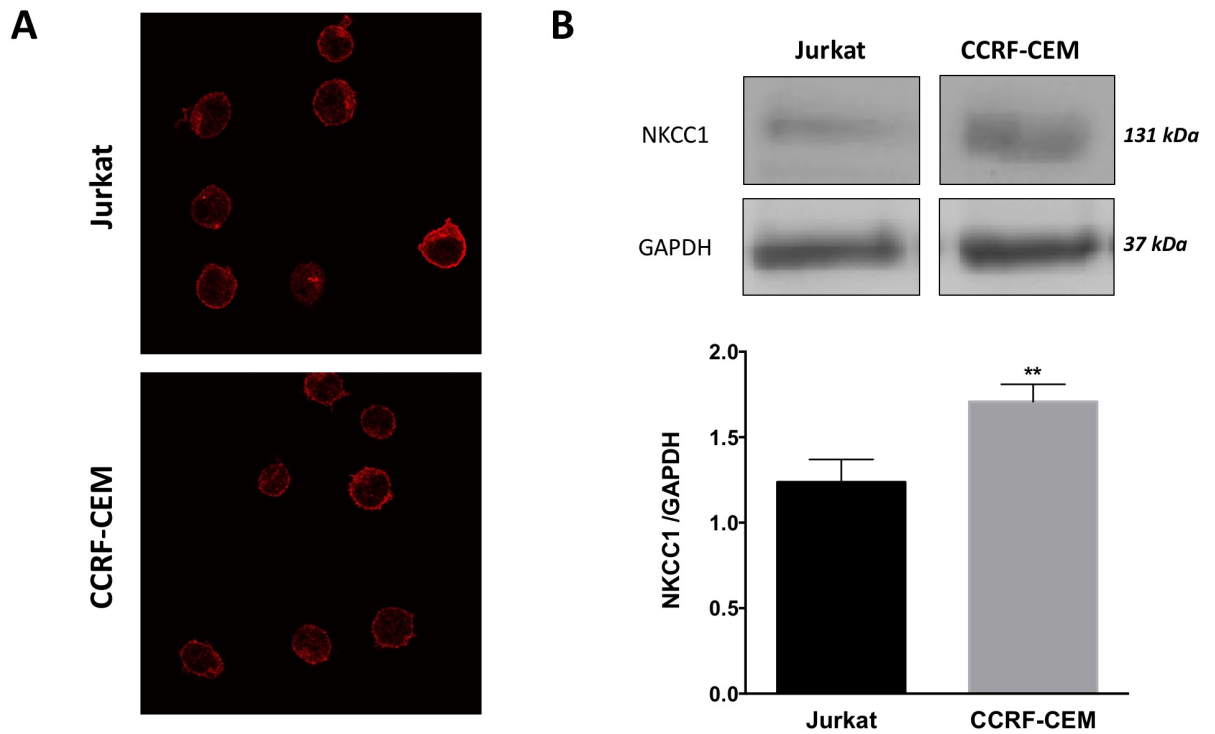


Figure 6.2 Protein expression and localization of NKCC1 in Jurkat and CCRF-CEM cells.

A) Representative immunofluorescence images of Jurkat and CCRF-CEM cells stained with anti-NKCC1 (Cy3, Red). **B)** Representative Western Blot of NKCC1 in whole cell lysates of Jurkat and CCRF-CEM cells. Note the higher expression levels of NKCC1 in the CCRF-CEM cells.

Appendix B: Permission for Reprints

License to reprint Figure 1.1

8/13/2017

RightsLink Printable License

NATURE PUBLISHING GROUP LICENSE TERMS AND CONDITIONS

Aug 13, 2017

This Agreement between Miss. Ying Lin ("You") and Nature Publishing Group ("Nature Publishing Group") consists of your license details and the terms and conditions provided by Nature Publishing Group and Copyright Clearance Center.

License Number	4141540099960
License date	Jul 03, 2017
Licensed Content Publisher	Nature Publishing Group
Licensed Content Publication	Nature Reviews Cancer
Licensed Content Title	Cytokines in cancer pathogenesis and cancer therapy
Licensed Content Author	Glenn Dranoff
Licensed Content Date	Jan 1, 2004
Licensed Content Volume	4
Licensed Content Issue	1
Type of Use	reuse in a dissertation / thesis
Requestor type	academic/educational
Format	print and electronic
Portion	figures/tables/illustrations
Number of figures/tables/illustrations	1
High-res required	no
Figures	Figure 1) The innate and adaptive immune response.
Author of this NPG article	no
Your reference number	
Title of your thesis / dissertation	Distinct roles of GABAAR signaling in regulation of two human T lymphocyte lines
Expected completion date	Aug 2017
Estimated size (number of pages)	112

License to reprint Figure 1.2

8/13/2017

RightsLink Printable License

NATURE PUBLISHING GROUP LICENSE TERMS AND CONDITIONS

Aug 13, 2017

This Agreement between Miss. Ying Lin ("You") and Nature Publishing Group ("Nature Publishing Group") consists of your license details and the terms and conditions provided by Nature Publishing Group and Copyright Clearance Center.

License Number	4141540324203
License date	Jul 03, 2017
Licensed Content Publisher	Nature Publishing Group
Licensed Content Publication	Nature Reviews Immunology
Licensed Content Title	Calcium signalling in lymphocyte activation and disease
Licensed Content Author	Stefan Feske
Licensed Content Date	Sep 1, 2007
Licensed Content Volume	7
Licensed Content Issue	9
Type of Use	reuse in a dissertation / thesis
Requestor type	academic/educational
Format	print and electronic
Portion	figures/tables/illustrations
Number of figures/tables/illustrations	1
High-res required	no
Figures	Figure 1) Store-operated calcium entry (SOCE) in T cells.
Author of this NPG article	no
Your reference number	
Title of your thesis / dissertation	Distinct roles of GABAAR signaling in regulation of two human T lymphocyte lines
Expected completion date	Aug 2017
Estimated size (number of pages)	112

License to reprint Figure 1.3

8/13/2017

RightsLink Printable License

NATURE PUBLISHING GROUP LICENSE TERMS AND CONDITIONS

Aug 13, 2017

This Agreement between Miss. Ying Lin ("You") and Nature Publishing Group ("Nature Publishing Group") consists of your license details and the terms and conditions provided by Nature Publishing Group and Copyright Clearance Center.

License Number	4141540433404
License date	Jul 03, 2017
Licensed Content Publisher	Nature Publishing Group
Licensed Content Publication	Nature Reviews Immunology
Licensed Content Title	T-cell development and the CD4[ndash]CD8 lineage decision
Licensed Content Author	Ronald N. Germain
Licensed Content Date	May 1, 2002
Licensed Content Volume	2
Licensed Content Issue	5
Type of Use	reuse in a dissertation / thesis
Requestor type	academic/educational
Format	print and electronic
Portion	figures/tables/illustrations
Number of figures/tables/illustrations	1
High-res required	no
Figures	Figure 1) Overall scheme of T-cell development in the thymus.
Author of this NPG article	no
Your reference number	
Title of your thesis / dissertation	Distinct roles of GABAAR signaling in regulation of two human T lymphocyte lines
Expected completion date	Aug 2017
Estimated size (number of pages)	112

Terms and Conditions for Permissions

8/13/2017

RightsLink Printable License

Total 0.00 CAD

[Terms and Conditions](#)

Terms and Conditions for Permissions

Nature Publishing Group hereby grants you a non-exclusive license to reproduce this material for this purpose, and for no other use, subject to the conditions below:

1. NPG warrants that it has, to the best of its knowledge, the rights to license reuse of this material. However, you should ensure that the material you are requesting is original to Nature Publishing Group and does not carry the copyright of another entity (as credited in the published version). If the credit line on any part of the material you have requested indicates that it was reprinted or adapted by NPG with permission from another source, then you should also seek permission from that source to reuse the material.
2. Permission granted free of charge for material in print is also usually granted for any electronic version of that work, provided that the material is incidental to the work as a whole and that the electronic version is essentially equivalent to, or substitutes for, the print version. Where print permission has been granted for a fee, separate permission must be obtained for any additional, electronic re-use (unless, as in the case of a full paper, this has already been accounted for during your initial request in the calculation of a print run). NB: In all cases, web-based use of full-text articles must be authorized separately through the 'Use on a Web Site' option when requesting permission.
3. Permission granted for a first edition does not apply to second and subsequent editions and for editions in other languages (except for signatories to the STM Permissions Guidelines, or where the first edition permission was granted for free).
4. Nature Publishing Group's permission must be acknowledged next to the figure, table or abstract in print. In electronic form, this acknowledgement must be visible at the same time as the figure/table/abstract, and must be hyperlinked to the journal's homepage.
5. The credit line should read:
 Reprinted by permission from Macmillan Publishers Ltd: [JOURNAL NAME] (reference citation), copyright (year of publication)
 For AOP papers, the credit line should read:
 Reprinted by permission from Macmillan Publishers Ltd: [JOURNAL NAME], advance online publication, day month year (doi: 10.1038/sj.[JOURNAL ACRONYM].XXXXX)

Note: For republication from the *British Journal of Cancer*, the following credit lines apply.
 Reprinted by permission from Macmillan Publishers Ltd on behalf of Cancer Research UK: [JOURNAL NAME] (reference citation), copyright (year of publication) For AOP papers, the credit line should read:
 Reprinted by permission from Macmillan Publishers Ltd on behalf of Cancer Research UK: [JOURNAL NAME], advance online publication, day month year (doi: 10.1038/sj.[JOURNAL ACRONYM].XXXXX)
6. Adaptations of single figures do not require NPG approval. However, the adaptation should be credited as follows:

 Adapted by permission from Macmillan Publishers Ltd: [JOURNAL NAME] (reference citation), copyright (year of publication)

Note: For adaptation from the *British Journal of Cancer*, the following credit line applies.
 Adapted by permission from Macmillan Publishers Ltd on behalf of Cancer Research UK: [JOURNAL NAME] (reference citation), copyright (year of publication)
7. Translations of 401 words up to a whole article require NPG approval. Please visit <http://www.macmillanmedicalcommunications.com> for more information. Translations of up to a 400 words do not require NPG approval. The translation should be credited as follows:

8/13/2017

RightsLink Printable License

Translated by permission from Macmillan Publishers Ltd: [JOURNAL NAME] (reference citation), copyright (year of publication).

Note: For translation from the *British Journal of Cancer*, the following credit line applies.

Translated by permission from Macmillan Publishers Ltd on behalf of Cancer Research UK: [JOURNAL NAME] (reference citation), copyright (year of publication)

We are certain that all parties will benefit from this agreement and wish you the best in the use of this material. Thank you.

Special Terms:

v1.1

Questions? customer@copyright.com or +1-855-239-3415 (toll free in the US) or +1-978-646-2777.

Curriculum Vitae

Name: Amy Lin

Post-secondary Education and Degrees: Physiology and Pharmacology Graduate Program; MSc
Western University
London, Ontario, Canada
2016-2017

Bachelor of Medical Science (BMSc) – Honors Specialization in
Physiology and Pharmacology
Western University
London, Ontario, Canada
2012-2016

Honors and Awards: Graduated with Distinction
2016

Dean's Honor List
2012-2016

Robarts Research Retreat – Top poster in category
2017

Related Work Experience: Teaching Assistant
Western University
2016-2017

Presentations: Physiology and Pharmacology Research day – Poster presentation
2015

Robarts Molecular Medicine Series – Oral presentation
2017

Robarts Research Retreat – Poster Presentation
2017

Robarts Research Retreat – Oral Presentation
2017